MASTER OF SCIENCE BY RESEARCH

Clinical practice

expression of circulating miRNAs linked to cardiac injury in left-sided radiotherapy breast cancer patients

Malik, Moona

Award date:
2017

Awarding institution:
Coventry University

Clinical Practice: Expression of circulating miRNAs linked to cardiac injury in left-sided radiotherapy breast cancer patients

By

Moona Malik

Module Code: HLSR013

MRes in Clinical Research (MScR)

Academic Supervisors: Professor Helen Maddock, Dr Hardip Sandhu, Dr Mayel Gharanei and Professor Tim James

May 2017

A thesis submitted in partial fulfilment of the University's requirements for the Degree of Doctor of Philosophy /Master of Philosophy/Master of Research

Coventry University

Certificate of Ethical Approval

Applicant:

Moona Malik

Project Title:

Evaluation of circulatory microRNAS as potential early biomarkers for acute radiotherapy induced cardiac injury

This is to certify that the above named applicant has completed the Coventry University Ethical Approval process and their project has been confirmed and approved as Medium Risk

Date of approval:

31 January 2017

Project Reference Number:

P46798

Acknowledgements

First and foremost I would like to begin thanking my academic supervisors for the opportunity of bringing to life such a wonderful research project. I am sincerely grateful to Professor Helen Maddock, Dr Hardip Sandhu and Dr Mayel Gharanei for their kindness, patience, guidance and their teaching. You have all played an integral role in transforming me from a student into a researcher who has started an amazing lifelong journey of a clinical researcher, and the successes and moments of progress I have encountered in the past two years with you, I shall never forget. I cannot thank you enough for your support in both my professional and personal life, your guidance and thoughts have helped me achieve over and above what was perhaps anticipated.I could not feel prouder in belonging to such an incredible and driven research team under the leadership of Professor Helen Maddock. To me all of you are an inspiration.

A special thank you also to Dr Vanessa Ferreira and Dr David Cutter for allowing us to work with Oxford University Hospital NHS Foundation Trust and conduct this piece of work. Your clinical expertise and passion for this area of research has been inspiring and I am very grateful for the opportunity to have worked with you.

To my mum, thank you for supporting me and loving me. Everything I do is to make you proud.

Thank you

Moona Malik

Table of Contents

Table of Contents 2
Figure List 4
List of Tables 5
Abstract 7
Abbreviations 9
Section 1. Introduction 10
1.1 Breast Cancer Incidence and Radiotherapy 10
1.2 Radiation Induced Heart Disease (RIHD) 11
1.2.2 Current Prevention and Management of Breast Cancer 15
1.2.2.1 Diagnosis of Breast Cancer usingImaging 15
1.2.2.2 Diagnosis of Breast Cancer using protein biomarkers 16
1.2.2.3 RIDH and current diagnostics issues RIHD 17
1.3 miRNA biogenesis and function 19
1.3.1 miRNAs are involved in biological processes including cardiovascular disease development 21
1.3.2 miRNAs as ideal biomarker candidates 21
1.3.3 Fluid- and tissue- specificity of cardiac miRNAs 22
1.3.4 miRNAs are cardiac development stage specific 24
1.3.5 miRNAs in the developing and healthy adult heart 24
1.3.6 Cardiac disease specific miRNA expression 24
1.3.6.1 miRNAs in Acute Myocardial Infarction (AMI)patients 25
1.3.6.2 miRNAs in Heart Failure (HF)patients 26
1.3.6.3 miRNAs in Coronary Artery Disease (CAD) patients 27
1.3.6.4 miRNA in Hypertension and Atherosclerosis patients 27
1.3.6.5 miRNA in Fibrosis and Arrhythmia 28
1.3.7 miRNAs in aiding cardiomyocyte cell survival 28
1.3.8 miRNAs in response to cancer therapy induced cardiotoxicity 28
1.3.8.1 miRNAs in Breast Cancer 29
1.3.9 Application of miRNAs in various disease states 29
1.3.10 Clinical detection of miRNAs 30
1.4 Research Area 30
1.4.1 Hypothesis 30

1.4.2Aim 30
1.4.3 Objectives 31
Section 2. Materials and Methods 32
2.1 Ethics Statement 32
2.2 Patient Population and Inclusion criteria 32
2.2.1 Exclusion Criteria 33
2.3 Radiotherapy planning and delivery 33
2.4 Blood Sample Collection and Analysis 33
2.5 List of Consumables and Suppliers 34
2.6 miRNA extraction from plasma 34
2.7 NanodropQuanitification 36
2.8Reverse Transcription PCR (RT-PCR) 36
2.9 Real Time PCR 37
2.10 Statistical Analysis 38
Section 3: Results 40
3.1 Experimental Design Summary 40
3.2 Characteristics of the 15 BC patients 41
3.3 Cardiac Radiation Dosimetry 41
3.4 Troponin and BNP Analysis 41
3.5 Cardiovascular Magnetic Resonance Results 43
3.6 miRNA values and RT-PCR 46
3.7 Total RNA 47
3.8 Reverse Transcriptase and Real Time PCR analysis 50
3.9Sample ratio values 51
3.10 Exclusion Criteria 60
3.11 miRNA expression change graphs from GraphPad Prism 65
Section 4. Discussion 87
4.1 Background, Purpose and Results 87
4.2 Limitations of the study 92
4.3 Conclusion 95
4.4 Future Perspectives 95
Appendix 97
References 109

Figure List:

Figure title and number	Page Number
Figure 1: Demonstration of the pathophysiology of RIHD induced injury	14
Figure 2: Diagram of miRNA maturation and function (see section 1.3 for a detailed description) (Macfarlane et al 2010)	21
Figure 3: Demonstration of the experiment	41
Figure 4: Graphical demonstration of the changes	46
Figure 5: Nanodrop profile of sample 32D	49
Figure 6A: miR-1 expression levels changes over time point A to D	67
Figure 6b: miR-1 expression changes from time point A to D	68
Figure 7A: miR-451expression levels changes over time point A to D	69
Figure 7b: miR-451 changes from A to D	70
Figure 8A: miR-27a expression levels changes over time point A to D	71
Figure 8b: miR-27a changes from time point A to D only	72
Figure 9A: miR-125 expression levels changes over time point A to D	73
Figure 9B: miR-125 expression changes from A to D	74
Figure 10a: miR-29b expression levels changes over all time points A-D	76
Figure 10b: miR-29b changes from A to D	77
Figure 11a: miR-30a expression levels changes over all time points A to D	78
Figure 11b: miR-30a expression level changes from A to D	79
Figure 12a: miR-133a expression levels changes over all time point A to D	80
Figure 12b: miR-133a changes from A to D	81
Figure 13a: miR-505 expression levels changes over all time point A to D	82
Figure 13b: miR-505a changes from A to D only	83
Figure 14a: miR-144 expression levels changes over all time point A to D	84
Figure 14b: miR-144 changes from A to D	85
Figure 15a: miR-133b expression levels changes over all time point A to D	86
Figure 15b: miR-133b expression changes from A to D	87

List of Tables

Table Title and Number	Page Number
Table 1: Volume (µl) for reverse-transcriptase master mix constituents needed for 1 reaction.	37
Table 2: Volume (µl) for real-time PCR master mix constituents needed for 1 reaction.	38
Table 3: Troponin values for all patients across the 4 different time points A to D. There were no significant changes in the expression of Troponin values for any patient.	43
Table 4: BNP values across all 4 time points for each individual patient. There were no significant changes in BNP levels for any of the patients.	44
Table 5: Ejection fraction values for all patients from time points A to D (n=15).	45
Table 6: Stroke volume (ml/beat) readings for all patients over time points A to D (n=15).	47
Table 7: Purity Levels for all samples.	50
Table 8a: Time point A. Calculated ratio values via excel per sample 2-26 with respect to their corresponding miR-1, miR-27, miR-133a, miR-133b, miR-29b, miR- 30a	53
Table 8b: Time point A. Calculated ratio values via excel per sample 2-26, with respect to their corresponding miR-208a, miR-505, miR-144, miR-451, miR-125	53
Table 8c: Time point A. Calculated ratio values via excel per sample 29-32 with respect to their corresponding miR-1, miR-27, miR-133a, miR-133b, miR-29b, miR- 30a	54
Table 8d: Time point A. Calculated ratio values via excel per sample 29-32, with respect to their corresponding miR-208a, miR-505, miR-144, miR-451, miR-125	54
Table 9a: Time point B. Calculated ratio values via excel per sample 2-26 with respect to their corresponding miR-1, miR-27, miR-133a, miR-133b, miR-29b, miR- 30a	55
Table 9b: Time point B. Calculated ratio values via excel per sample 2-26, with respect to their corresponding miR-208a, miR-505, miR-144, miR-451, miR-125	55
Table 9c: Time point B. Calculated ratio values via excel per sample 29-32, with respect to their corresponding miR-1, miR-27, miR-133a, miR-133b, miR-29b, miR- 30a	56
Table 9d: Time point B. Calculated ratio values via excel per sample 29-32, with respect to their corresponding miR-208a, miR-505, miR-144, miR-451, miR-125	56

Table 10a: Time point C. Calculated ratio values via excel per sample 2-26, with respect to their corresponding miR-1, miR-27, miR-133a, miR-133b, miR-29b, miR- 30a	57
Table 10b: Time point C. Calculated ratio values via excel per sample 2-26, with respect to their corresponding miR-208a, miR-505, miR-144, miR-451, miR-125	58
Table 10c: Time point C. Calculated ratio values via excel per sample 29-32. with respect to their corresponding miR-1, miR-27, miR-133a, miR-133b, miR-29b, miR- 30a	58
Table 10d: Time point C. Calculated ratio values via excel per sample 29-32, with respect to their corresponding miR-208a, miR-505, miR-144, miR-451, miR-125	59
Table 11a: Time point D. Calculated ratio values via excel per sample 2-26, with respect to their corresponding miR-1, miR-27, miR-133a, miR-133b, miR-29b, miR- 30a	59
Table 11b: Time point D. Calculated ratio values via excel per sample 2-26, with respect to their corresponding miR-208a, miR-505, miR-144, miR-451, miR-125	60
Table 11c: Time point D. Calculated ratio values via excel per sample 29-32, with respect to their corresponding miR-1, miR-27, miR-133a, miR-133b, miR-29b, miR- 30a	60
Table 11d: Time point D. Calculated ratio values via excel per sample 29-32 with respect to their corresponding miR-1, miR-27, miR-133a, miR-133b, miR-29b, miR- 30a	61
Table 12: Included ratio data for miR-1 by Time point	61
Table 13: Included Ratio data for miR-27a by time point.	62
Table 14: Included Ratio data for miR-133a by time point	62
Table 15: Included Ratio data for miR-133b by time point	63
Table 16: Included Ratio data for miR-29b by time point	63
Table 17: Included Ratio Data for miR-30a by time point	64
Table 18: Included Ratio Data for miR-505 by time point	64
Table 19: Included ratio data for miR-144 by time point	64
Table 20: Included Ratio data for miR-451 by time point	65
Table 21: Included Ratio data for miR-125 by time points	65

Abstract

Introduction: There is great long term concern over the adverse cardiotoxic effects of radiation therapy (RT) treatment particularly in left-sided breast cancer (BC) patients (Chapman et al 2008). There is currently an urgent need to find a more specific, sensitive and clinically valid biomarker which can be used for the earlier detection of radiation induced heart disease (RIHD). MicroRNAs (miRNAs) have appeared as ideal candidate biomarkers for early stage RIHD diagnosis due to their non-invasive, fluid-, tissue-, organ- and disease specific nature. To date there is no study which focuses upon the utility of previously recognised cardiovascular disease linked miRNAs as biomarkers for RIHD and specifically in the context of left-sided breast irradiation. The aim of this work was to thus evaluate whether miRNAs which have been previously linked to cardiac damage are differentially expressed in BC patients treated for left-sided RT, and if they could provide clues of cardiotoxic change earlier and with higher specificity and sensitivity than traditional heart imaging and circulation protein based biomarkers.

Method: This study recruited samples from a larger research study which focused on the utility of Cardiac Magnetic Resonance (CMR) imaging in the detection of RIHD at an earlier stage in low-radiation dose treated left sided BC women at Oxford University Hospital NHS Foundation Trust. A total of 15 low-dose radiation treated left-sided BC women from the larger study were recruited to this current study. Total miRNA was isolated from 15 BC patients receiving left-side radiotherapy at timepoints: A (baseline pre-radiotherapy), B (24-72h post radiotherapy), C (3 months post radiotherapy) and D (6 months post-radiotherapy). Mean dose to the whole heart ranged from 0.6–2.8 Gray of radiation. Real time PCR was performed using TaqMan microRNA assays for microRNAs linked to cardiotoxicity (miR-1, -27a, -133a, -133b, -29b, -30a, -505, -144, -208a, -451 and -125a) using sno U6 as internal reference. The ΔΔCT calculation method was used. Students t-test was performed to

analyse the data when time point A was compared to D alone ($p<0.05$). A one-way ANOVA was also conducted to explore individual relationships between A, B, C and D.

Results: None of the 15 BC patients were noted to have suffered myocardial damage from CMR imaging, BNP or troponin results. Significant miRNA expression changes were observed when utilising students t-test comparing time point A and D (n=8-15) for: miR-1 (increased nearly 3-fold, $p=0.0378$), miR-27a (decreased nearly 4-fold, $P=0.0464$), miR-451 (decreased more than 2-fold, $P= 0.0321$), and miR-125a (increased more than 3-fold, $P=0.0098$).miR-144 was also found to be upregulated from A (n=10) to C (n=7) ($P\leq0.01$) and decreased back to baseline levels from C (n=7) to D (n=12) ($P\leq0.0001$). Other statistically significant relationships include a more than 3-fold increase in the levels of miR-1 from time point B to D ($p=0.002$) and C to D ($p=0.003$). miR-125 levels also increased by more than 2-fold between time points B to D ($p=0.031$). miR-144a levels increased by more than 465-fold from time point A to C ($p<0.01$) and then decreased by more than 1600 fold from time point C to D ($p<0.0001$). miR-133b levels were found to significantly decrease by more than 40-fold between A (n=10) to B (n=8) ($p=0.015$). The expression levels of miR-133a, miR-29b, miR-30a and miR-505 were not altered 6 months post-radiotherapy. The expression of miR-208a was undetectable at all time points in this study (n=7-13).

Conclusion:This study has shown that miR-1, miR-27a, miR-125 and miR-451 were altered from the pre-radiation to the 6 month post-radiation stage in left sided RT BC patients, whereas imaging and circulation cardiac injury protein biomarkers did not change at all. In addition it was also observed that miR-144 and miR-133b shows a differential regulation pattern in response to RT. As none of the patients within this study developed clinically diagnosed cardiotoxicity as a result of radiation, the link between RIHD as a cause of these expressional changes cannot be established. However this study does highlight that miRNAs warrant further investigation in larger patient cohorts for potential as early stage biomarkers of RIHD as changes in expression patterns are seen.

.

Abbreviations

AMI: Acute myocardial infarction

BC: Breast Cancer

BNP: Brain Natriuretic Peptide

CMR: Cardiac Magnetic Resonance

CAD: Coronary Artery Disease

cTnI: Cardiac troponin I

cTnT: Cardiac troponin

EF: Ejection Fraction

Gy: Gray

HF: Heart Failure

IHD: Ischaemic Heart Disease

miR: microRNA

miRNAs:microRNAs

MI: Myocardial Infarction

NICE: National Institute of Clinical Excellence

qRT-PCR: quantitative reverse transcription-polymerase chain reaction

RT: Radiation Therapy

RIHD: Radiation Induced Heart Disease

SPECT: Single photon emission computed tomography

TIC: Therapy Induced cardiotoxicity

TTE: Transthoracic Echocardiography

Section 1. Introduction

1.1 Breast Cancer Incidence and Radiotherapy

More than one million cases of breast cancer (BC) are diagnosed each year worldwide (Perry et al 2008). It is the most commonly occurring neoplasm in women in both high resource and low resource settings and accounts for over one-fifth of the estimated annual 4.7 million cancer diagnosis in females (Beiki et al 2012). It is also the second most common tumour after lung cancer in both sexes (Ferlay et al 2001). Furthermore, it is the primary cause of cancer death amongst women globally and is responsible for more than 500,000 deaths each year worldwide (Siegel et al 2016).

Radiation Therapy (RT) is a critical component of the multidisciplinary management of invasive BC. It is estimated that 50% of patients will receive RT at some stage of their clinical treatment. In appropriately selected patients, RT not only improves local control, by reducing morbidity and chances of local recurrence but also improves survival by preventing seeding and reseeding growth of distant metastases from persistent reservoirs of locoregional disease (Jagsi et al 2013). Timothy *et al.* showed that adjuvant RT statistically significantly reduced the risk of mortality (odds ratio = 0.83, 95% confidence interval [CI] =0.74 to 0.94; p=.04) (Timothy et al 2003).

It is possible to summarise and group the stages of BC into early stage various different stages based upon the size of the tumour and whether the cancer has spread. Stage I is a tumour no larger than 2cm and has not spread to lymph nodes. Locally advanced stage disease encompasses stage II and III whereby the tumour is between 2-5cm and may have spread to lymph nodes under the arm or surrounding breast tissue. Advanced or metastatic stage disease encompasses stage IV whereby tumour has spread to other organs in the body for examples lungs, liver or bone. Stages I, IIA, IIIB, are considered ‘early stage’ breast cancer and refer to cancers that may have spread to nearby lymph nodes but have not metastasized. It is therefore not surprising that treatment options for early stage are

different to those for advanced stage disease (Kirova et al 2010). Approximately of the 55,000 new cases of BC diagnosed each year in the UK, 60% of patients are diagnosed with early stage BC, 33% patients are diagnosed at the locally advanced stage and 5% of patients are diagnosed with advanced or metastatic BC (McNeely et al 2006). Approximately 98% of patients will survive for 5 years if they have early stage BC. Around 74% of patients with locally advanced BC will survive for 5 years and roughly 20% of BC patients with advanced or metastatic disease will survive for 5 years. (Joshi et al 2007).Unsurprisingly, restoring the quality of life in patients with early stage breast cancer remains a clinical priority due to their increased chances of living longer.

The four main applications of RT in the primary treatment of BC are in treating early stage invasive disease, locally advanced BC and as postmastectomy therapy (Taghian et al 1999). The primary treatment of BC patients with early stage BC is usually breast-conserving surgery followed by RT as adjuvant therapy, where RT is used to destroy any remaining mutated cells that remain in the breast or armpit area post-surgery (Jacob et al 2016). Lim *et al.* who conducted a prospective study of lumphectomy alone without RT in early stage BC patients found at 7 year follow up the local recurrence rate to be unacceptably high at 23%. We can thus conclude that RT given after breast conservative surgery among patients, at moderate or high risk of dying from cancer, has favourable effects on survival. In fact multiple clinical trials have also shown a substantial risk of local recurrence if RT is omitted after breast conserving surgery (Cutuli et al 2009; Whelan et al 2010).

1.2 Radiation Induced Heart Disease (RIHD)

Radiation-induced heart disease is a term used to refer to the spectrum of cardiac pathologies, including myocardial fibrosis and cardiomyopathy, coronary artery disease, valvular disease, pericardial disease, and arrhythmias which are a result of radiation to the chest (Madan et al 2015).

Unfortunately, while breast radiotherapy improves overall survival, there is strong evidence that due to incidental exposure of the heart to RT adverse effects from radiation exposure can lead to development of heart disease, in particular left-sided RT, which can progress to heart failure and death (Madan et al 2015). Patients who receive post-mastectomy RT for left sided breast cancer are 2-3 times at a higher risk of developing cardiovascular disease as compared to right sided BC patients. (Madan et al 2015). This is because in left sided BC, the apex and anterior wall of the heart typically receive the highest dose of radiation and consequently the left anterior descending and distal diagonal regions are most prominently involved due to the national positioning of the heart which pre-disposes the heart to developing clinically significant cardiac abnormalities (Donnellan et al 2016). Approximately 51% of patients have left sided BC, 46% of patients have right sided breast cancer, and 3% of patients have simultaneous bilateral malignancy (Amer et al 2014). As left sided BC patients receive higher RT doses and that too specifically to the heart, this study focused upon left sided BC patients as miRNA signals would be hypothetically stronger in these patients. No statistical significance has been noted in survival between left and right sided breast cancer as a result of the cancer itself although as discussed above RIHD is of greater risk in left sided BC patients contributing to risk of mortality (Amer et al 2014).

Considering RT pathogenesis, RT can cause both acute and chronic effects on the heart as shown below in Figure 1. Radiation-related cardiac disease is known to induce pathological changes including endothelial damage causing perfusion abnormalities, myocardial oedema, scarring and fibrosis, valvular disease, coronary artery disease (CAD) and MI (Vasu et al 2013).

Figure 1: *Demonstration of the pathophysiology of RIHD induced injury and end-clinical manifestations. Radiation to the heart can induce both acute and chronic effects by implication of Tumour Necrosis Factor and interleukins resulting in an immune response which causes damage to vessels, conductive tissue, myocardium and pericardium (Taunk et al 2015).*

Various alternative approaches to minimise the burden of treatment have been sought due the increased chance or mortality due to Radiation Induced Heart Disease (RIHD). This includes hypofractionation of radiation treatment which involves the use of larger daily doses of radiation and decreases the total number of fractions that must be administered. The UK Standardisation of Breast Radiotherapy Trial B compared contemporary 50 Gray (Gy) of RT in 25 fractions and 40 Gy in 15 fractions over 3 weeks in 2125 BC women. They found that there was a significantly lower rates of adverse effects in the group who received the

accelerated hypofractionated RT regime (40 Gy in 15 fractions over 3 weeks)(Kim et al 2016). Combined with the fact that radiation doses received by the heart are generally lower from contemporary RT then older RT techniques, it is likely that the cardiac injury risk from modern day RT treatments is lower than the past (Taylor et al 2007). However, RT treated BC patient hearts still receives a mean radiation dose of between 1 and 5 Gy on average during treatment of the left-sided BC and there is evidence that even this low dose poses a significant risk (Carr et al 2005; Shimizu et al 2010;, Darby et al 2013).

Cardiac damage has been shown to be correlated with the heart-absorbed dose of RT. Darby *et al.* who conducted a population based case control study of major coronary events in BC patients demonstrated that rates of major coronary events such as myocardial infarction (MI), coronary revascularisation, or death from ischaemic heart disease increased linearly with a mean dose to the heart by 7.4% per increase in Gy with no apparent threshold. They found the increase in risk to start within the first 5 years after completed RT and continued into the third decade after RT. Interestingly, the proportional increase in risk in the rate of major coronary events per Gy was similar in women with and women without cardiac risk factors at the time of RT. Furthermore, they also found the percentage increases in the rate of major coronary events per Gy of radiation according to the number of years since radiation exposure were as follows: 0 to 4 years, 16.3%; 5 to 9 years, 15.5%; 10 to 19 years, 1.2%; and 20 or more years, 8.2% (Darby et al 2013).

BC RT of the heart has been shown to be associated with long-term cardiotoxicity, such as heart failure (HF) and myocardial infarction (MI) and finally cardiovascular death. More than 10 years after RT the relative risk is in the range of 1.2 to 3.5 times by comparing left-breast treated patients who are at a higher risk to those that are unexposed or treated on the right-side (Giordano et al 2005).

Cardiotoxicity is described as either subclinical myocardial injury (development of asymptomatic cardiac abnormalities) or clinical toxicity (objective cardiac damage). More specifically, clinically, cardiac toxicity can be defined as one of the following:
1) Reduction of LVEF, either global or specific in the intraventricular septum; 2) symptoms or signs associated with heart failure (HF); 3) reduction in LVEF from baseline ≤ to 5% to <55% in the presence of signs or symptoms of HF (Seidman et al 2002). It is these three criteria which were used to assess patients for the presence of cardiotoxicity.

Risk factors for RIHD include radiation dose >30-35 Gy, dose/fraction more than 2 Gy, large volume of irradiated heart, younger age at exposure, longer time since exposure, use of cytotoxic chemotherapy, endocrine therapy or trastuzumab. Other risk factors for RIHD include diabetes, hypertension, dyslipidemias, obesity and smoking (Bovelli et al 2010).

1.2.2 Current Prevention and Management of Breast Cancer

The European Society of Medical Oncology has issued guidelines for the prevention, diagnosis and management for cardiovascular disease development associated with cancer therapy. Briefly the guidelines call for aggressive cardiac risk-factor risk modification through weight-loss, exercise, blood pressure control and smoking cessation, in addition to early identification of RIHD. The current approach to RIDH diagnosis includes imaging and measurement of circulating cardiac injury protein biomarkers.

1.2.2.1 Diagnosis of Breast Cancer usingImaging

Baseline comprehensive transthoracic echocardiography (TTE) is advocated in all patients before starting RT to detect anomalies. Beyond this, an annual history and physical examination, paying close attention to the signs and symptoms of cardiopulmonary disease is essential.

In asymptomatic patients, screening TTE at 10 years after RT is recommended. In patients with no pre-existing cardiac disease, surveillance TTE is recommended should be at 5-year intervals thereafter. In asymptomatic high-risk patients, those who have undergone anterior or left sided RT and have at least one risk factor for RIHD, initial screening TTE is recommended 5 years post RT. If this initial examination is negative, stress CMR is recommended.

The imaging modality that has been used most frequently to study RIHD following BC is single photon emission computer tomography (SPECT) nuclear myocardial perfusion imaging. More recently tissue Doppler echocardiography has also been used (Erven et al 2011). However, there is currently no data advocating the use of any of these imaging techniques as screening tools (Lancelloti et al 2013).

1.2.2.2 Diagnosis of Breast Cancer using protein biomarkers

Circulating cardiac injury protein biomarkers can be used in the assessment of myocardial injury. Cardiac troponin I (cTnI) is cardiac-muscle-specific, whereas cardiac Troponin T (cTnT) is expressed in damaged skeletal muscle (Jaffe et al 2000). It has been found that cTnI and cTnT are released into the blood circulation at levels which reflect the extent of myocardial injury, therefore they could be said to be specific and sensitive to a certain extent (Collinson et al 2005). However cardiac cell injury which does not result in an altered cardiac muscle cell membrane disruption may not be associated with increases in serum proteins. This is significant as apoptotic signalling can be generated by interaction of ionising radiation with cellular membranes (Sharma et al 2004). In addition in cases of altered ion homeostasis, valvular diseases and contractile dysfunction, levels of serum troponins may not be increased (Collinson et al 2005). In a study of 50 women with BC, no change in serum troponin was found after a total dose of 45 to 46 Gy (Sharma et al 2004).

Brain Natriuretic Peptide (BNP) is a cardiac neuro-hormone which is secreted by the ventricular myocardium in response to changes in volume expansion and pressure overloading during myocardial stress or HF (Maisel et al 2002). It has been shown that the release of BNP is directly correlated with the degree of ventricular wall tension and generally BNP secretion correlates with echocardiographic indices of systolic and diastolic dysfunction and clinical HF (Sandri et al 2005). However, BNP is not recommended for diagnostic screening of therapy-induced cardiotoxicity (TIC) due to poor sensitivity and the fact that levels vary significantly based upon the physiological characteristics of the patient, thus making it difficult to establish a cut off (Nousianen et al 2002; Daugaard et al 2005).

Hence based on current knowledge, circulating cardiac injury protein biomarkers are not recommended for evaluation of radiation-induced cardiotoxicity but remain a useful research tool.

1.2.2.3 RIDH and current diagnostics issues RIHD

The most important issue however remains that subclinical cardiac damage occurs in more than 50% of BC patients who undergo RT (Darby et al 2013). Subclinical cardiac injury can be defined as development of asymptomatic cardiac abnormalities in previously healthy cancer survivors (Carr et al 2005). As can be seen from the above clinical guidelines, patients are not reviewed until 5-10 years post RT when damage to the heart is often chronic and irreversible (Lancelloti et al 2013). There is currently no active monitoring either of patients either for cardiac abnormalities post RT unless they complain of cardiac-related symptoms by which time the cardiac damage has progressed significantly.

Nilsson et al demonstrated a four- to sevenfold increased risk of stenosis in the coronary arteries post left sided BC irradiation with 70% of abnormalities occurring in the left anterior descending coronary artery (Nillson et al 2012).

Marks et al (2005) found that in 114 left-sided BC patients treated with RT 42% developed new perfusion defects. Up to 70-90% of patients with significant mediastinal radiation exposure can develop pericardial disease (Veinot et al 1996). Furthermore nearly 20% of these patients may have initially have had effusions (Stewart et al 1984). Patients who receive at least 32 Gy of radiation to the heart then upto 81% of patients have been discovered to be suffering from valvular dysfunction and fibrosis (Brosius et al 1981). The aortic and mitral valves are more commonly involved than the tricuspid and pulmonary valves. Conduction abnormalities arise due to micro vascular damage which lead to cardiac myocyte conduction abnormalities or direct damage to critical structures such as sinoatrial or atrio-ventricular nodes. In 200 BC survivors, ECG results showed that the risk of developing conduction abnormalities increased from 19% to 45% at 6 months post RT, T-wave changes were post predominant in this group. The risk remained at 45% 10 year post treatment with the pathology changing to fewer T wave abnormalities but more ST depression and ectopic beats (Strender et al 1986). However unlike other RIHD types, cardiac conduction abnormalities are largely reversible and the peri-myocardial damage indicated is functionally insignificant.

Subclinical myocardial injury is progressive and can develop into HF over time. Therefore, early identification of RIHD is key to minimising the harmful side effects of cancer therapy and would allow clinicians to personalise the programme of cancer therapy for patient's there improving survival

Furthermore, it is imperative to recognise that RIHD may be detectable within a matter of days to months post RT. It has been found that amongst 200 BC survivors, a significant percentage had conduction abnormalities at both 6 months and 10 years after treatment (Taunk et al 2015). Pericarditis may develop over a period ranging from a few months to few years with a typical presentation at 12 months (Madan et al 2015). Importantly asymptomatic pericardial perfusion is the most common mode of presentation for the development of

delayed pericarditis (Zhuang et al 2017). Perfusion defects of the heart have been shown to be evident in 50% to 63% of patients 6 to 24 months after RT (Darby et al 2013). Gayed et al have further supported these findings by demonstrating 27%, 29%, 38%, 42% incidence of myocardial perfusion abnormalities in asymptomatic patients with BC at 6, 12, 18 and 24 months after RT, respectively (Gayed et al 2009).

Due to the limited sensitivity and specificity as well as high cost of currently used techniques which may be used to detect RIHD, there is an urgent need for the development of a new non-invasive and cost effective diagnostic biomarker that can be used for the earlier detection of RIHD.

1.3 miRNA biogenesis and function

Small non-coding RNAs (~ 22 nucleotides) known as miRNAs have a critical role in the regulation of mRNA or protein levels through mRNA degradation or attenuation of mRNA translation (Bartel et al 2004). One miRNA can target several mRNAs, and one mRNA can be regulated by several different miRNAs. Up until now more than 2000 mature unique miRNAs have been identified in humans (https://www.mirbase.org) and it is estimated that at least 60% of all mammalian mRNAs are regulated by miRNAs (Friedman et al 2009).

Figure 2demonstrates the process of miRNA maturation and function. The miRNA gene is transcribed under the control of RNA polymerase II (though some can be generated by RNA polymerase III) to generate a primary microRNA (pri-miRNA) precursor molecule that undergoes nuclear cleavage by the RNase III enzymes Drosha in the nuclear and Dicer in the cytosol to form a precursor microRNA (pre-mRNA). The pre-miRNA is cleaved in the cytoplasm to create a microRNA duplex (miRNA:miRNA*, passenger strand is indicated by asterix) containing the mature miRNA. The duplex unwinds and the guide strand of this duplex associates with RNA-induced silencing complex (RISC) whereas the passenger strand of this miRNA duplex is either degraded or utilised as functional miRNA by the same

cell or exported to another cell (O'Toole et al 2016). The miRNA base-pairs with target mRNA to direct gene silencing via mRNA cleavage or translation based upon the level of complementarily between the miRNA and the mRNA target(Friedman et al 2009).

Figure 2: *Diagram of miRNA maturation and function (see section 1.3 for a detailed description)(Friedman et al 2009).*

Both the miRNA sequences and the miRNA-processing are evolutionary conserved, indicating the critically important role of miRNAs in biological function (Bartel et al 2004; Zhao et al 2007).

1.3.1 miRNAs are involved in biological processes including cardiovascular disease development

miRNAs participate in many cellular processes, such as apoptosis (Xu et al., 2007), fat metabolism (Xu et al 2007), cell differentiation (Chang et al 2008), tumourigenesis (Zhao et al 2007), cardiogenesis and angiogenesis (Zhao et al 2007).

In the cardiovascular system, miRNAs have been shown to be critical regulators of development and physiology. They control basic functions in virtually all cell types relevant to the cardiovascular system (such as endothelial cells, cardiac muscle, smooth muscle, inflammatory cells, and fibroblasts) and therefore are directly involved in the pathophysiology of many cardiovascular diseases. As a result of their role in disease, they are being studied for exploitation in diagnostics, prognostics and therapeutics.

Interestingly, the promoters of RNA polymerase II often containing toxicologically significant enhancer regions, indicating that miRNAs play a role in response to cellular stresses and gene changes following exposure to toxic substances. It has already been shown that ionising radiation induces oxidative stress hence altering expression of miRNAs (Friedman et al 2010).

1.3.2 miRNAs as ideal biomarker candidates

An ideal diagnostic biomarker has to fulfil a number of criteria, such as accessibility through non-invasive methods, high-specificity indicating myocardial origin, a reliable indication of early detection of the disease before clinical symptoms appear, high-sensitivity to changes in pathology: disease progression or therapeutic response, and they must be robust and translatable (Vasan et al 2006). As with all healthcare services, clinical effectiveness has to be balanced with cost and it essential for an ideal biomarker to be cost effective and also offer high-throughput testing such that the test can be performed simply and quickly and results should be available in a timely manner.

miRNAs resemble the characteristics of an ideal biomarker incredibly well. Advantageously, miRNA sequences are stable in a variety of different body fluids, such as blood plasma and serum (Mitchell et al 2008), urine (Dimov et al 224), saliva (Michael et al 2010), amniotic fluid and pleural fluid (Gilad et al 2008). In 2008 it was discovered that miRNAs are also present in blood where they were found in plasma, erythrocytes, platelets and nucleated blood cells (Chen et al 2008). Stability of miRNAs is due to protection from degradation by ribonucleases, RNA-binding proteins and lipid vehicles (Valadi et al 2007). Importantly as discussed below miRNAs are tissue/fluid, disease type and stage specific (Etheridge et al 2011). Furthermore, it is viable to detect homogenous miRNA by quantitative PCR and next generation sequencing. All of the above discussed qualities make miRNAs thus a very attractive diagnostic biomarker (Mitchell et al 2008).

The introduction of a reliable early-stage miRNA biomarker for RIHD would allow clinicians to introduce preventative adjunct therapy to protect the heart at an earlier stage, thus limiting and stopping heart disease progression. Furthermore, clinicians could tailor anti-cancer therapy regimes for BC patients in a more personalised manner reducing risk of cardiotoxicity. This would undoubtedly improve the quality of life and increase the survival of BC patients.

1.3.3 Fluid- and tissue- specificity of cardiac miRNAs

Plasma miRNAs were found to be remarkably stable even under conditions as harsh as boiling, low or high pH, long storage at room temperature and multiple freeze thaw cycles (Mitchell et al 2008).

miR-208a and miR-499 are expressed specifically in heart tissue (van et al 2007; Adachi et al 2010), whereas miR-1 and miR-133 have been found in injured skeletal muscle (van et al 2009; Chen et al 2006). These miRNAs which are highly expressed in cardiac muscle have been noted to be involved with heart development and myocyte differentiation (Zhao et al 2007; Liu et al 2007).

It has also been noted that miRNAs are differentially expressed depending upon on the various compartments of the organ. For example it has been noted that the arteries of the heart express a different miRNA profile than the heart, suggesting a cell-type-specific miRNA expression profile. Cardiac muscle cells express miR-30c, miR-1 and miR-133 (Lagos-Quintana et al 2002). Coronary atrial smooth muscle cells express miR-1, miR-133, miR-125a, miR-145 and miR-143 (Schmidt et al 2007). In contrast coronary atrial endothelial cells express miR-126, which is responsible for controlling angiogenic sprouting of aortic arch vessels (Nicoli et al 2010).

The presence of miRNAs in microparticles has intrigued the idea that circulating miRNAs could have a role in cell to cell communication. This would further suggest that miRNAs are selectively targeted for secretion in one cell and taken up by a distant, target cell, possibly in order to regulate gene expression. Subsequent studies have revealed that miRNAs may indeed function as mediators of cell to cell communication (Zhang et al 2010).
miRNAs can be readily accessed in body fluids and based on the above it is unsurprising that in HF similar responses in miRNA levels in the circulation and in myocardial tissue have been observed. For example Tijsen*et al. (2010).*found higher levels of miR-423-5p in both circulation of the heart failure patients and in post mortem samples of patients suffering from dilated cardiomyopathy (Tijsen et al 2010). However it is certain that potential miRNA targets need to be further scrutinized for their true clinical value with respect to cardiovascular disease, especially as there is much debate over which targets may actually be of use. For example the group of *Vogel et al.* (2013) found that miR-423-5p was not significantly dysregulated in whole peripheral blood of HF patients with reduced ejection fraction. It should be noted that *Tijsen et al*. (2010) measured miRNAs from plasma samples whilst *Vogel et al. (*2013) assessed whole peripheral blood samples. The advantage of analysing miRNAs in whole blood peripheral samples is that tissue-related miRNAs can be sought and a more wholistic view of miRNAs from all circulating cells can be obtained.

1.3.4 miRNAs are cardiac development stage specific

Functional miRNA studies reported that a variety of miRNAs play a role in pathogenic mechanisms leading to heart failure, such as remodelling, hypertrophy, apoptosis, and hypoxia (Tijsen et al 2012). Furthermore, in response to the progression of heart failure, miRNAs were shown to behave in a dynamic and stage-specific way. For example, decreased levels of miRNAs (including miR-1 and miR-133a) were found before development of disease (Ji et al) while an increasing number of miRNAs exhibited a dysregulated and mainly up-regulated pattern in the later stages towards end-stage heart failure (Mitchel et al 2008). Others demonstrated that the aetiology of heart failure (ischaemic, aortic stenosis, or idiopathic cardiomyopathy) was associated with differentially expressed miRNA patterns (Ji et al 2007). Thus, compelling evidence suggests that miRNAs play an active role in the onset and progression of heart failure.

1.3.5 miRNAs in the developing and healthy adult heart

miRNAs have been identified in cardiac tissue at all stages of development and those highly expressed in the foetal heart include miR-21, miR-29a, miR-129, miR-210, miR-211, miR-320, miR-423, and let-7c (Thum et al 2007). The critical role of miRNAs during embryonic and postnatal cardiac development has been established in the literature.

In the healthy adult heart it has been established that a huge number of miRNAs which are highly expressed in non-diseased cardiac tissue, are likely to play a key role in both normal cardiac maintenance and disease development. These include miR-1, miR-16, miR-27b, miR-30d, miR-126, miR-133, miR-143, miR-208 and the let-7 family(Bartel et al 2004; Thum et al 2008).

1.3.6 Cardiac disease specific miRNA expression

The next section focuses upon key cardiac injury specific miRNAs, which are involved in specific heart diseases.

1.3.6.1 miRNAs in Acute Myocardial Infarction (AMI) patients

It has been demonstrated that measuring miR-1 in plasma is a good approach for blood-based detection of AMI in patient as they correlated well with infarct size (Ai et al 2010; Cheng et al 2010). Also increased miR-1 is well correlated with abnormal electrical activation in AMI patients, and after treatment plasma miR-1 recovered to normal value (Taurino et al 2010).

A miRNA microarray study demonstrated that mIR-1, miR-133a, miR-499 and miR-208a were elevated in the plasma from 33 AMI patients compared to as well as healthy subjects, patients with non-AMI coronary heart disease or patients with other cardiovascular diseases. This study demonstrates a specific nature of miRNA to differentiate between different subtypes of cardiovascular disease. Notably, within 4 h of the onset of symptoms, miR-208a was easily detectable in AMI patients, but remained undetectably in non-AMI patients (Wang et al 2010). However the study by D'Alessandra et al showed miR-208a to not be detectable at all in AMI patients. This could have been due to two reasons. Firstly D'Alessandra et al collected samples approximately 9 hours post AMI onset whereas Wang et al collected them sooner at 4 hours post onset. All miRNAs have different times at which they peak depending on the type of initiation or response they are involved in with respect to myocardial injury and repair. For example it is known that miR-208a levels peak within the first 2 hours post injury which could explain why the study by D'Alessandra et al failed to detect any miRNA. Furthermore, the methods used to detect miRNA between the study of D'Alessandra and Wang et al differed. Thus when interpreting miRNA findings the timing of sample collection and method utilised appear to be crtitical factors in establishing differential regulation patterns and must be critiqued to truly establish the clinical utility of candidate markers. Also, Adachi et al pointed out that very low levels of mIR-208a and mIR-208b exist in human hearts thus deeming it as an unsuitable marker of myocardial injury in humans due to it not being particularly involved in normal human heart and development. Therefore it is

important to only recognise and take those miRNA candidates forward in research where possible which have an organ- disease and tissue specific origin.

Devaux and colleagues reported that a panel of four miRNAs (miR-16, miR-27a, miR-101, miR-150) improved the prediction of left ventricle contractility six months after AMI, in a multivariable model that included NT-proBNP, an established biomarker of heart failure (Devaux et al 2013). These findings built upon their previous demonstration that reduced levels of miR-150 levels were associated with increased left ventricle remodelling after ST segment elevation myocardial infarction and herald promise in the use of miRNAs, or panels of miRNAs, as diagnostic and prognostic predictors of heart failure.

1.3.6.2 miRNAs in Heart Failure (HF)patients

Plasma levels of heart-muscle enriched miR-1, miR-133a, miR-208b, mIR-499; fibrosis associated miR-21, miR-29b, and leukocyte associated miR-146, miR-155, miR-223 have all been tested as candidate biomarkers of HF (Corsten et al 2010). This study demonstrated that in humans, diverse conditions of myocardial damage are associated with striking perturbations of plasma levels of cardiac miR-208b and miR-499 in acute HF (minimal), viral myocarditis (marked) and AMI (extensive). An intriguing observation was the correlation of miR-133a plasma levels with BNP in asymptomatic patients with diastolic dysfunction, which was not observed in acute HF patients. Corsten et al supported these findings by showing that expression of miR-208b, miR-499, miR-1 and miR-133a in acute HF patients. They found that the expression of all four of these myocardial injury miRNAs were elevated in acute HF patients (Corsten et al 2010). However in interpreting the significance of these findings it must be remembered that this study utilised incredibly small N numbers thus reducing the statistical power of the findings. This study recruited only 32 AMI patients, 39 patients with diastolic dysfunction and 33 acute heart failure patients which is not a substantial enough sample size to ascertain strong statistical significance. Furthermore acute heart failure can be the result of a huge range of cardiac abnormalities including valvular complications, arrhythmias, and coronary artery disease. It was unclear from this

study the exact causes of the congestive heart failure in the patients the study focused upon and certainly larger studies focusing one each cause of heart failure would be necessary to be confident that these miRNAs do indeed play a role in acute heart failure.

1.3.6.3 miRNAs in Coronary Artery Disease (CAD) patients

Plasma miRNA are also differentially regulated in CAD patients. Analysis in patients with stable CAD revealed that myocardial-injury-specific miR-133 and miR-208a were up regulated, whereas inflammation associated miR-155 and smooth muscle enriched miR-145 were down regulated (Chen et al 2006). It has been shown that circulating miR-155 and miR-145 are also decreased in cases of CAD and could act as diagnostic biomarkers of coronary artery disease (Bartel et al 2004)

1.3.6.4 miRNA in Hypertension and Atherosclerosis patients

Numerous studies have been conducted to detect circulating miRNAs implicated in hypertension patients. The results indicated that the plasma miR-505 was significantly elevated in essential hypertensive patients, thus circulating miR-505 maybe a circulating biomarker for hypertension (Ji et al 2007).

A recent study also identified several novel up-regulated miRNAs (miR-23b, miR-130a, and miR-191) and down-regulated miRNAs (miR-451 andmiR-1246) in the circulation of patients suffering from pulmonary hypertension (PH) (Wei et al 2013). Another research also found that reduced miR-150 was closely associated with poor survival in pulmonary hypertension patients (Rhodes et al 2013). Furthermore, Santovito et al have shown that miR-145 is over-expressed in atherosclerotic plaques of hypertensive versus normotensive patients undergoing carotid endarterectomy, implicating miR-145 as a potentially key regulator of blood pressure mediated vascular damage (Santavito et al 2013).

1.3.6.5 miRNA in Fibrosis and Arrhythmia

The miR-29 family has been implicated in cardiac fibrosis following a report showing down-regulation of miR-29 family, miR-29a, miR-29b and miR-29c in the border of human hearts during MI. Multiple target genes of the mIR-29 family were identified including extracellular membrane proteins, such as collagens, fibrillins, and elastin and it was speculated that transforming growth factor (TGF-β) mediated down regulation of miR-29 would enhance fibrosis (van Rooji et al 2008). Furthermore, it has been shown that miR-1 levels are markedly reduced in atrial tissue of patients with atrial fibrillation compared to those patients without (Liao et al 2016).

1.3.7 miRNAs in aiding cardiomyocyte cell survival

It has been noted in the literature that miR-144/451 individually augment cardiomyocyte survival which is further improved by over-expression of both of these miRNAs in response to ischaemia/reperfusion injury (Zhang et al 2010).

1.3.8 miRNAs in response to cancer therapy induced cardiotoxicity

To date there is no study which focuses upon the utility of miRNAs as a marker for RIHD and specifically in the context of left-sided breast irradiated cancer patients.Very few studies have looked upon miRNA expression patterns during chemotherapy-induced cardiotoxicity. For example, it has been noted that plasma miR-29b and miR-499 are acutely elevated (at 6-12h) in cases of anthracycline induced cardiotoxicity amongst children and young patients with leukaemia (Leger et al 2017). Interestingly here too there was a dose response relationships observed with anthracycline dose and markers of cardiac injury. In the plasma of 59 BC patients treated with doxorubicin chemotherapy miR-1 was significantly found to be upregulated in cardiotoxicity-affected patients (Horrie et al 2010)

1.3.8.1 miRNAs in Breast Cancer

It should be noted that in cancer miRNAs play a role in oncogenesis, metastasis and resistance to various therapies and can be classified as oncogenes (oncomirs) or tumour suppressor genes (Ahmad et al 2011). Interestingly, it has been noted that miR-155 promotes proliferation of human breast cancer cells (Zhang et al 2010)

It has also been noted that quantification of certain miRNAs could even be used to predict response to radiotherapy. For example low levels of miR-34a rendered BC cells more resistant to radiotherapy (Kato et al 2009).

It has even been suggested that microRNAs such as miR-21 and miR-34 are very promising new targets for RNA-based therapy in non-invasive and invasive BC (Kaboli et al 2015).

1.3.9 Application of miRNAs in various disease states

It is important to recognise when assessing the potential clinical value of miRNAs that they are not only differentially regulated in myocardial conditions but in a variety of cancers (e.g. lung cancers, gastric cancers, oesophageal cancers), viral diseases, immune related diseases (e.g. diabetes, multiple sclerosis, diabetes), neurogenerative diseases (for example Parkinson's and Alzheimer's disease), and therefore have a role in diagnosis and therapy in multiple disease states (Li et al 2012).

Interestingly to highlight the utility of miRNA in the diagnosis if neurogenerative disease the University of Melbourne Centre of Research, Innovation and Commercialisation have developed a blood test for the early detection of Alzheimer's disease which they are currently commercialising as a patient orderable blood test (Hill et al 2014).

1.3.10 Clinical detection of miRNAs

microRNAs can be detected clinically relatively simply in tissues and tissue fluids using quantitative reverse transcription-polymerase chain reaction (qRT-PCR). With technical advancements, it is now possible to detect low copy numbers of both the precursor and the mature forms of miRNAs with great sensitivity and specificity (Chen et al 2005). With technological advancement and increasing interest, novel analytical approaches for profiling miRNA expression continue to emerge (Srivastava et al 2013).

1.4 Research Area

We hypothesise that RT will result in a signature of differentially affected cardiac injury specific miRNAs and this could potentially be used as a more effective early stage RIHD screening tool. The study will assess cardiac injury specific genomic miRNA substances in the bloodstream to help identify specific mIRNAs which could be used for the earlier identification of RIHD. The long-term goal of this study is to identify a genomic biomarker high throughput screening platform to profile sub-clinical myocardial injury and drug-induced cardiotoxicity and potential use in evaluating agents used to prevent cytotoxic induced injury.

1.4.1 Hypothesis

We hypothesise that RT treatment will result in a signature of differentially affected cardiac specific miRNAs which could then be exploited to identify RIHD at an earlier stage.

1.4.2Aim

The work aims to evaluate whether miRNAs which have been previously linked to cardiac damage are differentially expressed in BC patients receiving left sided RT

1.4.3 Objectives

1. Undertake miRNA assessment for cardiotoxicity in the circulation following RT in left sided RT treated patients where risk of cardiotoxic damage is the greatest compared to right-sided RT.

2. Compare miRNA expression profiles in patient over various time points of RT to see changes across time. Time points to investigate include Time point A (pre-RT), Time point B (24-72h from final fraction of treatment), Time point C (3 months post RT) and Time point D (6 months post RT).

3. Compare the sensitivity and specificity of miRNAs to traditional proteomic biomarkers (such as Troponin I and BNP) and CMR.

Section 2. Materials and Methods

2.1 Ethics Statement

This study was performed in accordance principle of the Declaration of Helskinki as well as adhering to the requirements of good clinical practice (GCP). This study has gained the relevant ethical approval from each partner institution including Coventry University (CU), Oxford University Hospital NHS Foundation Trust (OUH NHS Trust) and Health Research Authority (HRA). Written informed consent was obtained from all patients before blood sample and imaging collection.

Ethical Approval Number: OUH NHS Trust and HRA- 09H060483; CU- P46798. Please find ethics approval confirmations from Coventry University and OUH NHS Trust attached to the front of the thesis.

2.2 Patient Population and Inclusion criteria

This study recruited samples from a larger research study which focused on the utility of imaging in the detection of RIHD at an earlier stage in low radiation dose treated left sided BC women based on availability of samples across all 4 time points as mentioned in section 2.4. This larger study was conducted at Oxford University Hospital NHS Foundation Trust. This study had previously revealed that CMR imaging was in agreement with troponin and BNP findings in that none of the patients had developed RIHD at 6 months post their RT. A total of 15 low-dose radiation treated left-sided BC women from the larger study were recruited to this current study. The 15 women whose date and samples were used all had had early stage BC or Ductal Carcinoma in Situ post breast-conserving surgery treated with low dose left sided RT and had been treated at the Cancer Centre, Oxford University Hospital NHS Foundation Trust. These patients were routinely treated in accordance with Trust Approved RT Guidelines in line with those recommended by the National Institute of Clinical Excellence (NICE 2009) on the Early and locally advanced BC: diagnosis and treatment. Mean dose to the whole heart ranged from 0.6–2.8 Gray of radiation.

2.2.1 Exclusion Criteria

Women who were <18 or 65> years, adjuvant cytotoxic chemotherapy, previous significant heart disease, diabetes, oestrogen receptor positive tumours receiving hormone therapy were all excluded from this study.

2.3 Radiotherapy planning and delivery

The prescribed dose was 40 Gy in 15 fractions, 5 fractions per week, prescribed to a normalisation point in the centre of the breast, with 50 Gy in 25 fractions used for exceptional cases (women with very large breasts). A boost dose of 10 Gy in 5 daily fractions was given where indicated, using electrons of appropriate energy to a clinically defined tumour bed.

2.4 Blood Sample Collection and Analysis

Blood samples in EDTA tubes would be obtained at each time point A, B. C and D. Where:

- A = baseline pre-RT
- B = 24h-72h immediately after first RT Dose
- C = 3 months post-final fraction of RT
- D = 6 months post-final fraction of RT

EDTA blood samples were then processed for plasma within 1 hour of collection. Blood was centrifuged at 3000g for 20 minutes at 10˚C, followed by further centrifugation of the supernatant at 15000g for 10 minutes at 10˚C to remove the cell debris. Plasma samples were then analysed for Troponin and BNP using an Abbott Architect analyzer in the routine biochemistry laboratory. After this the samples were aliquoted into tubes, labelled and stored at -80˚C in preparation for miRNA analysis. MRI scans would also be performed where routine measurements and more sophisticated measures on MRI provided information on the structural integrity of the heart and assessment of ventricular function

including (i.e. Ejection fraction (EF), stroke volume, left ventricular end systolic volume and left ventricular end diastolic volume).

Information that was available to this study included amount of radiation dose, Troponin value, BNP value, stroke volume, ejection fraction at each visit. Unfortunately data surrounding more intricate measures of cardiac magnetic resonance from the larger study as well as details of co-morbidities were not available to this study. However all medical histories were reviewed by clinicians to ensure appropriate inclusion utilising the patients' medical records and therefore the inclusion and exclusion criteria strictly applies to this patient cohort.

2.5 List of Consumables and Suppliers

RNaseZAP (Ambion), Qiagen RNeasy Mini Kit inclQIAzol(Qiagen), MS2 RNA (Roche) Chloroform (Ambion), microRNA primer assays (Thermofisher Scientific), Applied Biosystems TaqMan microRNA Reverse Transcription Kit- (Thermofisher Scientific), TaqMan Universal PCR Mastermix (Thermofisher Scientific).

2.6 miRNA extraction from plasma

Total RNA was extracted from 1000 ml of plasma with the miRNeasy Mini Kit (Qiagen) and the modified Exiqon protocol explained below which includes the addition of MS2 RNA (Roche), a carrier RNA that ensures the highest and also the most consistent yield of RNA in the samples. All plastic consumables handling the plasma samples were RNase free and tips were in addition with filters. The samples were handled with gloves sprayed with RNaseZAP (Ambion) in order to reduce the spread of RNase. A volume of 0.5 ml plasma was defrosted for each patient in time points A, B, C and D totalling a sample volume of 0.5ml. Samples were transferred into 2.0 ml tubes appropriately labelled and spun at 1000 g for 5 minutes at 4˚C in order to remove the cell debris. Plasma was carefully transferred into

fresh 2 ml tubes avoiding the debris. To each plasma sample 5 µl of MS2 RNA and 1ml of Qiazol was added. This mixture was then vortexed and allowed to stand at room temperature for 5 minutes. To each sample 500 µl of chloroform was added. During the uptake of chloroform, the pipette was fully compressed upon entering the acid phenol: Chloroform solution (piercing through the phenol layer which is used to neutralize and suppress the action of the chloroform) producing bubbles visible to the eye and where uptake of the solution could be visualised. The samples were once again vortexed and allowed to stand for 2 minutes at room temperature after which point the samples were spun down at 14000 RPM for 20 minutes at 4˚C. At this stage centrifugation resulted in the formation of distinct layers within the sample; the upper phase containing RNA, and the interphase and lower phase. Only the upper aqueous containing the RNA was carefully extracted and transferred to fresh RNAase free collection tubes leaving a small layer on the interphase line to prevent the phases being disturbed and therefore contaminating the isolated RNA. In the proportion of 50µl upper phase to 1150µl ethanol was added to each sample. RNeasy Mini Spin columns were labelled with patient number and time point. A total of 750µl of lysate/ethanol mixture and successive applications from the same patient sample and time point were made to the filter until all the sample was used up. Once complete, 700 µl of RWT was solution was added to the filter cartridge and centrifuged followed by three-times500µl RPE wash solution. Samples were centrifuged at 14000 RPM for 1 minute at 4 ˚C and the flow-through was discarded until all the lysate/ethanol/wash buffer mixture was washed through the filter. Following the last wash the filter cartridges were transferred back into fresh collection tubes and centrifuged at 14000 RPM for 1 minute at 4 ˚C in order to remove the residual fluid from the filter. After the filter had dried for 1 minute at RT 50µl of nuclease free water from the Qiagen Kit was used and added to the centre of the membrane. This was incubated for 1 minute and then spun at 14000 RPM for 1 minute at 4 ˚C in order to recover the RNA. The resulting eluate was stored at -20˚C in preparation for real time PCR analysis.

2.7 NanodropQuanitification

The extracted RNA concentration and purification was determined via the ND 1000 Spectrophotometer (Thermo Scientific USA). RNA-40 sample type was selected prior to analysis on the analyser, and the analyser was blanked prior to each reading using 1 µl of RNAse free water on the Nanodrop pedestal and run in order to calibrate the spectrophotometer. Sample purity was observed via the A260/280 and A260/230 ratios.

2.8 Reverse Transcription PCR (RT-PCR)

A total of 1800ng of miRNA was reverse transcribed into cDNA for U6, miR-1, miR- 27a, miR-133a, miR-133b, miR-29b, miR-30a, miR-144, miR-451, miR-505 and miR-208a via the microRNA Reverse Transcription Kit. These specific miRNAs were chosen for investigation due to their involvement in both normal cardiac development as well as changes in expression patterns in both acute and chronic cardiac disease states ranging from AMI to heart failure as discussed in the introduction. The miRNAs were also chosen due to varying times of expressional changes post cardiac injury ranging from hours to months in order to capture changes in our own sample population which ranged from 24 hours post radiation up to 6 months. The reverse transcriptase mastermix was produced as shown in Table 1.

Table 1: *Volume (µl) for reverse-transcriptase master mix constituents needed for 1 reaction.*

Reverse Transcriptase Mastermix	Volume for 1 reaction (µl)
Enzyme	3
dNTPS	1
Inhibitors	1
Buffer	7.5
Specific primer sets	1.5 each
H_2O + miRNA	43

Samples were diluted with 75 µl of H2O after RT-PCR.

The reverse transcriptase PCR reaction was performed using the master cycler gradient via the following set up; 16˚C for 30 minutes, 42˚C for 30 minutes and 85˚C for 5 minutes. This reaction resulted in the production of cDNA.

2.9 Real Time PCR

Upon preparation of the cDNA, the real time PCR reaction was performed as shown in Table 2.

Table 2: *Volume (µl) for real-time PCR master mix constituents needed for 1 reaction.*

Real Time PCR mastermix	For 1 reaction (µl)
Taqman	10
Specific Primer	0.5
H2O	4
cDNA	5.5

14.5µl of the Real Time Mastermix (Taqman, Primer and H_2O) mixture would be aliquoted into each well and 5.5µl of the prepared cDNA was added.

The cDNA samples were carefully loaded in duplicates with the pipette tips carefully changed in order to prevent any contamination. Once prepared in the configuration shown below the PCR plates were gently centrifuged for 1000 RPM for 1 minute at 4 °C to ensure all the sample content migrated to the bottom of the well.

The real time PCR process was utilised using 1800ng of starting cDNA alongside the specific primer sets and a standard Taqman Universal PCR mastermix (as per the manufacturer's instructions) on the CFX Connect Real Time PCR system (BioRad, USA). The real time PCR sequence detection software CFX manager (Applied Biosystems USA)

was used to monitor the amplification of DNA by means of real time optics and imaging via the binding of SYBR green fluorescent dye to double stranded DNA.

The real time PCR thermal cycling reaction was programmed to run at 50 °C for 2 minutes, 95 °C for 10 minutes and then 40 cycles of 95˚C for 15 seconds followed by 60˚C for 1 minute.

The cycle threshold values for all patient time points were compared to U6 snRNA which was used as an internalised reference.

2.10 Statistical Analysis

CT data obtained from the above was initially entered and analysed using Microsoft Excel whereby the mean, average, standard derivation (SD), Standard error of mean (SEM) was calculated . Analysis of the miRNA data was performed using the comparative ΔΔCT method. Relative quantities of miRNAs were calculated using the CT values obtained via Real-Time PCR analysis of target miRNAs: miR- 1, miR-27a, miR-133a, miR-133b, miR-29b, miR-30a, miR-208a, miR-505, miR-144, miR-451 and miR-505) in relation to the U6 snRNA values in the sample via the following formula:

$X0/R0=2^{CTR-CTX}$

Where *X0* is the original amount of target miRNA, *R0* is considered the original amount of U6 snRNA, *CTR* is the CT value for U6 snRNA, and *CTX* is the CT value for the target miRNA. The average miRNA sample ratio values was calculated for each time point. Any samples which were 5-fold above or below the mean were discarded. A prospective statistical power calculation revealed that a larger N number was needed of at least 30 samples per time point. A total of 15 subjects were recruited into this study and generally N numbers between 7-12 were included once outliers had been discarded miRNA analysis. Though the N numbers in this study did not meet the requirement for statistical power the main reason for this was that the study relied upon samples being available across all 4 time points from the larger CMR imaging study which unfortunately was the case for only 15 patients.

The miRNA ratio values produced from the formula were further analysed graphically using GraphPad PRISM. GraphPad Prism was initially used to construct graphs of average changes in expression levels of miRNA over the 4 time points (A, B, C and D). One-way ANOVA test was used in GraphPad prism based upon the above ratios to determine significant expression differences between points: A-B, A-C, A-D, B-C and C-D where significant differences $P<0.05$. In addition a student's T-test was used to compare A and D (RT treatment start and end-points), where significant differences were considered at p-values <0.05 (* = $p<0.05$, ** = $p<0.01$ and *** = $p<0.001$).

Section 3: Results

3.1 Experimental Design Summary

A total of 15, left sided RT treated subjects were taken through the experimental design shown in Figure 3 below in the order in which they were obtained are described below.

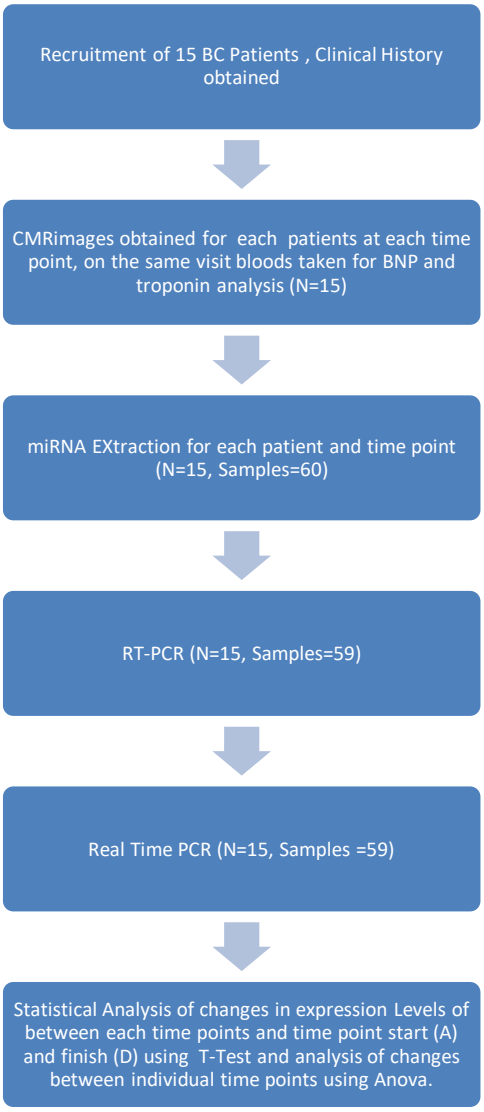

Figure 3: *Demonstration of the experimental process. Each of the 15 BC patients recruited into the study were taken through the above experimental design process.*

3.2 Characteristics of the 15 BC patients

The mean age of patients was 56.8 years with the lowest age being 41 and the highest age being 62. Cardiac risk factors within some but not all of these patients included smoking (both current and previous), hypertension, hypercholesterolaemia, and a family history of previous cardiac disease.

3.3 Cardiac Radiation Dosimetry

The mean dose to the whole heart, left ventricle, and left coronary artery was 1.4 Gy, 2.0 Gy, and 6.6 Gy, respectively. The maximum dose given to the whole heart, left ventricle and left coronary artery was 32.89 Gy, 30.18 Gy, 30.50Gy respectively.

3.4 Troponin and BNP Analysis

All patients has normal levels of Troponin I, below the limit of detection for the assay (<0.04 µg/L) at all time points as shown in table 3. Any result greater than 0.04µg/L is deemed to be indicator of ischaemic heart disease. Even a slight increase is deemed to be clinically significant especially for acute episodes such as AMI.

Table 3: Troponin values for all patients across the 4 different time points A to D. There were no significant changes in the expression of Troponin values for any patient.

Troponin Levels (ug/L) over time points				
	A	B	C	D
1	<0.2	<0.2	<0.2	<0.04
2	<0.2	<0.2	<0.04	<0.04
3	<0.04	<0.04		<0.04
4	<0.04	<0.04	<0.04	<0.04
5	<0.04	<0.04	<0.04	<0.04
6	<0.04	<0.04	<0.04	<0.04
7	<0.04	<0.04	<0.04	<0.04
8	<0.04	<0.04	<0.04	<0.04
9	<0.04	<0.04	<0.04	<0.04
10	<0.04	<0.04	<0.04	<0.04
11	<0.04	<0.04	<0.04	<0.04
12	<0.04	<0.04	<0.04	<0.04
13	<0.04	<0.04	<0.04	<0.04
14	<0.04	<0.04	<0.04	<0.04
15	<0.04	<0.04	<0.04	<0.04

All measures of BNP were also normal (0.6-28.9 pmol/L) as shown in Table 4. Transient changes in BNP were considered clinically insignificant. BNP levels greater than 236 pmol/L are considered to be an indicator of HF. Raised levels greater than 47 pmol/L are considered to be an indicator of acute ischaemic heart disease.

Table 4: *BNP values across all 4 time points for each individual patient. There were no significant changes in BNP levels for any of the patients.*

Changes in BNP Levels (pg/ml)					
Patient	A	B	C	D	Changes
1	17.0	27.6	33.8	20.1	+3.1
2	3.5	7	6.4	2.5	-1.0
3	1.6	2.5		2.6	+1.0
4	9.3	14.3	12.7	15.6	+6.3
5	11.4	2.1	4.6	7.5	-3.9
6	12.8	3.8	9.8	8.8	-4.0
7	4.6	0.9	2.6	4.1	-0.5
8	8.2	6.7	3.1	5.5	-2.7
9	2.1	<0.6	3.8	0.7	-1.4
10	13.8	2.4	3.8	1.8	-12.0
11	13.8	4.8	7.5	6.5	-7.3
12	2.6	4.8	2.7	3.1	+0.5
13	5.0	4.3	5.2	3.3	-1.7
14	4.7	5.7	4.2	3.9	-0.8
15	24.4	12.4	30.6	18.4	-6.0

3.5 Cardiovascular Magnetic Resonance Results

A consultant cardiologist was responsible for reviewing the CMR images who was blinded to the study and the dose of RT received by the patients however was informed that the patients were part of the research study.

There was no evidence of any change in basic indices of left ventricle function between the time points studied. A normal EF of greater than 55% is usually considered as normal. The EF readings for all of the patients remained normal across all 4 time points (n=15) as shown in Table 5 and Figure 4.

Table 5: *Ejection fraction values for all patients from time points A to D (n=15). There were no changes for EF for any of the patients.*

Ejection Fraction (%)					
Patient	**A**	**B**	**C**	**D**	Change in EF from onset (%)
1	82	83	81	81	-1
2	74	74	78	82	+8
3	73	75	70	78	+5
4	76	75	75	74	-2
5	77	79	80	81	+4
6	81	79	74	79	-2
7	68	65	64	63	-5
8	62	66	70	64	+2
9	79	73	77	75	-4
10	73	76	74	68	-5
11	79	72	75	72	-7
12	75	73	72	75	0
13	71	72	66	67	4
14	79	79	76	79	0
15	77	83	74	76	-1

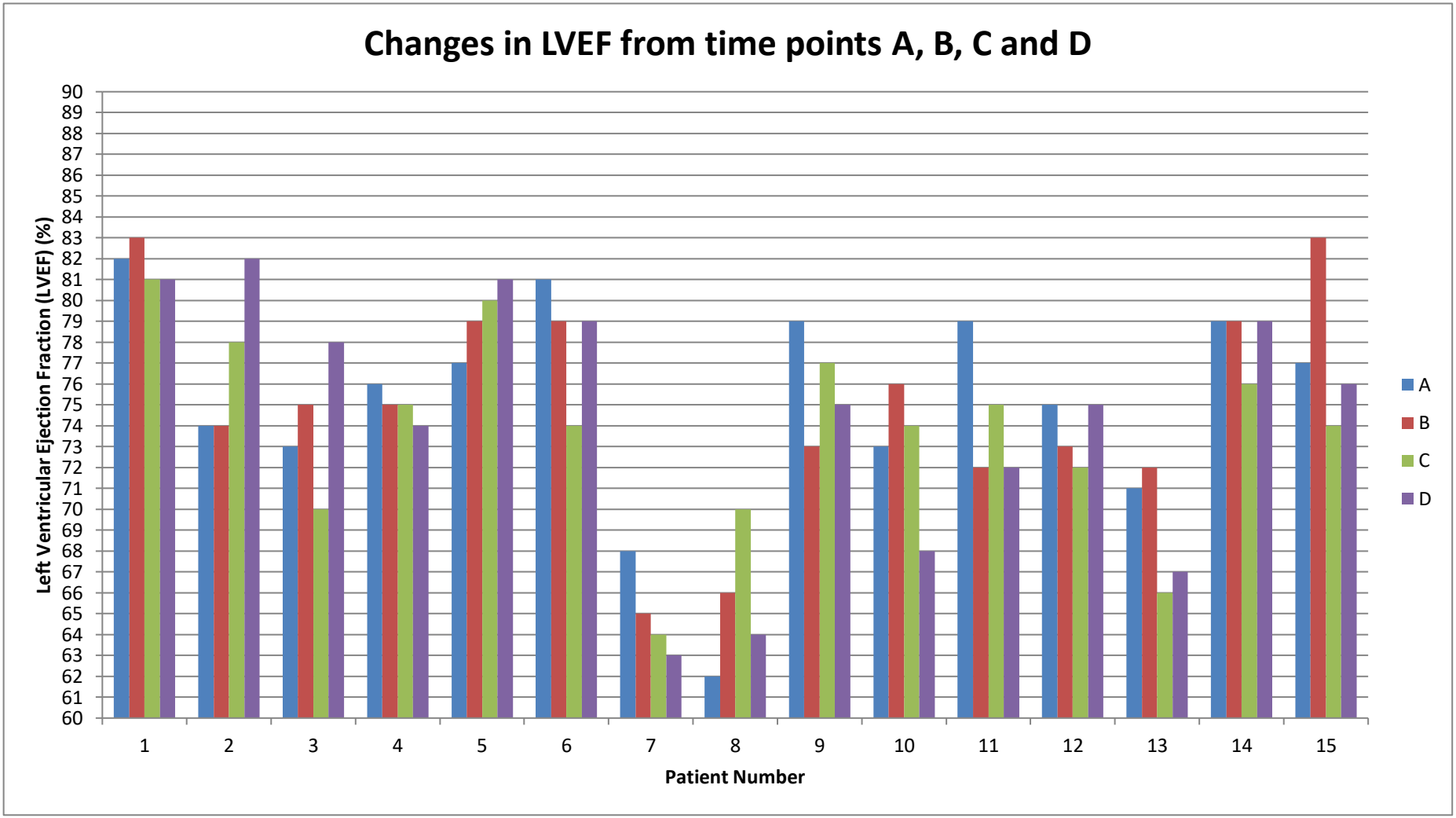

Figure 4*: Graphical demonstration of the changes in EF over the course of the 4 time points A to D. All the patients had normal EF readings during the course of the study, no patient changed from normal to abnormal EF readings to slight individual EF variations between patient visits was seen (n=15).*

A normal stroke volume is deemed to be between 50ml-100ml /beat (Vella et al 2005). No patients had any significant changes in stroke volume post-RT as shown in table 6.

***Table 6**: Stroke volume (ml/beat) readings for all patients over time points A to D (n=15). There were no significant changes in stroke volume for any of the patients from start to the end of radiotherapy*

Time Points					
		A	B	C	D
Patient	**Age**	**SV (ml/beat)**	**SV (ml/beat)**	**SV (ml/beat)**	**SV (ml/beat)**
1	61	77	79	77	86
2	52	111	111	116	108
3	61	78	84	71	87
4	62	83	79	88	91
5	60	107	115	116	115
6	58	90	101	93	84
7	55	93	78	77	71
8	61	75	80	102	77
9	61	91	88	95	74
10	52	105	118	121	87
11	58	101	83	98	77
12	57	87	81	67	73
13	41	86	95	84	82
14	52	81	91	83	91
15	61	85	87	66	88

3.6 miRNA values and RT-PCR

miRNA purification analysis using Nanodrop Spectrophotometer

The nanodrop technique is used to quantify the purification quality. Purines and pyrimides in nucleid acids usually show a peak absorbance at 260nm whereas proteins and phenolic compounds absorb UV light near 280nm.

The 260/280 ratio specifies the purity of the nucleic acid.The RNA extraction was considered pure and free from contamination if this ratio was ~2.0, which is reflected by the 260/280 ratio. Furthermore, absorbance measured at 230nm is a result of concomitants such as

phenol, guanidine and other buffers such as QIAzol. Therefore, the 230/260 ratio is utilised as a secondary measure of the nucleic acid purity, and the values obtained for ‘pure’ nucleic acid are generally greater than the respective 260/280 ratios with expected values ranging generally in the range of ~2.0-2.2. Where the value is appreciably lower than expected, it is there that contamination is suspected.

Initially, 1µl of RNase was free water was pipette onto the measuring pedestal of the ND-100 Nanodrop to both zero and calibrate the Nanodrop to ensure the analyser was functioning and the RNase free water was not contaminated. After which, the miRNA samples were then successively pipette onto the Nanodrop ND-100 measuring pedestal following vigorous scraping of the surrounding Eppendorf walls of the sample via the pipette tip, dislodging and exposing the residual RNA. A spectrophotometric reading was drawn following the sample measurement between 2 optic fibres

3.7 Total RNA

The total RNA (including miRNA) concentration values using Nanodrop spectrophotometer ranged from 20.4-268.4 ng/µl.

The diluted concentrations of the miRNA samples ranged from 6.7-44ng/µl.

Due to sample insufficiency, the miRNA concentration could not be quantified in sample 11B. Of the samples that presented protein purity (260/280), all of the samples were considered around the acceptable pure range, contrasting with the 260/230 ratio where fewer samples were considered free of organic compound contamination.

A peak of 230nm was seen in most samples. Figure 5, showing sample 32D, demonstrates an example of the contamination peak seen at 230nm. Contamination as a result of phenol and QIAzolwas seen in most samples.

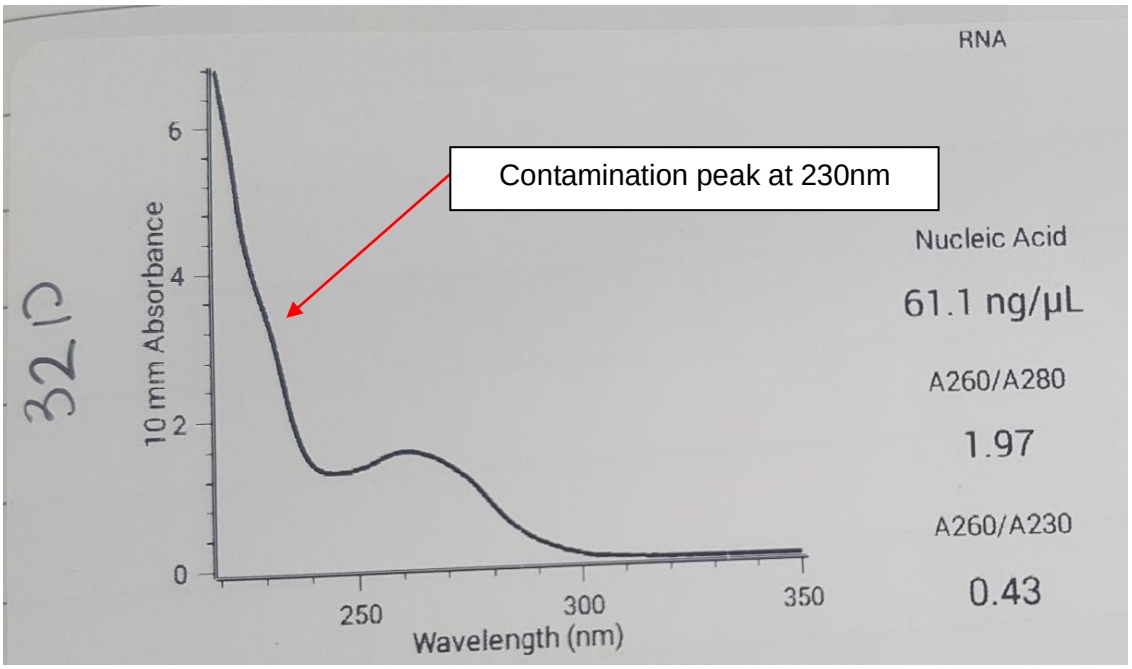

.***Figure 5:*** *Nanodrop profile of sample 32D showing a peak at 230nm. This peak was a result of contamination of phenol, guanidine and QIAzol buffer. The red arrow indicates the presence of the contamination peak.*

The concentration of total RNA and of the diluted miRNA samples retrieved from Nanodrop spectrophotometer is shown in Table 7, the purity levels are indicated by the 260/280 and 260/230 ratios.

Table 7: Purity Levels for all samples.*Sample purity levels indicate good quality sample purity levels however the 260/230 ratio values for each sample do indicate contamination as a result of phenol, QIAzol*

.

Patient	Extraction date	ng/ul	A260/A280	A260/A230	1800ng miRNA	H2O (Vt44.5)
2A	20170307	78.8	1.89	1.08	22.8	21.7
2B	20170307	60	2.03	1.18	30.0	14.5
2C	20170307	54.9	2.05	1.5	32.8	11.7
2D	20170307	268.4	2.11	2.19	6.7	37.8
7A	20170307	71.1	1.89	1.05	25.3	19.2
7B	20170307	66.6	2.04	1.75	27.0	17.5
7C	20170307	47.9	2.05	1.89	37.6	6.9
7D	20170307	53.1	2.01	1.52	33.9	10.6
11A	20170307	51.4	2.03	1.95	35.0	9.5
11B	20170215	20.4	1.56	0.2		
11C	20170222	56.16	1.84	0.51	32.1	12.4
11D	20170222	63.94	2.1	1.68	28.2	16.3
12A	20170222	40.89	1.94	0.32	44.0	0.5
12B	20170222	58.23	2	1.47	30.9	13.6
12C	20170222	170.15	2.07	2.13	10.6	33.9
12D	20170222	158.9	2.07	2.06	11.3	33.2
13A	20170222	129.36	2.06	1.65	13.9	30.6
13B	20170222	139.68	2.09	2.15	12.9	31.6
13C	20170222	75.86	2	2.01	23.7	20.8
13D	20170222	143.01	1.96	2.03	12.6	31.9
14A	20170222	119.12	2.07	1.93	15.1	29.4
14B	20170307	48.2	2.03	1.59	37.3	7.2
14C	20170223	65.76	2.02	1.5	27.4	17.1
14D	20170223	58.37	2.02	1.58	30.8	13.7
16A	20170223	62.02	2.04	0.39	29.0	15.5
16B	20170223	62.34	2.03	1.61	28.9	15.6
16C	20170223	60.57	2.04	1.77	29.7	14.8
16D	20170223	63.93	2.07	1.06	28.2	16.3
20A	20170223	62.34	2.09	1.97	28.9	15.6
20B	20170223	62.73	2.05	1.66	28.7	15.8

20C	20170223	68.29	2.06	1.93	26.4	18.1
20D	20170223	57.48	2.02	1.46	31.3	13.2
22A	20170223	65.41	2	1.41	27.5	17.0
22B	20170223	59.38	2.03	1.59	30.3	14.2
22C	20170223	61.9	2.01	1.73	29.1	15.4
22D	20170223	60.58	1.97	1.68	29.7	14.8
23A	20170223	59.49	2.08	1.57	30.3	14.2
23B	20170223	95.37	1.8	0.94	18.9	25.6
23C	20170223	62.11	2.06	1.49	29.0	15.5
23D	20170223	60.24	1.98	1.29	29.9	14.6
26A	20170223	61.97	2.05	1.88	29.0	15.5
26B	20170223	54.95	1.95	1.17	32.8	11.7
26C	20170223	60.6	2.03	1.54	29.7	14.8
26D	20170223	58.43	2.03	1.3	30.8	13.7
29A	20170223	58.08	2.05	1.74	31.0	13.5
29B	20170223	67.74	1.99	1.24	26.6	17.9
29C	20170307	61.8	1.98	1.9	29.1	15.4
29D	20170307	83.4	1.95	0.39	21.6	22.9
30A	20170307	67.6	2.04	1.68	26.6	17.9
30B	20170307	98.3	1.81	1.1	18.3	26.2
30C	20170307	60.9	1.96	0.7	29.6	14.9
30D	20170307	73	1.91	1.29	24.7	19.8
31A	20170307	65	2.05	1.37	27.7	16.8
31B	20170307	66.5	2.01	1.01	27.1	17.4
31C	20170307	63.7	2	0.8	28.3	16.2
31D	20170307	54.7	1.99	0.63	32.9	11.6
32A	20170307	92.3	1.94	1.19	19.5	25.0
32B	20170307	64.3	2.04	1.99	28.0	16.5
32C	20170307	56.8	1.97	1.38	31.7	12.8
32D	20170307	61.1	1.97	0.43	29.5	15.0

3.8 Reverse Transcriptase and Real Time PCR analysis

Using the miRNA concentrations and purity readings from Nanodrop, the amount of miRNA required for each sample yielding a concentration of 1800ng/µl was calculated. miRNAwas

transcribed into cDNA successfully as real time PCR analysis gave CT value readings for all samples.

Determinations of the miRNA concentrations and purity via the Nanodrop spectrophotometer aided further calculations in determining the quantity of miRNA required for each sample to yield a concentration of 1800 ng/µl (as shown in Table 7 above) cDNA was efficiently transcribed using Real Time PCR as shown by the CT values in Table A-E in the appendix. miRNA target gene analysis was carried out in duplicate.

The real time PCR data was normalized to U6, the housekeeping gene for miRNA prior to analysis which is a crucial quality control aspect during quantification analysis. Each miRNA was screened for in each sample at each time point in duplicate (plate design shown in Table C, in the Methods and Methodology Section) and corresponded with the respective CT value obtained. Ct values for the majority of duplicate samples were considered consistent with one another and therefore reliable, however a few samples differed slightly by presenting a narrow variation in values.

Table 8a-11d shows individual miRNA analysis results for each patient across each time point with their subsequent time points, for ease of comparison data is shown divided by time point.

3.9Sample ratio values

Via Excel, the individual ratio values for each individual samples was calculated via the formula

$X0/R0=2^{CTR-CTX}$

Where *X0* is the original amount of target miRNA, *R0* is considered the original amount of U6 snRNA, *CTR* is the CT value for U6 snRNA, and *CTX* is the CT value for the target miRNA.

The corresponding miRNAs and their ratios for each time point and sample are shown below.

Ratio values from Real Time PCR for Time Point against each miRNA for Time Point A are shown in Table 8a-d below.

***Table 8a: Time point A**. Calculated ratio values via excel per sample 2-26 with respect to their corresponding miR-1, miR-27, miR-133a, miR-133b, miR-29b, miR- 30a*

Target Gene						
Sample	**1**	**27**	**133a**	**133b**	**29b**	**30a**
2	0.495879251	10.38101072	2.005958873		0.03394743	309.7006215
7	63.08887495	4798.706272	528.7314379	0.764557658	5.943537636	2444.553067
11	2.280973377	3.993694954	10.73613768	0.074017485	0.029174283	88.27827155
12	5.74092689	99.63211824	7.550233497	0.00562409	0.126426737	104.0022017
13	3.461809341	29.81393101	6.946969339	0.30679071	0.078057311	53.97989422
14	0.498143313	35.84428738	0.670671628	0.013334222	0.071039425	31.6810838
16	9.342693706	391.192125	38.93610244	0.303704917	1.892268223	102.597247
20	2.607942078	77.46560034	4.387073164	0.120174568	0.163759334	284.801775
22	2.336094154	338.580064	11.13983088	0.360647643	0.628407929	216.9115217
23	2.994865033	326.1033176	10.46041577	1.285314937	0.673203631	620.3079459
26	0.522807519	47.8018471	2.212045731	0.20736764	0.328827639	164.3125358
Mean	**8.488273601**	**559.9558426**	**56.70698881**	**0.344153387**	**0.906240871**	**401.9205605**
S.D	**18.29500993**	**1413.260305**	**156.9022325**	**0.398848702**	**1.757398424**	**697.6968619**
S.E.M	**5.516153042**	**426.1140147**	**47.30780308**	**0.126127034**	**0.529875562**	**210.3635189**
N	**11**	**11**	**11**	**10**	**11**	**11**

***Table 8b: Time point A.** Calculated ratio values via excel per sample 2-26, with respect to their corresponding miR-208a, miR-505, miR-144, miR-451, miR-125*

Target Gene					
Sample	**208 ***	**505**	**144**	**451**	**125**
2		1.765170108		845.0835679	21.63356182
7	0.628643501	54.65961005	19.155103	36010.00787	2605.493751
11		1.088061869	0.309215719	692.1016925	84.89814447
12		0.942072784	0.278699366	1403.823007	89.385408

13	0.025030546	0.399069776	0.113793986	892.5995275	21.42685189
14		0.43706301	0.086716833	294.208214	5.805244287
16	0.012269831	0.609239471	0.342923995	4422.407306	189.9096845
20		1.709945406	0.444590375	555.5238985	51.25614367
22	0.024854293	1.719328712	0.365702829	1338.019851	68.69300181
23		3.478435074	1.437009055	1346.121573	108.8586718
26	0.022005977	0.38533163	1.243971105	310.1309026	10.44321003
Mean	**0.142560829**	**6.108484353**	**2.377772626**	**4373.638856**	**296.1639703**
S.D	**0.271778299**	**16.12842284**	**5.912652685**	**10554.22559**	**767.8074476**
S.E.M	**0.12154295**	**4.862902456**	**1.86974495**	**3182.21875**	**231.5026559**
N	**5**	**11**	**10**	**11**	**11**

Table 8c: Time point A.*Calculated ratio values via excel per sample 29-32 with respect to their corresponding miR-1, miR-27, miR-133a, miR-133b, miR-29b, miR- 30a*

Target Gene						
Sample	1	27	133a	133b	29b	30a
29	0.399585	8.059494	0.769272	0.046392	0.028512	5.404522
30	0.443932	7.29461	0.77753	0.03622	0.013325	146.2681
31	0.425146	1.507932	0.357076	0.172154		16.50424
32	0.130633	4.463368	0.342975	0.023159	0.018542	19.16786
Mean	0.349824	5.331351	0.561713	0.069481	0.020126	46.83618
S.D	0.147253	2.981559	0.244527	0.069106	0.007716	66.55537
S.E.M	0.073627	1.490779	0.122264	0.034553	0.004455	33.27768
N	4	4	4	4	3	4

Table 8d: Time point A.*Calculated ratio values via excel per sample 29-32, with respect to their corresponding miR-208a, miR-505, miR-144, miR-451, miR-125*

Target Gene					
Sample	208 *	505	144	451	125
29		0.188824	2.396809	700.9776	11.65514
30		1.389741	0.214802	362.4287	32.53896
31		0.336543	0.035928	158.1674	1.087789
32		0.293716		35.58316	11.45912
Mean		0.552206	0.882513	314.2892	14.18525
S.D		0.561794	1.314465	290.916	13.19388

S.E.M		0.280897	0.758907	145.458	6.59694
N	0	4	3	4	4

* miRNA 208 failed to be detected in any sample

Ratio values from Real Time PCR for Time Point against each miRNA for Time Point B are shown in Table 9a-d below.

Table 9a: Time point B. *Calculated ratio values via excel per sample 2-26 with respect to their corresponding miR-1, miR-27, miR-133a, miR-133b, miR-29b, miR- 30a*

Target Gene						
Sample	1	27	133a	133b	29b	30a
2	0.090367709	14.71080843	0.915780271		0.043327143	81.06320478
7	34.05928681	3167.490851	157.469929	9.362715666	3.834065039	26889.05323
11						
12	3.583213021	107.6757099	13.06949728	0.145709483	0.297996512	353.2197598
13	0.883507048	3.854180155	0.357967027	0.035719478	0.017000686	20.45524739
14	1.140406601	23.23739118	1.458021613	0.263334738	0.048479531	303.7682361
16	0.054013588	0.389185119	0.069731144		0.000634134	1.160067728
20	1.598430775	129.4416384	3.547855047	0.036588807	0.524531099	93.27155628
22	0.090035173	16.61411863	0.245931899		0.002470222	81.48007422
23	3.271853699	188.3428106	5.383050911	0.432195484	1.449875777	22.47495319
26	0.111117383	13.36691711	1.243214316	0.15528833	0.212678847	41.73837807
Mean	4.488223181	366.5123611	18.37609785	1.490221712	0.643105899	2788.768471
S.D	10.47115412	986.279963	49.03179086	3.474171792	1.205544259	8468.83505
S.E.M	3.311269674	311.8891094	15.50521369	1.31311351	0.381226568	2678.080789
N	10	10	10	7	10	10

Table 9b: Time point B. Calculated ratio values via excel per sample 2-26, with respect to their corresponding miR-208a, miR-505, miR-144, miR-451, miR-125

Target Gene					
Sample	208 *	505	144	451	125
2		0.247158983	0.365296475	622.7708824	46.92848177
7		168.4634485	2.423479461	22596.90887	3900.550034

11					
12		0.889351362	0.611468736	1258.020085	134.5440273
13		0.048866847	1.086808921	552.2280269	6.696803065
14		5.884835511	2.481032343	3930.649048	21.67438332
16		0.005987277	0.001306374	5.392007728	0.399839221
20		0.273544017	1.17410892	389.2630335	35.09670964
22		0.096962588	0.903395449	1318.068785	2.143227122
23		3.113991608	3.637722529	2710.586184	125.1043675
26	0.002476964	0.180734432	1.390399974	451.9846673	5.586211345
Mean	0.002476964	17.92048811	1.407501918	3383.587159	427.8724084
S.D	#DIV/0!	52.92950671	1.118905265	6858.08131	1221.168859
S.E.M	#DIV/0!	16.73777966	0.353828912	2168.715732	386.1675001
N	1	10	10	10	10

Table 9c: Time point B. *Calculated ratio values via excel per sample 29-32, with respect to their corresponding miR-1, miR-27, miR-133a, miR-133b, miR-29b, miR- 30a*

Sample	1	27	133a	133b	29b	30a
29	502.4242	5466.888	169.1671	0.682188	11.40595	7190.75
30						
31	0.061393	8.21405	0.75832	0.167859	0.017259	24.3367
Mean	167.5152	1825.584	56.66204	0.284674	3.809243	2407.994
S.D	290.0397	3153.463	97.43282	0.353876	6.578945	4141.995
S.E.M	167.4545	1820.653	56.25287	0.20431	3.798356	2391.382
N	3	3	3	3	3	3

Table 9d: Time point B. *Calculated ratio values via excel per sample 29-32, with respect to their corresponding miR-208a, miR-505, miR-144, miR-451, miR-125*

Target Gene					
Sample	208 *	505	144	451	125
29		84.1857316	38.42094312	27660.56527	2577.729085
30					
31		0.779775886	0.020699954	223.9500939	50.36577773
32		0.120893123	0.005143767	26.01924536	8.515618108

* miRNA 208 failed to be detected in any sample

Ratio values from Real Time PCR for Time Point against each miRNA for Time Point C are shown in Table 10a-dbelow.

Table 10a: Time point C. *Calculated ratio values via excel per sample 2-26, with respect to their corresponding miR-1, miR-27, miR-133a, miR-133b, miR-29b, miR- 30a*

Target Gene						
Sample	1	27	133a	133b	29b	30a
2	0.648572721	15.53056941	0.674959549	0.018046471	0.065037905	153.733237
7	3.093693142	84.29207783	5.910532132	0.07817894	0.093193346	447.4349559
11	1.85216699	19.82365935	6.725742773	0.023559432	0.050086792	28.10814417
12	69.00035034	1506.396369	57.41428216	0.705245538	6.807448528	2631.656342
13	24.43389461	66.15322447	2.869578563	2.386426026	0.375001396	389.963861
14	0.223471265	39.54860267	4.409779206	0.118833126	0.200746584	58.43879794
16	3.310611205	19.69098934	2.896318914	0.002728374		11.01812124
20	0.008585848	1.460377938	0.026861242	0.000786428	0.003911844	2.116112219
22	0.313453537	50.46636431	0.838336499	0.004075071	0.148626638	57.12152504
23	0.987275924	104.8191993	3.795416166	0.01113838	0.162707686	0.296584673
26	1.27377557	51.21210659	8.200370628	0.218733979	0.307167526	246.080098
Mean	9.558713741	178.1266855	8.523834348	0.324341069	0.821392824	365.9970708
S.D	20.92876537	441.6373945	16.42021982	0.714446589	2.106439161	767.8656039
S.E.M	6.310260186	133.1586846	4.950882556	0.215413752	0.66611455	231.5201907
N	11	11	11	11	10	11

Table 10b: Time point C. *Calculated ratio values via excel per sample 2-26, with respect to their corresponding miR-208a, miR-505, miR-144, miR-451, miR-125*

Target Gene					
Sample	208 *	505	144	451	125
2		1.624889933	0.075816444	882.9068273	183.39882
7		5.348897907	0.121446153	1141.638427	84.78699104
11		0.302018899	0.222643151	178.7219748	44.23051519
12		24.44782941	32.95619001	39534.90089	1845.379022
13		0.29076426	0.334853558	4173.858383	65.10356731
14		1.684781283	0.075910943	655.9276063	26.69445474
16		0.080491909	0.097967349	3621.509551	73.31554471
20		0.001532339	0.047220485	27.92680614	0.219050783
22		0.279795308	0.021106798	108.4756777	20.53280594
23		0.957278439	0.531064512	239.0926437	55.5910525
26		2.585955054	1.540160931	1389.904216	91.29330181
Mean	#DIV/0!	3.418566795	3.274943666	4723.169364	226.4131933
S.D	#DIV/0!	7.14910701	9.853867252	11630.56227	539.1182128
S.E.M	#DIV/0!	2.155536867	2.971052765	3506.746469	162.5502572
N	0	11	11	11	11

Table 10c: Time point C. *Calculated ratio values via excel per sample 29-32. with respect to their corresponding miR-1, miR-27, miR-133a, miR-133b, miR-29b, miR- 30a*

Target Gene						
Sample	1	27	133a	133b	29b	30a
29	2.44286	2.883754	5.71241	0.006502	0.0155	4.492226
30	1.088788	237.8754	24.50594	0.680998	0.045422	566.4767
31	14.10424	29.4537	16.8276	0.112089	0.318979	213.9994
32	5.891399	44.05437	12.02105	1.71907	0.041909	311.4601
Mean	5.881821	78.56681	14.76675	0.629665	0.105452	274.1071
S.D	5.842597	107.5645	7.929247	0.784358	0.142976	233.224
S.E.M	2.921299	53.78225	3.964623	0.392179	0.071488	116.612
N	4	4	4	4	4	4

Table 10d: Time point C. *Calculated ratio values via excel per sample 29-32, with respect to their corresponding miR-208a, miR-505, miR-144, miR-451, miR-125*

Target Gene					
Sample	208 *	505	144	451	125
29		0.398148	0.132557	57.88371	15.49169
30		10.8479	3.512112	16620.88	186.6577
31	0.175669	27.53595	0.976445	1226.82	108.55
32	0.005035	0.940021	0.359806	1320.516	71.85636
Mean	0.090352	9.930505	1.24523	4806.524	95.63894
S.D	0.120657	12.68185	1.552742	7897.153	71.74099
S.E.M	0.085317	6.340926	0.776371	3948.577	35.8705
N	2	4	4	4	4

* miRNA 208 failed to be detected in any sample.

Ratio values from Real Time PCR for Time Point against each miRNA for Time Point D are shown in Table 11a-dbelow.

Table 11a: Time point D. *Calculated ratio values via excel per sample 2-26, with respect to their corresponding miR-1, miR-27, miR-133a, miR-133b, miR-29b, miR- 30a*

Target Genes						
Sample	1	27	133a	133b	29b	30a
2	2.142843908	54.50567878	5.779825026		0.39315108	87.20621762
7	31.06251816	865.1179326	91.29664137	1.003037683	1.435586738	3166.402137
11	9.220367019	41.64830408	15.09006863	0.027238053	0.129011001	45.13578299
12	0.433050582	6.372926768	0.215734979	0.018894809	0.039232663	48.88722964
13	0.034587926	0.259446963	0.062325306	0.000142452	0.00261742	6.124585705
14	7.448355303	118.92867	71.25741545	0.157467126	1.481140396	437.9648569
16	9.647017534	53.79039048	12.73023414	0.036695653	0.045120118	5.722027041
20	0.037174921	2.175635563	0.120441405		0.010852009	0.128635263
22	0.846101477	39.21465237	2.378358205	0.016432436	0.056316252	136.5404684

23	1.814232978	59.48222674	0.754994355	0.47657516	0.668086996	93.36014648
26	0.113533383	7.571530263	0.765269126	0.074731245	0.094129195	81.01507669
Mean	5.709071199	113.5515813	18.22284618	0.201246069	0.395931261	373.4988331
S.D	9.212555687	251.6976384	31.92170925	0.335746343	0.562458201	934.3139623
S.E.M	2.777690052	75.88969337	9.624757477	0.111915448	0.169587528	281.706259
N	11	11	11	9	11	11

Table 11b: Time point D. *Calculated ratio values via excel per sample 2-26, with respect to their corresponding miR-208a, miR-505, miR-144, miR-451, miR-125*

Target Gene					
Sample	208 *	505	144	451	125
2		0.64010569	0.166080894	955.847371	409.9064231
7		27.00362044	1.56391954	6832.600541	394.403677
11		0.71035356	0.2179977	239.0589407	158.3185599
12		0.321438605	0.715334517	732.6311171	11.3450997
13		0.03084167	0.105462157	157.3380331	0.177643344
14		0.009297763	7.944141785	2996.393136	195.3970251
16		0.183610902	0.03421399	172.8265059	103.8482879
20		0.022549474	0.015155928	83.59193243	0.812921038
22		0.98342984	0.022879977	124.1782277	16.12024637
23		1.309119323	0.506412051	133.7741503	54.86524506
26		0.2471984	9.183974311	2160.331742	4.263605236
Mean		2.860142333	1.861415714	1326.233791	122.6780667
S.D		8.01876496	3.356238559	2063.599957	153.452083
S.E.M		2.417748605	1.011944001	622.1987977	46.26754387
N	0	11	11	11	11

Table 11c: Time point D.*Calculated ratio values via excel per sample 29-32, with respect to their corresponding miR-1, miR-27, miR-133a, miR-133b, miR-29b, miR- 30a*

Target Gene						
Sample	1	27	133a	133b	29b	30a
29	2.442860331	2.883753882	5.712410018	0.006501793	0.015500454	4.492225923
30	1.088787978	237.875408	24.50594084	0.680998072	0.045421737	566.476732
31	14.10423631	29.45369546	16.82760055	0.112088885	0.318978793	213.9993992
32	5.891399005	44.05437242	12.0210538	1.719069536	0.04190858	311.4601242

Table 11d: Time point D. *Calculated ratio values via excel per sample 29-32 with respect to their corresponding miR-1, miR-27, miR-133a, miR-133b, miR-29b, miR- 30a*

Target Gene					
Sample	208 *	505	144	451	125
29		0.398148256	0.132556936	57.88371447	15.49168824
30		10.84789901	3.512112499	16620.87837	186.6577379
31	0.175669453	27.53595379	0.976445007	1226.819565	108.5499721
32	0.005034742	0.940020922	0.359805956	1320.515636	71.85635703

* miRNA 208 failed to be detected in any sample

Further analysis of the calculated sample ratio values by means of GraphPad PRISM produced graphs for each time miRNA against each time point.

3.10 Exclusion Criteria

Once the miRNA sample values were calculated in Excel using the comparative ΔΔCT method and average was calculated for each miRNA for each of the time points. Any samples which were 5-fold above or below the mean were discarded.
Ratio data that was included in the study post-outlier processing by miRNA is shown below in table 12-21.

Table 12: Included ratio data for miR-1 by Time point

A	B	C	D
0.495879	0.090368	0.648573	2.142844
2.280973	3.583213	3.093693	9.220367
5.740927	0.883507	1.852167	7.448355
3.461809	1.140407	0.223471	9.647018
0.498143	0.054014	3.310611	0.846101
2.607942	1.598431	0.313454	1.814233
2.336094	0.090035	0.987276	2.44286
2.994865	3.271854	1.273776	1.088788
0.522808	0.111117	0.755377	14.10424
0.399585	0.061393	0.390805	5.891399
0.443932	0.059987		
0.425146			

Table 13: Included Ratio data for miR-27a by time point.

A	B	C	D
	14.71081	15.53057	54.50568
		84.29208	
		19.82366	41.6483
99.63212	107.6757		6.372927
29.81393		66.15322	
35.84429	23.23739	39.5486	
391.1921		19.69099	53.79039
77.4656	129.4416		
338.5801	16.61412	50.46636	39.21465
326.1033	188.3428	104.8192	59.48223
47.80185	13.36692	51.21211	7.57153
		66.94536	
	8.21405		29.4537
		15.03932	44.05437

Table 14: Included Ratio data for miR-133a by time point.

A	B	C	D
2.005959	0.91578	0.67496	5.779825
		5.910532	
10.73614		6.725743	15.09007
7.550233	13.0695		0.215735
6.946969		2.869579	
0.670672	1.458022	4.409779	71.25742
38.9361		2.896319	12.73023
4.387073	3.547855		
11.13983		0.838336	2.378358
10.46042	5.383051	3.795416	0.754994
2.212046	1.243214	8.200371	0.765269
0.769272			5.71241
0.77753		1.459717	24.50594
	0.75832		16.8276
		0.54248	12.02105

Table 15: Included Ratio data for miR-133b by time point

A	B	C	D
10.73614		6.725743	15.09007
6.946969		2.869579	
0.670672	0.145709	4.409779	
38.9361	0.035719	2.896319	12.73023
4.387073	0.263335		
11.13983		0.838336	2.378358
10.46042	0.036589	3.795416	0.754994
2.212046		8.200371	
0.769272	0.432195		5.71241
0.77753	0.155288	1.459717	
	0.682188	0.567462	
			0.680998
	0.167859		
			1.71907

Table 16: Included Ratio data for miR-29b by time point

A	B	C	D
0.033947	0.043327	0.065038	0.393151
		0.093193	1.435587
0.029174		0.050087	0.129011
0.126427	0.297997		0.039233
0.078057		0.375001	
0.071039	0.04848	0.200747	1.48114
			0.04512
0.163759	0.524531		0.010852
0.628408		0.148627	0.056316
0.673204	1.449876	0.162708	0.668087
0.328828	0.212679	0.307168	0.094129
0.028512		0.946195	0.0155
0.013325		0.147442	0.045422
			0.318979
0.018542			0.041909

Table 17: Included Ratio Data for miR-30a by time point

A	B	C	D
309.7006	81.0632	153.7332	87.20622
		447.435	
88.27827			45.13578
104.0022	353.2198		48.88723
53.97989	20.45525	389.9639	
31.68108	303.7682	58.4388	437.9649
102.5972			
284.8018	93.27156		
216.9115	81.48007	57.12153	136.5405
	22.47495		93.36015
164.3125	41.73838	246.0801	81.01508
		221.7049	
146.2681		589.022	
	24.3367		213.9994
		197.7687	311.4601

Table 18: Included Ratio Data for miR-505 by time point

A	B	C	D
1.76517	0.247159	1.62489	0.640106
		5.348898	
1.088062		0.302019	0.710354
0.942073	0.889351		0.321439
0.39907		0.290764	
0.437063		1.684781	
0.609239			0.183611
1.709945	0.273544		
1.719329		0.279795	0.98343
3.478435	3.113992	0.957278	1.309119
0.385332		2.585955	0.247198
0.188824			0.398148
1.389741			
0.336543	0.779776		
0.293716		0.467121	0.940021

Table 19: Included ratio data for miR-144 by time point

A	B	C	D
	0.365296	882.9068	0.166081
	2.423479	1141.638	1.56392
0.309216		178.722	0.217998
0.278699	0.611469		0.715335
0.113794	1.086809		0.105462

	2.481032	655.9276	
0.342924			0.034214
0.44459	1.174109		0.015156
0.365703	0.903395	108.4757	0.02288
1.437009	3.637723	239.0926	0.506412
1.243971	1.3904	1389.904	
2.396809			0.132557
0.214802			
	0.0207		0.976445
			0.359806

Table 20: Included Ratio data for miR-451 by time point

A	B	C	D
745	622.7709	882.9068	955.8474
		1141.638	
692.1017			239.0589
1403.823	1258.02		732.6311
892.5995	552.228	4173.858	157.338
294.2082	3930.649	655.9276	
		3621.51	172.8265
555.5239	389.263		83.59193
1338.02	1318.069	108.4757	124.1782
1346.122	2710.586	239.0926	133.7742
310.1309	451.9847	1389.904	
700.9776		5686.541	57.88371
362.4287		8243.706	
158.1674	223.9501		1226.82
		676.7125	125

Table 21: Included Ratio data for miR-125 by time point

A	B	C	D
21.63356	46.92848	183.3988	409.9064
		84.78699	394.4037
84.89814		44.23052	158.3186
89.38541	134.544		
21.42685	6.696803	65.10357	
	21.67438	26.69445	195.397
189.9097		73.31554	103.8483
51.25614	35.09671		
68.693		20.53281	
108.8587	125.1044	55.59105	54.86525
10.44321		91.2933	
11.65514		682.1806	
32.53896		224.1777	186.6577
	50.36578		108.55
	8.515618	127.0302	71.85636

3.11 miRNA expression change graphs from GraphPad Prism

The miRNA ratio values were used to construct the below graphs on GraphPad Prism to demonstrate the changes in miRNA expression levels across the 4 time points. The anova test was performed on the data to test for a relationship between each of the time points: A= pre-RT, B=24-72h post-RT, C=3 months post-RT and D= 6 months post-RT. The student's T-Test was used to investigate the relationship between A (pre-RT) to D (6 months post-=RT).

Figure 6A: miR-1 expression levels changes over time point A to D

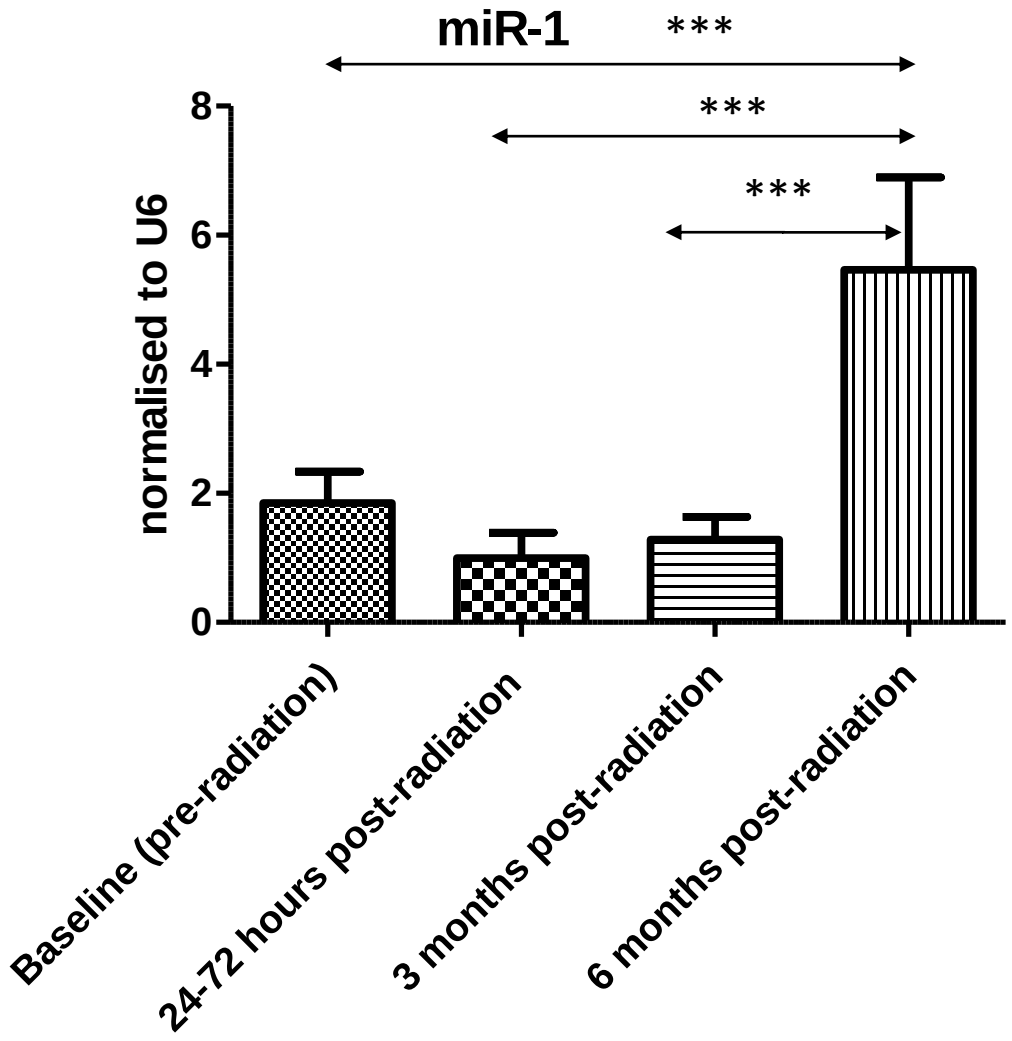

Figure 6A*: Effects of left-sided radiotherapy on breast cancer patients on the expression of miR-1 at different time point A =pre-RT, B =24-72h post first dose of RT, C=3 months post-first dose of RT, D=6 months post first dose of RT. Expression was determined by quantitative real-time PCR and the data were normalized to U6 as an internal control. Each data point is presented as mean± SEM (A: n=12, B: n=11, C: n=10, D: n=10), (p=0.0084).*

As can be seen from Figure 6a, levels decrease from time points A to B, and then rise from C through to time point D. The Anova test revealed a significant difference in the expression of miR-1 between the different groups (p=0.0084). As the graph reveals the expression of miR-1 from time point B to D increases by more than three-fold and C to D by more than 3 fold also. The expression from A to D changes by more than 2 fold. A Tukey HSD test

reveals the change from A to D (p=0.009), B to D (p=0.002) and C to D (p=0.003) and as tcarrying three star significance as illustrated in the graph above.

Figure 6b: miR-1 expression changes from time point A to D only

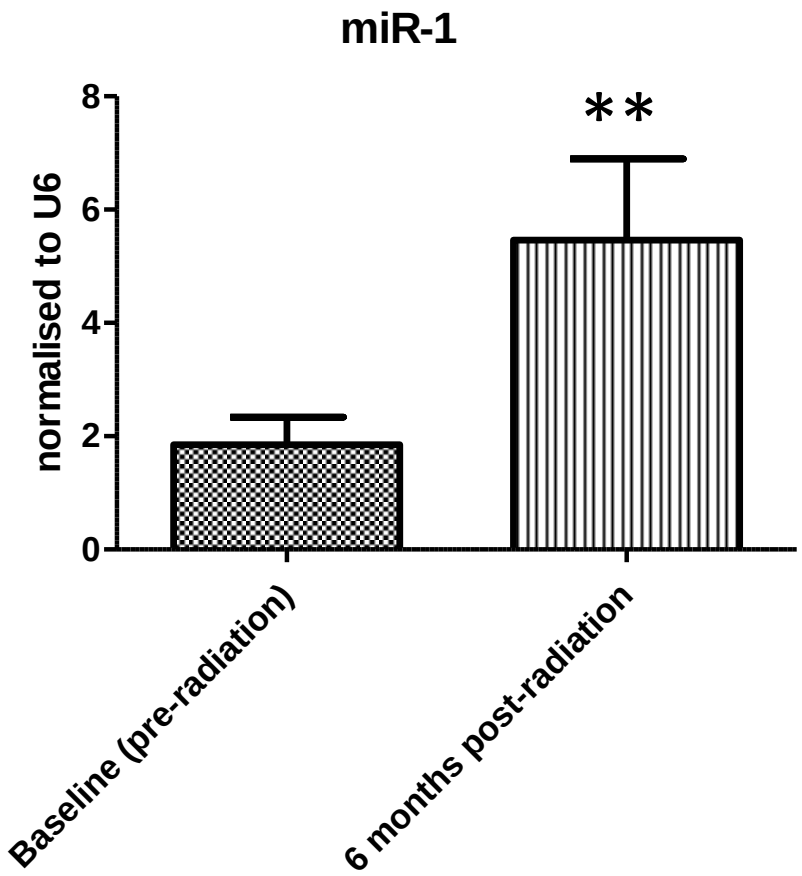

Figure 6b: *Effects of left-sided radiotherapy on breast cancer patients on the expression of miR-1 between time point A (baseline pre-RT reading) (n=12) and D (n=10) (6 months post RT reading) only. Expression was determined by quantitative real-time PCR and the data were normalized to U6 as an internal control. Each data point is presented as mean± SEM (A: n=12; D: n=10), (p=0.0378).*

As seen in Figure 6b above there was a significant increase in the levels from time point A to D. A students t-test in Fig 6b revealed a significant increase in miR-1 expression from time point A to D (p=0.0378).

Figure 7A: miR-451 expression levels changes over time point A to D

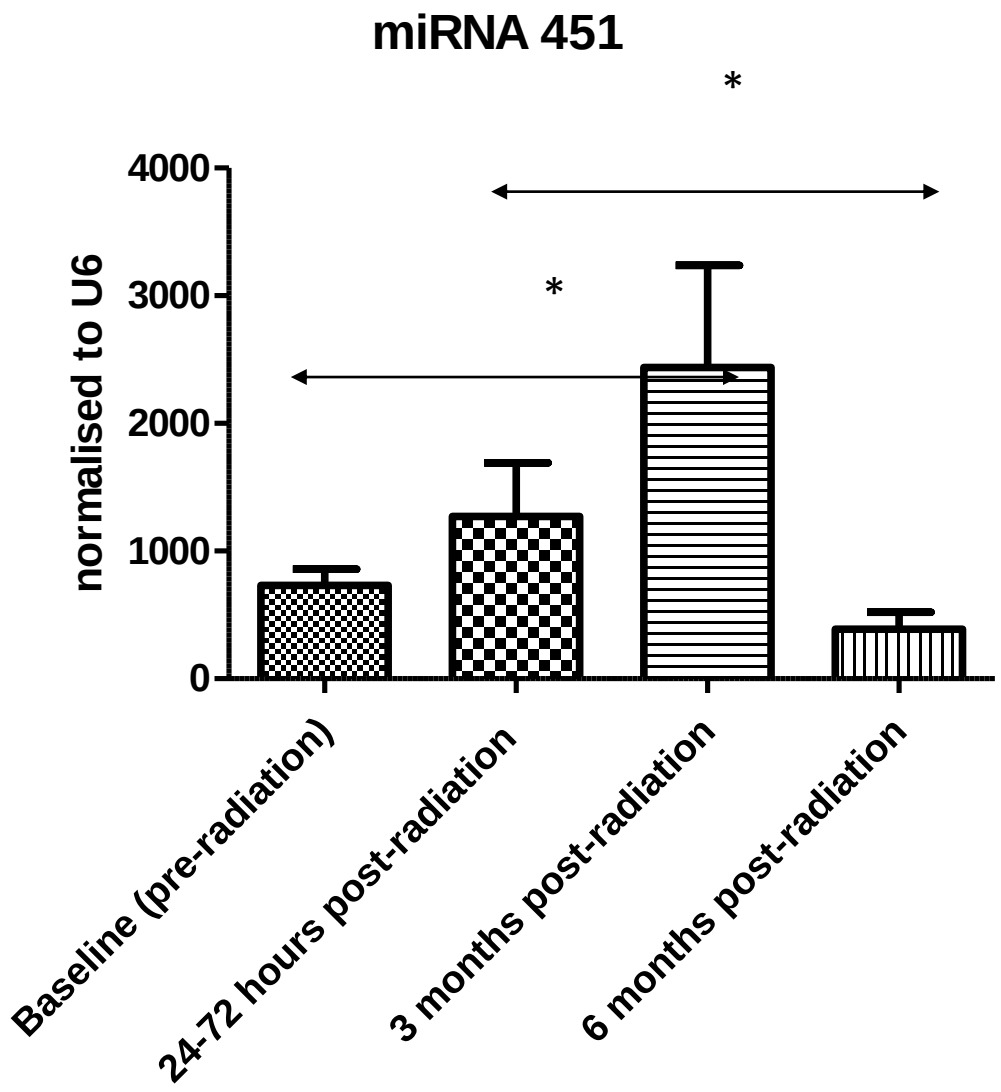

Figure 7a*: Effects of left-sided radiotherapy on breast cancer patients on the expression of miR-451 at different time point A =pre-RT, B =24-72h post first dose of RT, C=3 months post-first dose of RT, D=6 months post first dose of RT. Expression was determined by quantitative real-time PCR and the data were normalized to U6 as an internal control. Each data point is presented as mean± SEM (A: n=12, B: n=9, C: n=11, D: n=11), (p=0.0120).*

As can be seen from Figure 7A, levels from A-C rose by more than 3-fold and then decreased from C-D by more than 5-fold. A one way ANOVA test revealed there to be a significant relationship between the groups p=0.0120. The Tukey test revealed the increase from A-C to be significant (p=0.044) and the decrease from C-D to also be significant (p=0.012).

Figure 7b: miR-451 changes from time point A to D only

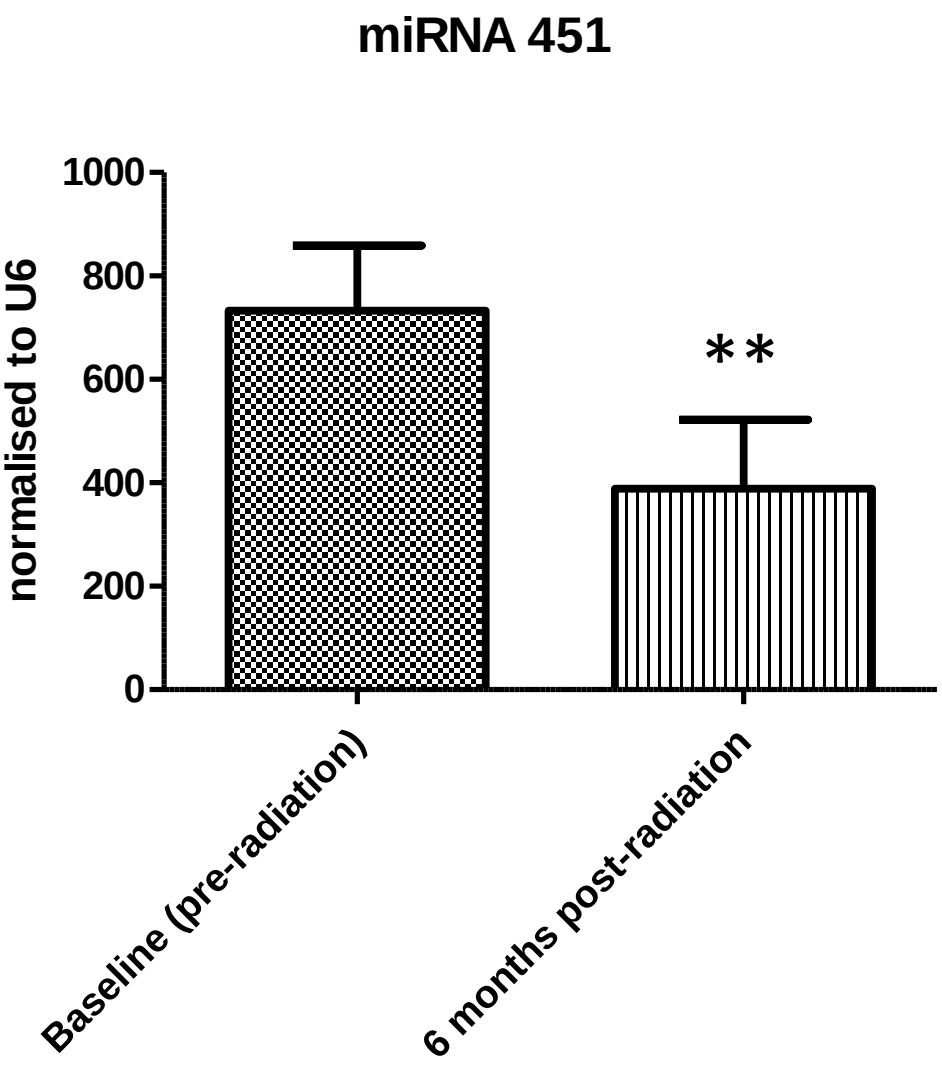

Figure 7b*: Effects of left-sided radiotherapy on breast cancer patients on the expression of miR-451 between time point A (baseline pre-RT reading) (n=12) and D (n=11) (6 months post RT reading) only. Expression was determined by quantitative real-time PCR and the data were normalized to U6 as an internal control. Each data point is presented as mean± SEM (A: n=12; D: n=11), (p=0.0321).*

As seen in Figure 7b there was a significant decrease in the levels from time point A to D. A students t-test in Fig 7B revealed a significant decrease in miR-451 expression from time point A to D (P=0.0321).

Figure 8A: miR-27a expression levels changes over time point A to D

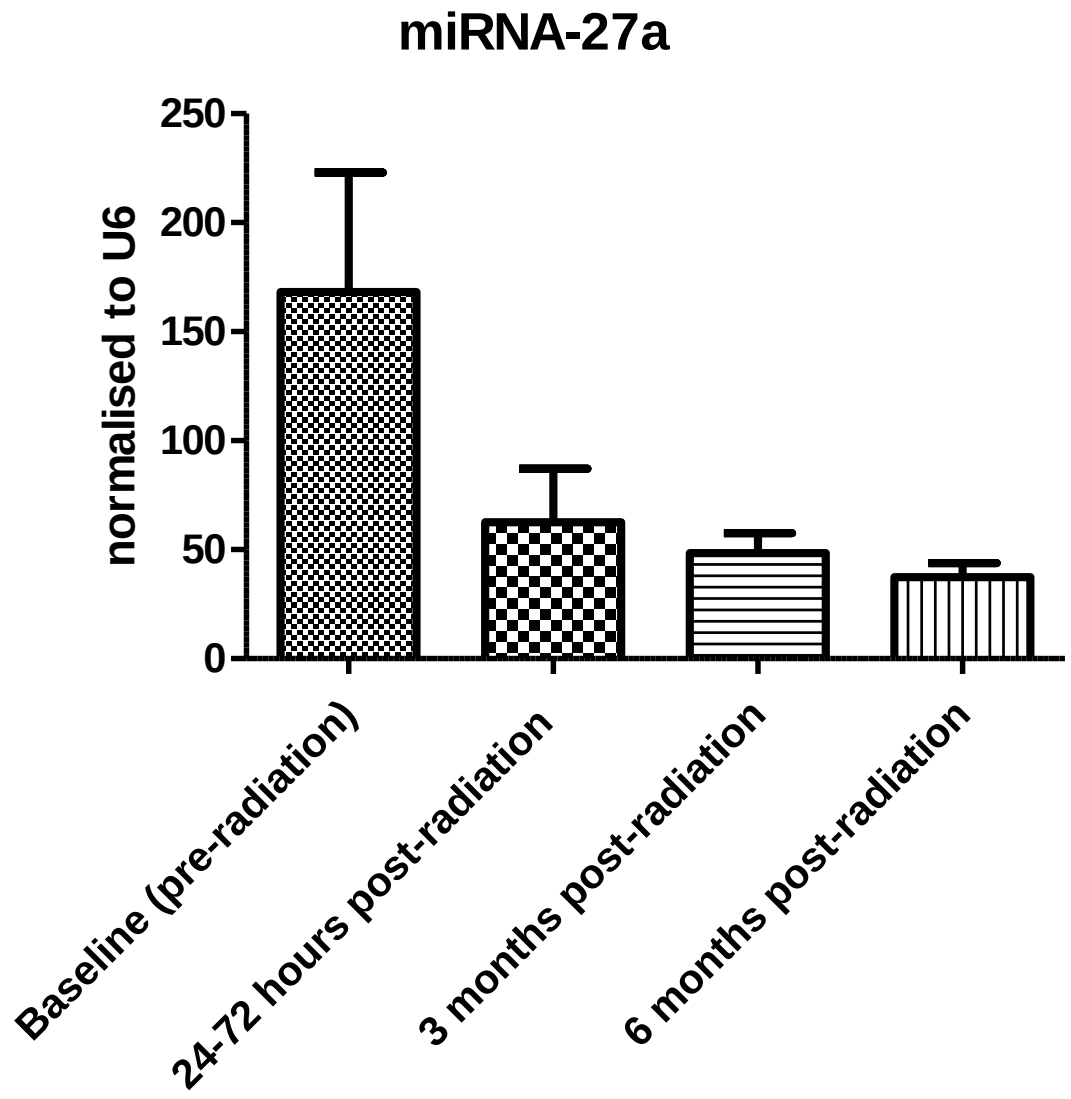

Figure 8a: *Effects of left-sided radiotherapy on breast cancer patients on the expression of miR-27a at different time point A =pre-RT, B =24-72h post first dose of RT, C=3 months post-first dose of RT, D=6 months post-first dose of RT. Expression was determined by quantitative real-time PCR and the data were normalized to U6 as an internal control. Each data point is presented as mean± SEM (A: n=8, B: n=8, C: n=11, D: n=9), (p=0.1387).*

As can be seen from Figure 8A, levels of miR-27a decreased by more than 3-fold by A t B, by more 4-fold from A to C and more than 5-fold A to D. However the ANOVA test revealed no significant difference between these time points (A-B, A-C, B-C, B-D, C-D (p=0.1387). A

T-test was conducted to explore the difference between groups to A to D where there was the greatest fold-decrease as shown in Figure 8b.

Figure 8b: miR-27a changes from time point A to D only

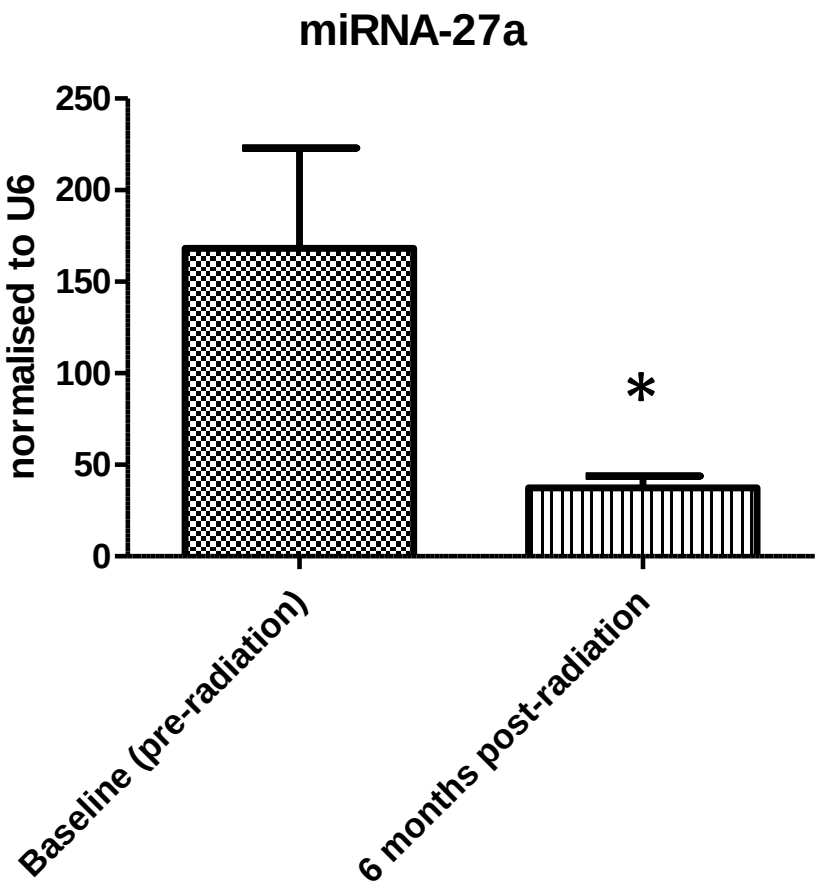

Figure 8b: Effects of left-sided radiotherapy on breast cancer patients on the expression of miR-27a between time point A (baseline pre-RT reading) (n=8) and D (n=9) (6 months post RT reading) only. . Expression was determined by quantitative real-time PCR and the data were normalized to U6 as an internal control. Each data point is presented as mean± SEM (A: n=8 D: n=9), (p=0.0464).

As seen in Figure 8b there was a significant decrease in the levels from time point A to D. A students t-test in Fig 8B revealed a significant decrease in miR-27a expression from time point A to D (P=0.0464).

Figure 9a: miR-125 expression levels changes over time point A to D

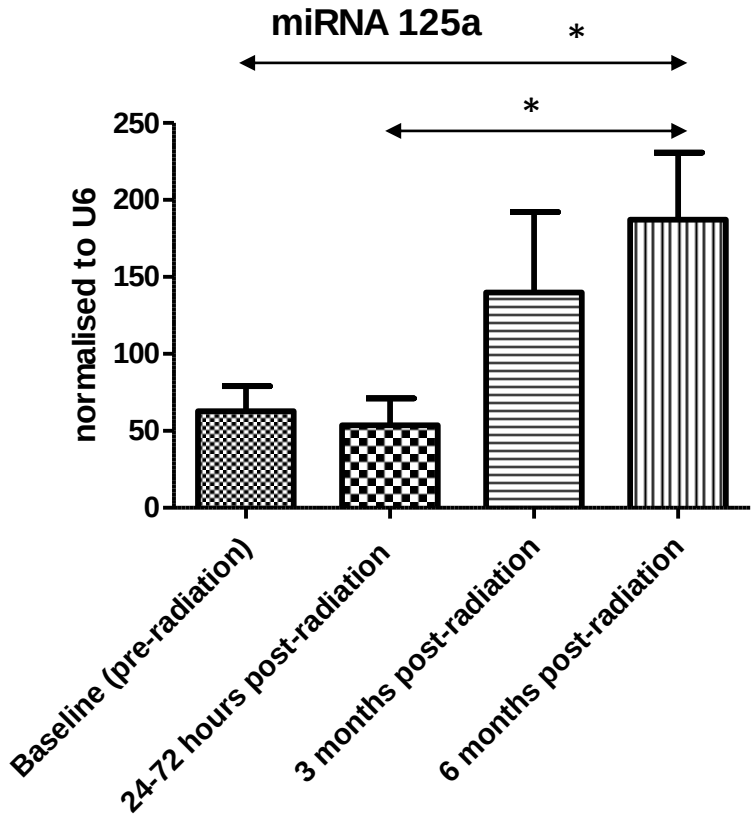

Figure 9a: *Effects of left-sided radiotherapy on breast cancer patients on the expression of miR-125a at different time point A =pre-RT, B =24-72h post first dose of RT, C=3 months post-first dose of RT, D=6 months post-first dose of RT. Expression was determined by quantitative real-time PCR and the data were normalized to U6 as an internal control. Each data point is presented as mean± SEM (A: n=11, B: n=8, C: n=12, D: n=9), (p=0.0146).*

As can be seen in Figure 9A, levels of miR-125a increased by 3-fold between time points B-D and A to D. A one way ANOVA found the relationship between the groups to be statistically significant (p=0.0146). A Tukey HSD test did not reveal which groups were statistically significant. A LSD Test went onto reveal that the increase from B- D was significant (p=0.031) as was the increase from A to D (p=0.032)

Figure 9b: miR-125a changes from time points A to D only

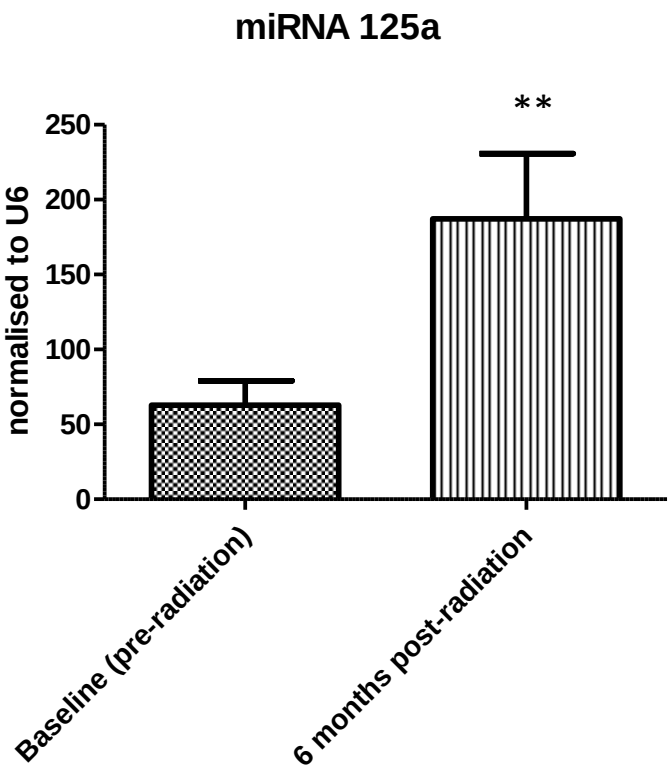

Figure 9b: *Effects of left-sided radiotherapy on breast cancer patients on the expression of miR-125a between time point A (baseline pre-RT reading) (n=11) and D (n=9) (6 months post RT reading) only. Expression was determined by quantitative real-time PCR and the data were normalized to U6 as an internal control. Each data point is presented as mean± SEM (A: n=11 D: n=9) (p=0.0098)*

As seen in Figure 9b there was a significant increase in the levels from time point A to D. A students t-test in Fig 9B revealed a significant decrease in miR-125a expression from time point A to D (P=0.0098).

Considering significant relationships from time points A to D as shown in Figure 6b to 9b it can be seen that, miR-1 expression increased significantly (p=0.0378) from a mean miRNA ratio value of 1.9 at time point A (baseline pre-RT) to 5.5 at time point D (6 months post RT) which is nearly a 3 fold increase.miR-125a expression increased significantly (p= 0.0098) from a mean miRNA ratio value of 62.7 at time point A (baseline pre-RT) to 187 at time point D (6 months post-RT) which is more than a 3 fold increase.

miR-451 expression decreased significantly (p=0.0321) from a mean miRNA ratio value of 733 at time point A (baseline pre-RT) to 388 at time point D (6 months post-RT) which is more than a 2 fold decrease in level.

miR-27a expression also decreased significantly (p=0.0464) from a mean miRNA ratio value of 167 at time point A (baseline pre-RT) to 37 at time point D (6 months post RT) which is more than a four-fold decrease.

Figure 10a: miR-29b expression levels changes over all time point A to D

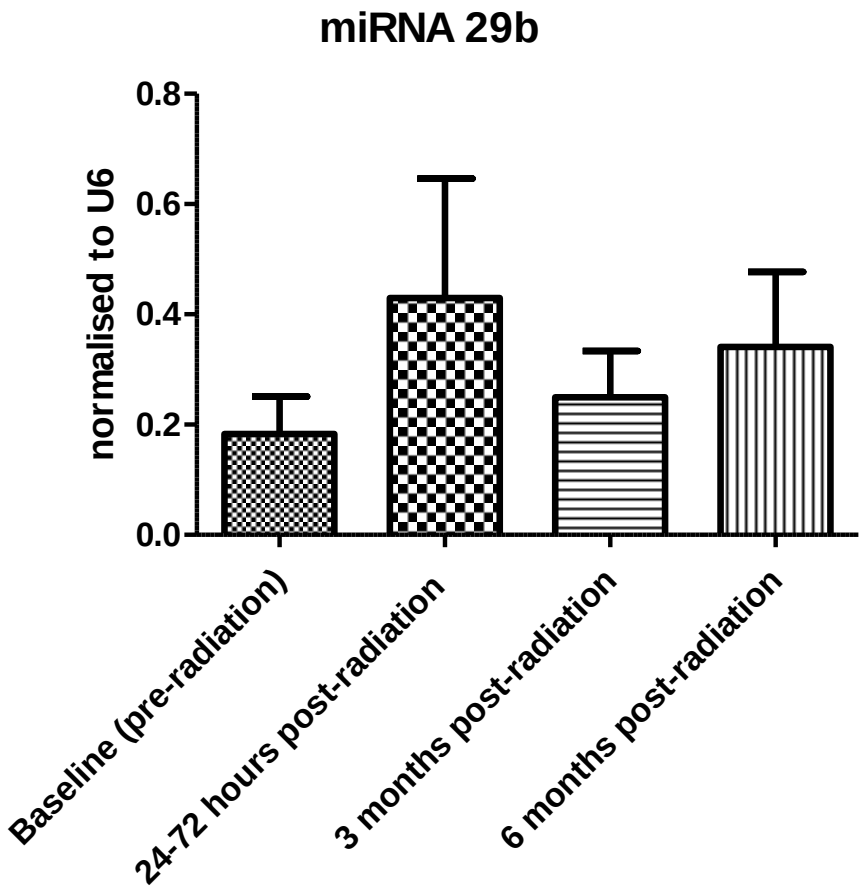

Figure 10a: *Effects of left-sided radiotherapy on breast cancer patients on the expression of miR-29b at different time point A =pre-RT, B =24-72h post first dose of RT, C=3 months post-first dose of RT, D=6 months post-first dose of RT. Expression was determined by quantitative real-time PCR and the data were normalized to U6 as an internal control. Each data point is presented as mean± SEM (A: n=12, B: n=6, C: n=9, D: n=14), (p=0.4050).*

As can be seen in Figure 10a there was minimal variation in the levels of miR-29b between time points A, B, C and D. The ANOVA test revealed no significant difference between the time points (A-B, A-C, B-C, B-D, and C-D). There was no significant change in miR-29b between A and D either as shown in Figure 10b.

Figure 10b: miR-29b changes from time points A to D only

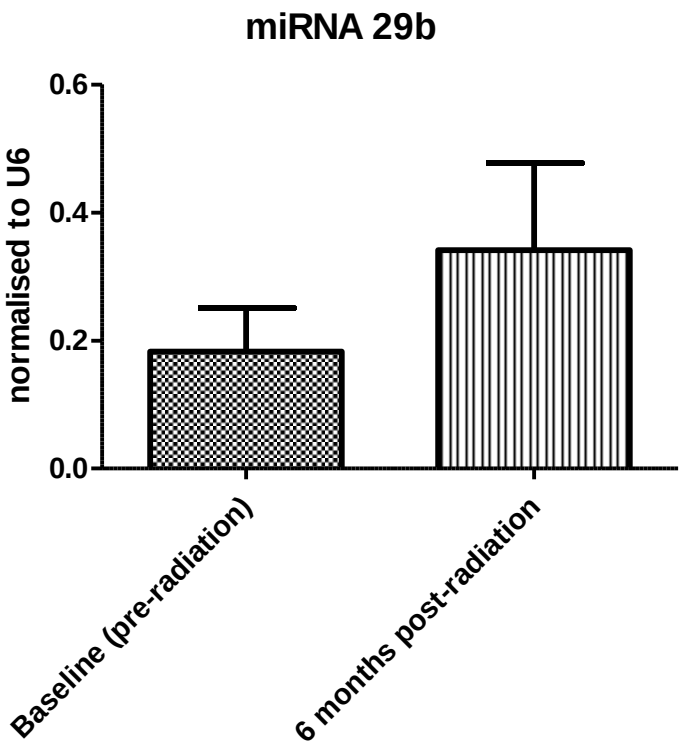

Figure 10b:*Effects of left-sided radiotherapy on breast cancer patients on the expression of miR-29b between time point A (baseline pre-RT reading) (n=12) and D (n=14) (6 months post RT reading) only. Expression was determined by quantitative real-time PCR and the data were normalized to U6 as an internal control. Each data point is presented as mean± SEM (A: n=12 D: n=14) (p=0.5892).*

As seen in Figure 10b, a student's t-test revealed no significant change from A to D (P=0.5892)

Figure 11a: miR-30a expression levels changes over time points A to D

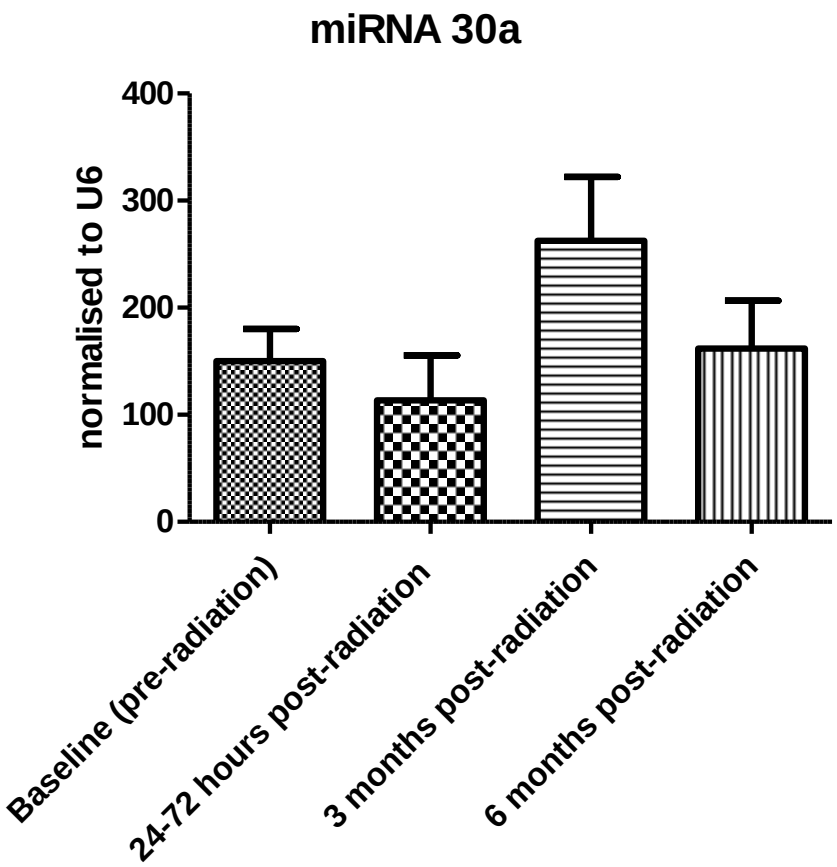

Figure 11a: *Effects of left-sided radiotherapy on breast cancer patients on the expression of miR-30a at different time point A =pre-RT, B =24-72h post first dose of RT, C=3 months post-first dose of RT, D=6 months post-first dose of RT. Expression was determined by quantitative real-time PCR and the data were normalized to U6 as an internal control. Each data point is presented as mean± SEM (A: n=10, B: n=9, C: n=9, D: n=9), (p=0.1128).*

As can be seen in Figure 11a there is not much variation in the levels of miR-30a between time points A, B, C and D. The ANOVA test revealed no significant difference between the time points (A-B, A-C, B-C, B-D, and C-D). There was no significant change in miR-30a between A and D either as shown in Figure 11b.

Figure 11b: miR-30a expression level changes from time points A to D only

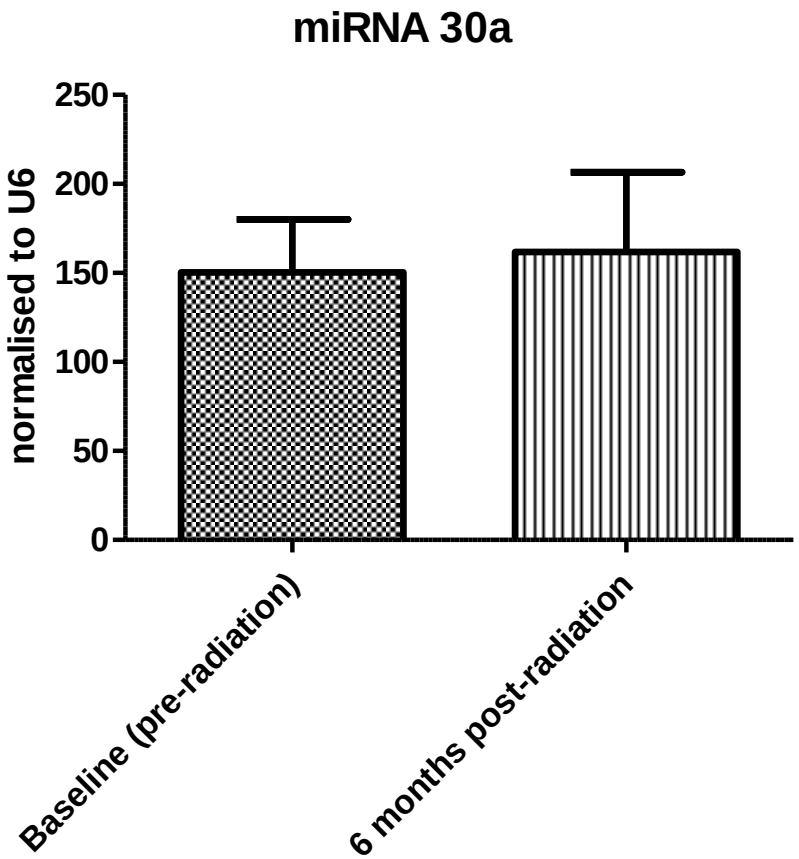

Figure 11b: *Effects of left-sided radiotherapy on breast cancer patients on the expression of miR-30a between time point A (baseline pre-RT reading) (n=10) and D (n=9) (6 months post RT reading) only. Expression was determined by quantitative real-time PCR and the data were normalized to U6 as an internal control. Each data point is presented as mean± SEM (A: n=10 D: n=9) (p=0.7802)*

As seen in Figure 11b, a student's t-test reveals no significant change from A to D

(P=0.7802).

Figure 12a: miR-133a expression levels changes from time point A to D

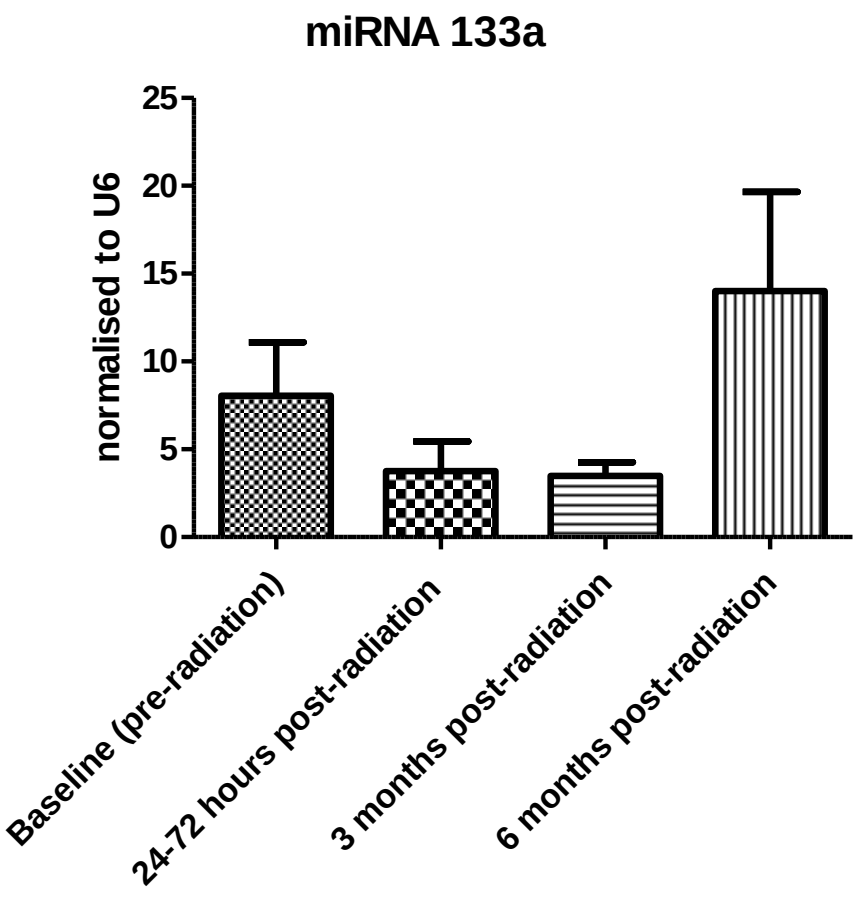

Figure 12a: *Effects of left-sided radiotherapy on breast cancer patients on the expression of miR-133a at different time point A =pre-RT, B =24-72h post first dose of RT, C=3 months post-first dose of RT, D=6 months post-first dose of RT. Expression was determined by quantitative real-time PCR and the data were normalized to U6 as an internal control. Each data point is presented as mean± SEM (A: n=12, B: n=7, C: n=11, D: n=12) (p=0.3443).*

As can be seen in Figure 12a there is no significant variation in the levels of miR-133a between time points A, B, C and D. The ANOVA test revealed no significant difference between the time points (A-B, A-C, B-C, B-D, and C-D). There was no significant change in miR-133a between A and D either as shown in Figure 12b.

Figure 12b: miR-133a changes from A to D only

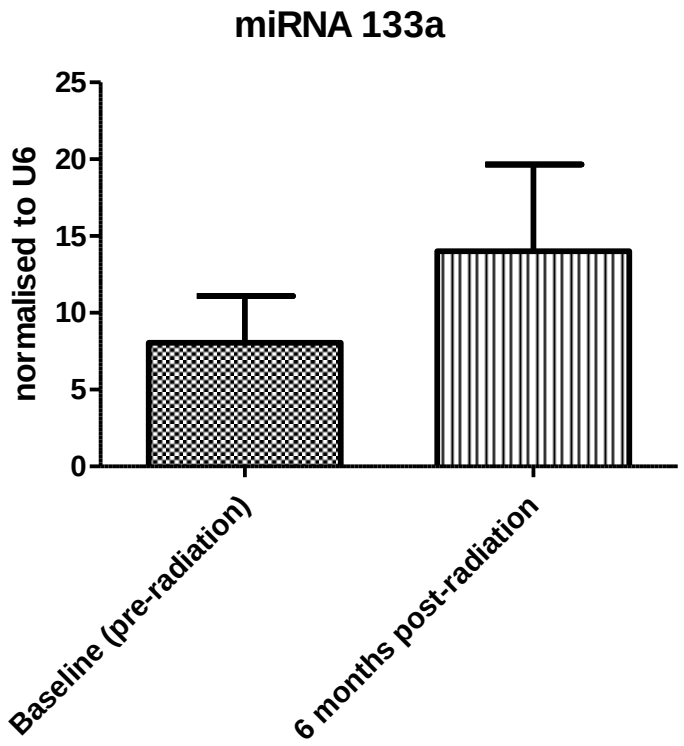

Figure 12b: *Effects of left-sided radiotherapy on breast cancer patients on the expression of miR-133a between time point A (baseline pre-RT reading) (n=12) and D (n=12) (6 months post RT reading) only. Expression was determined by quantitative real-time PCR and the data were normalized to U6 as an internal control. Each data point is presented as mean± SEM (A: n=12, D: n=12) (p=0.4357).*

A students t-test in Fig 12b revealed no significant change from A to D in miR-133a levels (P=0.4357)

Figure 13a: miR-505 expression levels changes from time point A to D

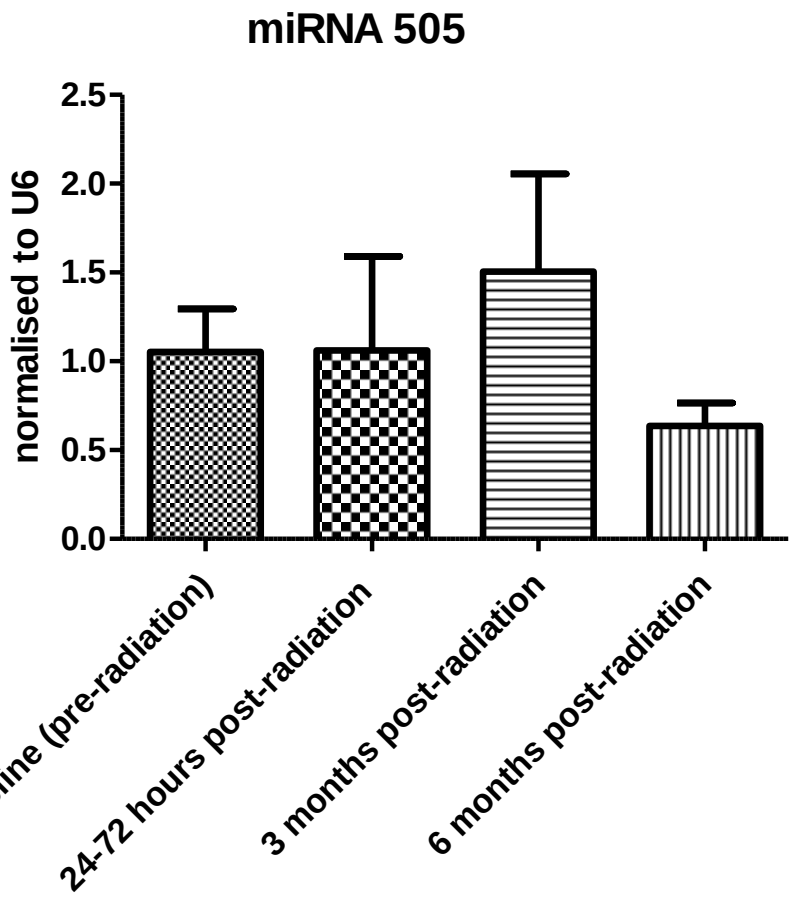

***Figure 13a**: Effects of left-sided radiotherapy on breast cancer patients on the expression of miR-505a at different time point A =pre-RT, B =24-72h post first dose of RT, C=3 months post-first dose of RT, D=6 months post-first dose of RT. Expression was determined by quantitative real-time PCR and the data were normalized to U6 as an internal control. Each data point is presented as mean± SEM (A: n=14, B: n=5, C: n=9, D: n=9), (p=0.2703).*

As can be seen in Figure 13a there is no significant variation in the levels of miR-505 between time points A, B, C and D. The ANOVA test revealed no significant difference between the time points (A-B, A-C, B-C, B-D, and C-D). There was no significant change in miR-505 between A and D either as shown in Figure 13b.

Figure 13b: miR-505a changes from time points A to D only

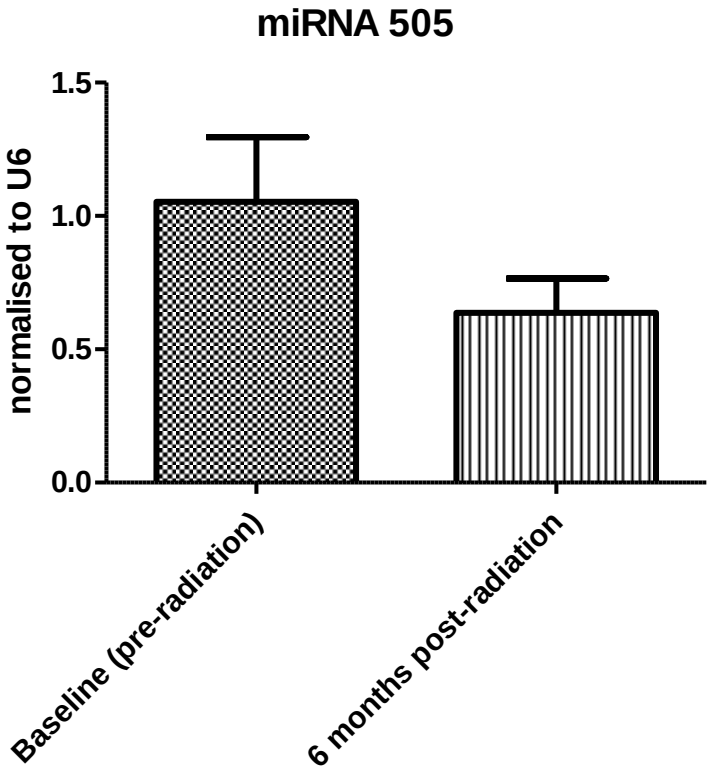

Figure 13b *Effects of left-sided radiotherapy on breast cancer patients on the expression of miR-505 between time point A (baseline pre-RT reading) (n=14) and D (n=9) (6 months post RT reading) only. Expression was determined by quantitative real-time PCR and the data were normalized to U6 as an internal control. Each data point is presented as mean± SEM (A: n=14, D: n=9) (p=0.2703)*

A students t-test in Fig 13b revealed no significant change from A to D in miR-505 levels

(P=0.2703).

Figure 14a: miR-144 expression levels changes from time point A to D

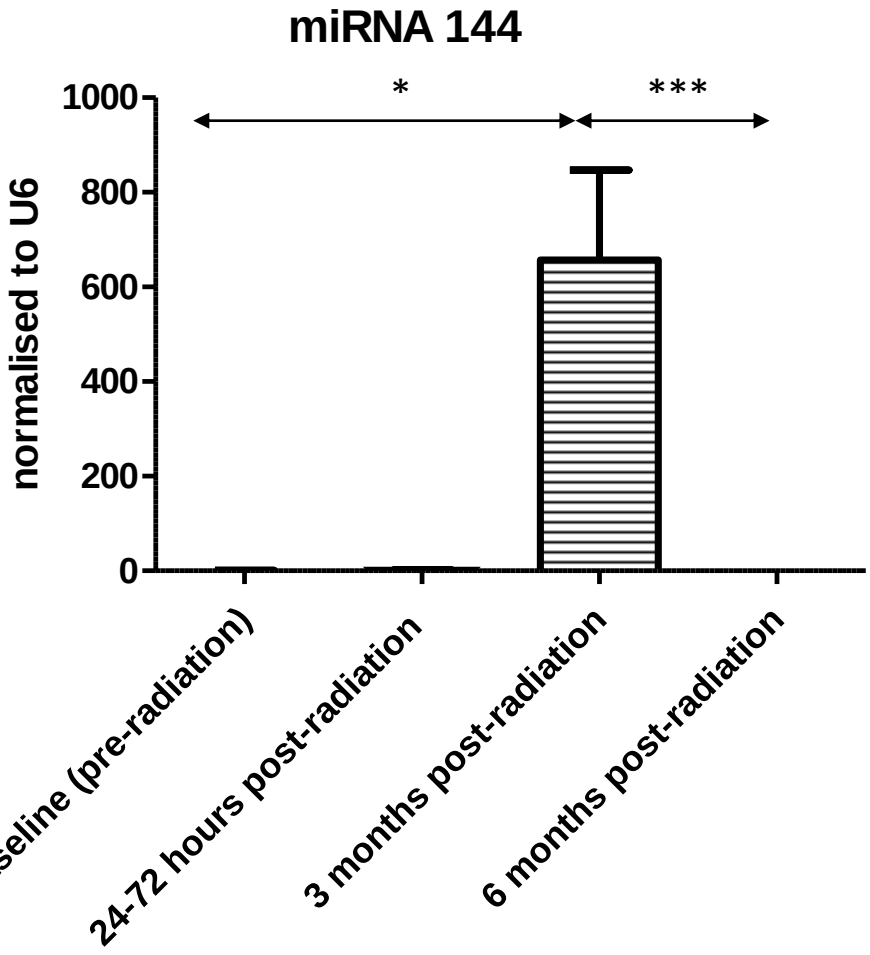

Figure 14a*: Effects of left-sided radiotherapy on breast cancer patients on the expression of miR-144 at different time point A =pre-RT, B =24-72h post first dose of RT, C=3 months post-first dose of RT. D=6 months post-first dose of RT. Expression was determined by quantitative real-time PCR and the data were normalized to U6 as an internal control. Each data point is presented as mean± SEM (A: n=10, B: n=10, C: n=7, D: n=12), (p=<0.0001)*

As can be seen in Figure 14a, there is more than 900 fold increase from A (0.7) to B (656), more than a 465 fold increase from A (0.7) to C (656) accompanied by more than 1600 fold decrease from C (656) to D (0.40). Using the Anova test, the increase from A (n=10) to C (n=7) was found to be statistically significant (p=<0.01) as well as the decrease from C (n=7) to D (n=12) (p=<0.0001).

Figure 14b: miR-144 changes from A to D only

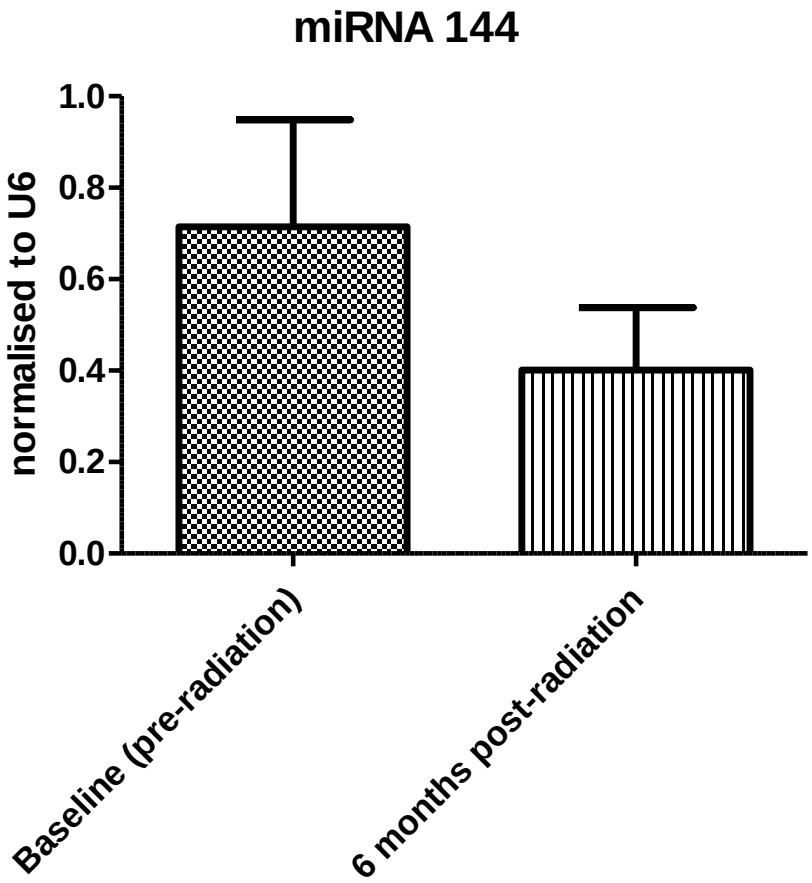

Figure 14b: *Effects of left-sided radiotherapy on breast cancer patients on the expression of miR-144 between time point A (baseline pre-RT reading) (n=10) and D (n=12) (6 months post RT reading) only. Expression was determined by quantitative real-time PCR and the data were normalized to U6 as an internal control. Each data point is presented as mean± SEM (A: n=10, D: n=12) (p=0.1765)*

A students t-test revealed no significant change from A to D in miR-144 (P=0.1765).

Figure 15a: miR-133b expression levels changes from time point A to D

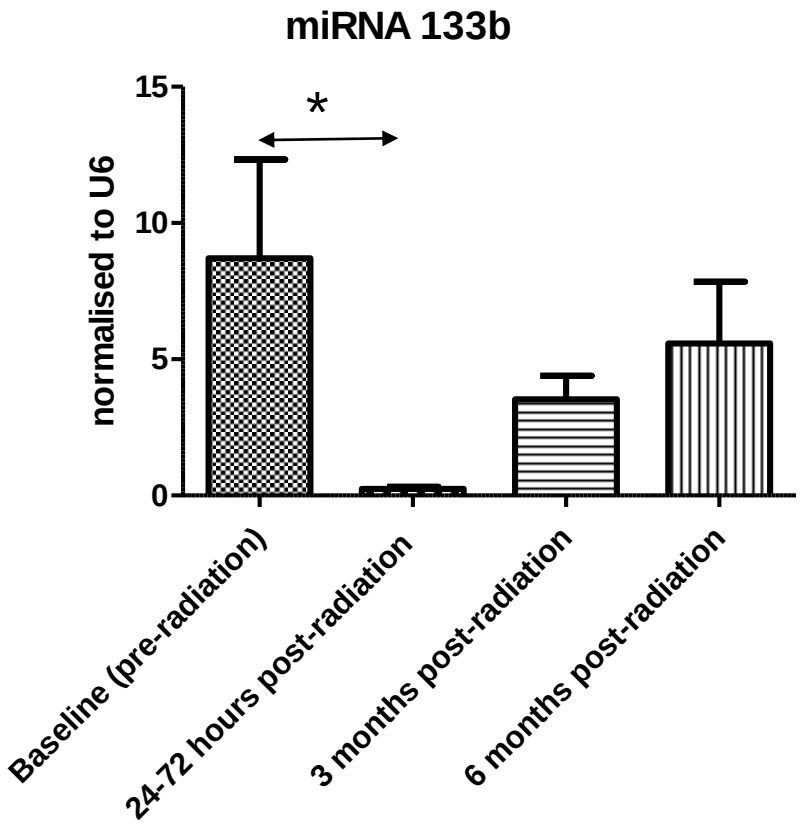

Figure 15a: *Effects of left-sided radiotherapy on breast cancer patients on the expression of miR-133b at different time point A =pre-RT, B =24-72h post first dose of RT, C=3 months post-first dose of RT, D=6 months post-first dose of RT. Expression was determined by quantitative real-time PCR and the data were normalized to U6 as an internal control. Each data point is presented as mean± SEM (A: n=10, B: n=8, C: n=9D: n=7), (p=0.0006).*

miR-133b levels decreased significantly (p=<0.001) from a mean miRNA ratio at time point A (baseline pre-RT) of 8 to 0.2 at time point B (24-72h post RT), which is more than a 40 fold decrease. miRNA levels continued from then on to rise significantly (p=<0.01) as the mean miRNA ratio increased at time point B (0.2) to 3.5 at time point C (3 months post RT) which is an 18 fold increase. From time point B, the mean ratio value of 0.2 was seen to rise significantly (p=<0.01) compared to 5.5 at time point D (6 months post RT) which is a 24 fold increase. A one way ANOVA test revealed the changes between the groups to be significant (P=0.0006). The Tukey test did not reveal the group in which the significant change relied within. The LSD test however showed that the change from A to B was significant (p=0.015).

Figure 15b: miR-133b expression changes from time point A to D only

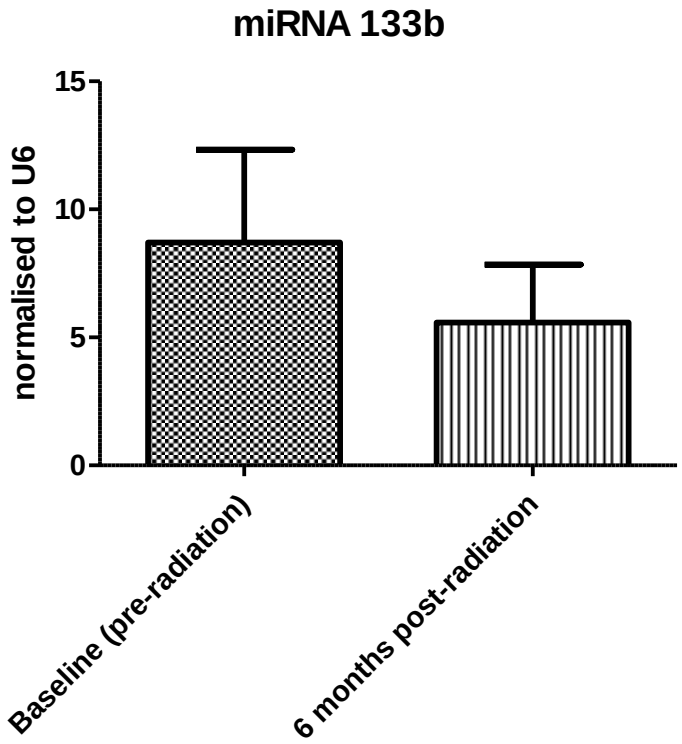

Figure 15b: *Effects of left-sided radiotherapy on breast cancer patients on the expression of miR-133b between time point A (baseline pre-RT reading) (n=10) and D (n=7) (6 months post RT reading) only. Expression was determined by quantitative real-time PCR and the data were normalized to U6 as an internal control. Each data point is presented as mean± SEM (A: n=10, D: n=7) (p=0.8125).*

A student's t-test in Fig 15b revealed no significant change from A to D in miR-133b (P=0.8125)**.**

As can be seen from Figures 10a to 13b the levels of miR-29b, miR-30a, miR-133a, miR-505 did not change significantly from time point A to D neither were they noted to have any significant variation between time point A, B, C or D.

Section 4. Discussion

4.1 Background, Purpose and Results

Though survival rates following BC have improved a great deal over the past few decades, there is a greater long term concern over the adverse effects of treatment, especially as patients live for longer (Chapman et al 2008).

Unfortunately one major risk of radiation is the damaging effect this has on the heart, in particular where cancer patients receive left-sided RT (Darby et al 2013). Cardiac dysfunction due to radiation involves a spectrum of disease processes in patients who have undergone mediastinal, thoracic, or breast RT, and may involve any cardiac structure, including the pericardium, myocardium, valves, conduction system, and coronary arteries (Darby et al 2013). RIHD encompasses a broad spectrum of acute and coronary conditions including perfusion abnormalities, myocardial oedema, scarring and fibrosis, valvular disease, CAD and acute MI (Vasu et al 2013).

There is currently an urgent need to find a more specific, sensitive and clinically valid biomarker which can be used for the earlier detection of RIHD. miRNAs have appeared as ideal candidate biomarkers for early stage RIHD diagnosis due to their non-invasive, fluid-, tissue-, organ- and disease specific nature. To date there is no study which focuses upon the utility of previously recognised cardiovascular disease miRNAs as a marker for RIHD and specifically in the context of left-sided breast irradiation. The aim of this novel work was to thus to evaluate whether miRNAs which have been previously linked to cardiac damage are differentially expressed in BC patients treated for left sided RT and thus could potentially provide clues of cardiotoxic change earlier than imaging or traditional protein based biomarkers.

It is important to note that of the 15 BC patient in this study, none to date have developed clinical signs of cardiotoxicity at their most recent 6 month-review post RT and these patients would not have been reviewed since then unless they became symptomatic for myocardial injury. These patients are however due for their 5 year-review this year where they will be assessed for their cardiac function through clinical history taking, miRNA, CMR imaging, Troponin and BNP analysis once again where their clinical presentation and complaints may be very different. It is important to note that these patients were treated with low doses of RT in a hypofractionated therapy regime which is known to minimise risk of adverse effects of RT (Kim et al 2016). At doses above 30 Gy, radiation related heart disease may occur within a year or two of exposure and risk increases with higher radiotherapy dose, therefore it could be that these patients have undetected signs of myocardial change (Beikei et al 2012). Though these patients received 40 Gy in 15 fractions over 5 weeks, the mean dose to the whole heart, left ventricle, and left coronary artery was 1.4 Gy, 2.0 Gy, and 6.6 Gy, respectively and they were deemed as receiving low-dose radiation where the latent period can be much longer and often be more than a decade (Darby et al 2013).

All patients included in this study had normal levels of Troponin I, below the limit of detection for the assay (<0.04 µg/L). All measures of BNP were also normal (0.6-28.9 pmol/L). CMR imaging results which are a more specific and sensitive measure of stroke volume and ejection fraction compared to echocardiography (Lancelloti et al 2013) showed that patients had no significant changes in stroke volume or EF.

Significant miRNA expression changes were observed when utilising students t-test comparing time point A and D (n=8-15) for: miR-1 (increased nearly 3-fold, p=0.0378), miR-27a (decreased nearly 4-fold, P=0.0464), miR-451 (decreased more than 2-fold, P= 0.0321), and miR-125a (increased more than 3-fold, P=0.0098).miR-144 was also found to be upregulated from A (n=10) to C (n=7) (P≤0.01) and decreased back to baseline levels from C (n=7) to D (n=12) (P≤0.0001). Other statistically significant relationships include a more

than 3-fold increase in the levels of miR-1 from time point B to D ($p=0.002$) and C to D ($p=0.003$). miR-125 levels also increased by more than 2-fold between time points B to D ($p=0.031$). miR-144a levels increased by more than 465-fold from time point A to C ($p<0.01$) and then decreased by more than 1600 fold from time point C to D ($p<0.0001$). miR-133b levels were found to significantly decrease by more than 40-fold between A (n=10) to B (n=8) ($p=0.015$). The expression levels of miR-133a, miR-29b, miR-30a and miR-505 were not altered 6 months post-radiotherapy. The expression of miR-208a was undetectable at all time points in this study (n=7-13).

These 6 candidate markers of cardiovascular disease are all dysregulated in the acute stages of myocardial injury (Darby et al 2013).Our findings might suggest of acute injury incidence detectable by miRNA profiling, which was not picked up by troponin, BNP or imaging, suggesting a more sensitive and specific role of miRNA biomarker detecting RIHD at an early stage. This would allow adjuvant therapy to be administered to aptinets to minimise the risk of cardiac damage and allow for RT regimes to be planned more effectively as treatment progresses to once again minimise the risk of cardiac damage.

Cardiac specific miRNA miR-1is suggested to plan essential role in endothelial function and angiogenesis and cardiac myocyte differentiation. It has previously been reported that miR-1 is a more sensitive biomarker that the gold standard biomarker Troponin in the diagnosis of acute coronary syndrome and is significantly increased in these cases (Ghao et al 2015). In our study miR-1 was also increased which suggests the existence of acute myocardial change in these patients. Depletion of miR-1 levels have also been show to cause a loss of conductivity through potassium channels resulting in cardiac arrhythmias thus an increase in expression levels may be a response to conduction abnormalities a a result of RIHD (Yang et al 2008). Acute coronary syndromes refer to a spectrum of clinical presentations ranging from arrhythmia, MI, and even unstable angina. However the diagnostic value of miR-1 in CAD which is also an important manifestation of RIHD may of limited value. Studies have

found no differential regulation of CAD patients compared to control group patients (Gacori et al 2016).

miR-125a has previously been reported as increased in patients with HF in patients with reduced ejection fraction (Vegter et al 2015). Our study also found levels of miR-125a to rise significantly from the start to the end of RT. Though it is unlikely that patients would have developed HF so promptly, the rise could be suggestive of damage to the myocardium. Interestingly, it has been reported that miR-125a partly regulates the inflammatory response in heart muscle cells and an increase is suggestive of an inflammatory response. It is known that one of the causes of RIHD is the host immune response to radiation which makes miR-125a a particularly valid marker in the contact of RIHD. It is likely therefore that the significant increase in miR-125a was related to the immune response to the radiation hosted by the heart muscle cells in response to the radiation.

A decrease in miR-27a has been shown to increase the production of cardioprotective genes. miR-27a is specifically noted to be an inhibitor of angiotensin converting enzymes (He et al 2011). In fact, it has even been suggested that modulation of mIR-27a could serve as a useful tool in preventing or reducing incidence of cardiovascular disease (Consistent up regulation of miR-27a was found during ischaemic stroke (Sepramaniam et al 2014). Our study agreed with these findings in that levels of miR-27a decreased from the start to the end of radiotherapy. A decrease in miR-27a could be suggestive of damage to the myocytes and therefore a reduction in the proportion of cardioprotective genes. It would be interesting to note whether levels of miR-27a would now be restored to normal levels thus promoting the increase in cardioprotective genes now that much time has elapsed since their last dose of RT. miR-27a as has also been noted to be decreased in cases of acute HF and correlates well with cases of cardiac hypertrophy (He et al 2011).

It has been reported that miR-451 is significantly decreased in cardiovascular disease (Zheng et al 2016). It has also been shown that miR-451 protects against atherosclerotic plaque formation and therefore can protect against CAD. In our study levels of miR-451 were found to significantly decrease, which would be suggestive cardiomyocyte damage, an increase in miR-451 and thus a decrease in the production of cardioprotective genes.

It has been shown that increased levels of miR-144 confer protection against stimulated ischaemia/reperfusion injury induced cardiomyocyte cell death (Zhang et al 2010) . In our study we found that miR-144 levels peaked at 3 months post=RT and then decreased again at 6 months post-RT. Upregulation at time point C would suggest occurrence of cardiomyocyte cell damage which induced miR-144 upregulation after which at time point D, another 3 months post RT, levels again subsided with improving cardiomyocyte cell function (Zhang et al 2010).

We also noted that miR-133b levels were seen to significantly drop at baseline ART and 24-72 hour post RT. Levels then continued to rise from time point B to time point C and D significantly. Upregulation of miR-133b is noted in cases of ischaemic reperfusion injury and an increase is noted to be associated with improved myocyte function and recovery from ischaemia. In our study levels dropped post administration of RT suggesting cardiomyocyte cell damage and the increase in levels between time point B-C and C-D are suggestive of upregulation of mIR-133b as a compensatory mechanism to improve cardiomyocyte function.

We found that within our study miR-208a could not be detected in any time point in any of these samples (N=7-13). The study by Wang et al has shown that miR-208, miR-1 and miR-133 could be detected at an early stage (within a few hours) of the onset of symptoms in the plasma of AMI patients when compared to a control group. However,the expression of miR-208a was undetectable in the control subjects. Furthermore,miR-208a expression was

elevated at anearlier stage than cTnI. Interestingly miR-208a was found to be elevated in all patients whereas cTNI was only detected in 85% of patients.However, a study conducted byD'Alessandra et al showed that miRNA 208a was not detected in all AMI patients. However, this variation compared to the group of Wang et al may have been due to the fact that D'Alessandra et al collected the samples approximately 9 hours post the onset of myocardial injury whereas Wang et al collected them at 4 hours post injury. It is known in the literature that miRNA 208a peaks within the first2 hours of myocardial injury onset and therefore it is valid that no miRNA 208a would have been detected at the 9 hour stage. None of our samples were collected and processed within 1-2 hours post administration of RT and therefore we may have missed the cut off for the differential readings of miR-208a in our clinical samples. This perhaps also demonstrates a limitation with this miRNA, in that though sensitive and specific, only prompt readings would be of any clinical value. However as it is not usually detected this marker could also be useful in the diagnosis of AMI as suggested previously if timed correctly due to its highly specific nature (Wang et al 2010).

The expression levels of miR-133a, miR-29b, miR-30a andmiR-505werenot altered 6 months post-radiotherapy. The expression of miR-208a was undetectable in this study (n=7-13). Though one may initially assume that this means there was no cardiotoxic change as these markers were not differentially regulated, it is more likely that mechanism of RIHD injury did not involve the dysregulation of these microRNAs (Darby et al 2006)

4.2 Limitations of the study

The largest limitation of this study currently is that these patients have not yet had their 5 year review and it is not yet known whether following on from their last 6 month review whether any patients have developed cardiotoxicity. Therefore form our study it cannot be confidently concluded that that differential expression of the miRNAs we observed was due therapy-induced cardiotoxicity.

In this study, a single consultant cardiologist was responsible for reviewing the CMR images. The consultant cardiologist was not informed of the radiation dose and completely blinded to the study but was aware that these patients had been recruited for research purposes as well clinical diagnostic purposes. Although this may ensure a consistent approach to interpretation there are numerous limitations to this approach.

It would also have been advisable to not inform the consultant cardiologist that these patients were recruited into the research study to ensure that the patients were detected for cardiac damage as would any other routine patient. This could cause positive bias in which findings may be overestimated in a bid to estimate findings that may not be objectively present. Secondly, this could lead to negative bias in which findings may be missed by adopting an over-cautious approach. Inter-assay variability may occur whereby simply reviewing images on different days may cause a difference in interpretation and errors. This inter-assay variability could also have occurred in the microRNA analysis phase of the experiments as the plates were run over different days which could have led to experimental errors due to inconsistent laboratory practice. Intra-assay variability in the interpretation of images could have also occurred whereby variation in interpretation occurred from reviewing one scan to another and a 'normal' scan being specific and unique to each individual patient. Intra-assay variability could have also occurred in the microRNA analysis phase as replicates were loaded by hand on each plate and thus experimental errors could have arisen due to variation in pipetting and inaccuracies in the loading of samples.

In an ideal experimental design to add more robustness to the experiment it would be beneficial to have a control group consisting of healthy patient volunteers who do not have cardiovascular disease as disease states such as hypercholesterolaemia are known to cause a differential expression of miRNAs (Chen et al 2015). Furthermore, miRNAs need to be profiled in patients known of suffering from RIHD or TIC in order to confidently ascertain the differential expression of miRNAs due to mechanisms of cancer therapy damage.

This study undoubtedly would also need to be conducted in a larger number of patients in order to clinically validate these results. The N number for our study was 15 and these findings in order to be deemed as clinically applicable would have to be replicated in a much larger patient cohort. Our power calculation has also revealed at the beginning of the study that we required greater than 15 patients per group in order to ensure statistical power to our findings, unfortunately due to patient retention and the fact samples from a larger study were used we could not achieve this. Therefore to add more statistical power we would need more recruits per group.

If more time was available then more time would have been spent on optimising the method. We used 1ml of plasma in our study as this seemed to give us acceptable quality and quantities of detectable miRNAs. However it has been suggested in the literature that 2-3ml of plasma/serum must be processed in order to obtain sufficient miRNA levels (Chen et al 2008).

As will be evident with the results in this study we adopted a stringent process for discarding outliers. There were outliers present within our study which may have been avoided if better experimental technique was used such as quicker processing of samples and reduction in the risk of contamination. Adequate spinning of the samples is key to reducing the proportion of contamination by cellular components (Zampetaki et al 2012).

There are however also several challenges regarding the analysis of circulating miRNAs: short length, unequal melting temperatures, existence of miRNAs which have only single nucleotide differences, and their low abundance High throughput sequencing technologies offer a unique opportunity for detecting and profiling miRNA pools with unprecedented sensitivity. However the cost of these is incredibly high and thus only feasible for a limited number of samples (Chen et al 2008).

For most laboratories however real time PCR as used in this study for the quantification of miRNA remains the gold standard for assessing circulating miRNAs in large clinical studies with its superior sensitivity compared to northern blotting, cloning, primer extension and microarrays (Bartel et al 2004).

4.3 Conclusion

Our study has shown that miR-1, miR-27a, miR-125 and miR-451 were altered from the pre-radiation to the 6 month post-radiation stage in left sided RT BC patients, whereas imaging and circulation cardiac injury protein biomarkers did not change at all. We also showed that miR-144 and miR-133b shows a differential regulation pattern in response to RT. As none of the patients within this study developed clinically diagnosed cardiotoxicity as a result of radiation, the link between RIHD as a cause of these expressional changes cannot be established. However this study does highlight that miRNAs warrant further investigation in larger patient cohorts for potential as early stage biomarkers of RIHD as changes in expression patterns are seen.

4.4 Future Perspectives

In order to now move to clinically validating this technique and measurement of these miRNAs there are a number of steps that need to be taken. The results from these studies would need to be validated in a larger patient cohort. It would also be recommended that miRNA Array analysis be carried out within samples in order to start from the beginning in seeing which miRNA are differentially regulated in RIHD. We chose a panel of 11 microRNAs we knew from the literature were previously associated with cardiovascular disease. However, the mechanism by which RIHD induces heart disease is not fully understood. A lack of understanding of the different pathways may mean that this study did not focus on other miRNAs which may be clinically significant in the context of RIHD and may have been missed, therefore utilising miRNA Array analysis would ensure that many

more miRNAs are checked and screened for an not just those which are linked to cardiovascular disease.

For the use of any biomarker clinically valid cut offs or reference ranged need to be established. Therefore, by investigating values of the microRNAs of interest in healthy patients, patients with different co-morbidities, those with cardiovascular disease, those with cancer, those with RIHD, appropriate reference ranges could be established for each group. Importantly in the context of miRNAs as genomic biomarkers and represented in a huge range of organs and tissues, investigation needs to be carried out to the effect of age, sex and different co-morbidities which have all been noted to cause differential expression in their levels (Darby et al 2013).

There has also been concern in the literature that miRNA signals from BC may interfere with signals from therapy induced cardiotoxicity. By adopting miRNA analysis and investigating the molecular mechanisms further by which microRNA can be dysregulated in BC, other cancers, and therapy induced cardiotoxicity will help broaden our understanding of which microRNAs serve as the best targets for RIHD.

The hope therefore remains that if a panel of specific and sensitive microRNAs to RIHD can be defined with cut offs and reference ranges then microRNAs may indeed prove to become a valid diagnostic tool for early identification and assessment of RIHD instead of using imaging and Troponin and BNP analysis which, as discussed, have their limitations. Clinically this would allow adjuvant therapy to be administered to patients in order to minimise the risk of cardiac damage and allow for RT regimes to be planned more effectively as treatment progresses to prevent RIHD.

Word Count: 15200

Appendix

Table A: Patient 2, 7 and 11 Cq Values obtained from RT-PCR

Target	Sample	Ct	Target	Sample	Ct	Target	Sample	Ct
U6	2A	34.19	U6	7A	38.56	U6	11A	33.45
U6	2A	36.04	U6	7A	39.20	U6	11A	33.40
1	2A		1	7A	32.90	1	11A	32.48
1	2A	35.20	1	7A	32.96	1	11A	32.02
27a	2A	31.13	27a	7A	27.20	27a	11A	31.10
27a	2A	32.41	27a	7A	26.43	27a	11A	31.88
133a	2A	33.54	133a	7A	29.86	133a	11A	30.73
133a	2A	34.76	133a	7A	29.87	133a	11A	29.50
133b	2A		133b	7A		133b	11A	37.02
133b	2A		133b	7A	39.59	133b	11A	37.37
29b	2A	39.07	29b	7A	36.43	29b	11A	38.48
29b	2A		29b	7A	36.29	29b	11A	38.57
30a	2A	26.48	30a	7A	27.49	30a	11A	27.01
30a	2A	27.37	30a	7A	27.78	30a	11A	26.91
208a	2A		208a	7A		208a	11A	
208a	2A		208a	7A	39.87	208a	11A	
505	2A	34.14	505	7A	32.58	505	11A	33.63
505	2A	34.72	505	7A	33.67	505	11A	33.03
144	2A		144	7A	34.35	144	11A	35.33
144	2A		144	7A	34.89	144	11A	34.93
451	2A	24.96	451	7A	24.81	451	11A	23.77
451	2A	25.96	451	7A	23.37	451	11A	24.26
125	2A	30.11	125	7A	27.91	125	11A	26.91
125	2A	31.33	125	7A	27.39	125	11A	27.13
U6	2B	33.17	U6	7B	38.03	U6	11B	Ins
U6	2B	34.11	U6	7B	39.66	U6	11B	Ins
1	2B	36.64	1	7B	33.85	1	11B	Ins
1	2B		1	7B	34.02	1	11B	Ins
27a	2B	29.86	27a	7B	27.84	27a	11B	Ins
27a	2B	29.83	27a	7B	27.33	27a	11B	Ins
133a	2B	32.99	133a	7B	33.12	133a	11B	Ins
133a	2B	34.64	133a	7B	31.51	133a	11B	Ins
133b	2B		133b	7B		133b	11B	Ins
133b	2B		133b	7B	36.44	133b	11B	Ins
29b	2B	38.78	29b	7B	38.39	29b	11B	Ins

29b	2B	38.03	29b	7B	36.88	29b	11B	Ins
30a	2B	27.40	30a	7B	26.32	30a	11B	Ins
30a	2B	27.37	30a	7B	24.04	30a	11B	Ins
208a	2B		208a	7B		208a	11B	Ins
208a	2B		208a	7B		208a	11B	Ins
505	2B	37.12	505	7B	30.75	505	11B	Ins
505	2B	35.33	505	7B	32.16	505	11B	Ins
144	2B		144	7B	37.14	144	11B	Ins
144	2B	35.56	144	7B	38.08	144	11B	Ins
451	2B	24.71	451	7B	25.44	451	11B	Ins
451	2B	24.31	451	7B	24.41	451	11B	Ins
125	2B	29.98	125	7B	27.05	125	11B	Ins
125	2B	27.71	125	7B	27.17	125	11B	Ins
U6	2C	33.03	U6	7C	35.10	U6	11C	31.88
U6	2C	33.22	U6	7C		U6	11C	31.60
1	2C		1	7C	33.40	1	11C	30.35
1	2C	33.84	1	7C	33.53	1	11C	31.91
27a	2C	29.60	27a	7C	28.58	27a	11C	26.81
27a	2C	28.88	27a	7C	28.83	27a	11C	29.02
133a	2C	33.62	133a	7C	32.50	133a	11C	28.46
133a	2C	33.77	133a	7C	32.56	133a	11C	30.13
133b	2C		133b	7C	39.52	133b	11C	36.54
133b	2C	39.01	133b	7C	38.28	133b	11C	38.62
29b	2C	36.17	29b	7C	38.59	29b	11C	36.02
29b	2C	39.16	29b	7C	38.45	29b	11C	36.12
30a	2C	28.58	30a	7C	26.56	30a	11C	27.20
30a	2C	25.06	30a	7C	26.07	30a	11C	26.66
208a	2C		208a	7C		208a	11C	
208a	2C		208a	7C		208a	11C	
505	2C	32.85	505	7C	33.02	505	11C	33.75
505	2C	32.14	505	7C	32.40	505	11C	33.19
144	2C	37.47	144	7C	38.15	144	11C	33.70
144	2C	36.47	144	7C	38.12	144	11C	34.22
451	2C	23.58	451	7C	24.84	451	11C	24.28
451	2C	23.16	451	7C	25.05	451	11C	24.24
125	2C	25.69	125	7C	29.09	125	11C	26.24
125	2C	25.54	125	7C	28.38	125	11C	26.33
U6	2D	36.54	U6	7D	37.90	U6	11D	31.74
U6	2D	35.30	U6	7D	35.00	U6	11D	30.89
1	2D	35.25	1	7D	32.34	1	11D	29.08
1	2D	34.42	1	7D	31.10	1	11D	27.30
27a	2D	30.55	27a	7D	27.35	27a	11D	25.79
27a	2D	29.79	27a	7D	27.19	27a	11D	26.47
133a	2D	33.39	133a	7D	30.55	133a	11D	27.34
133a	2D	33.89	133a	7D	30.75	133a	11D	27.70
133b	2D		133b	7D	37.14	133b	11D	37.39

133b	2D		133b	7D	36.70	133b	11D	35.75
29b	2D	37.89	29b	7D	36.78	29b	11D	34.05
29b	2D		29b	7D	35.53	29b	11D	35.01
30a	2D	30.65	30a	7D	25.46	30a	11D	26.03
30a	2D	28.45	30a	7D	25.40	30a	11D	25.65
208a	2D		208a	7D		208a	11D	
208a	2D		208a	7D		208a	11D	
505	2D	37.07	505	7D	32.33	505	11D	32.27
505	2D	36.07	505	7D	32.30	505	11D	31.35
144	2D	39.96	144	7D	36.70	144	11D	33.59
144	2D	37.36	144	7D	35.28	144	11D	33.55
451	2D	26.31	451	7D	24.35	451	11D	23.47
451	2D	25.83	451	7D	24.32	451	11D	23.49
125	2D	27.77	125	7D	28.48	125	11D	24.01
125	2D	26.72	125	7D	28.34	125	11D	24.19

As can be seen in table A for patient 2, 7 and 11 Cq Values obtained from RT-PCR, as can be seen from this table sample 11b was insufficient for analysis. Furthermore mIR-208a was not detected in these patients

Table B: Patient 12, 13 and 14 Cqvalues as obtained from RT-PCR

Target	Sample	Ct	Target	Sample	Ct	Target	Sample	Ct
U6	12A	33.61	U6	13A	34.07	U6	14A	32.95
U6	12A	32.33	U6	13A	34.27	U6	14A	33.10
1	12A	30.53	1	13A	35.84	1	14A	35.06
1	12A	30.73	1	13A	31.54	1	14A	33.49
27a	12A	26.67	27a	13A	28.93	27a	14A	27.86
27a	12A	26.07	27a	13A	29.67	27a	14A	27.87
133a	12A	30.36	133a	13A	31.00	133a	14A	32.90
133a	12A	29.84	133a	13A	31.81	133a	14A	34.82
133b	12A		133b	13A	34.89	133b	14A	39.18
133b	12A	39.80	133b	13A	38.64	133b	14A	
29b	12A	36.09	29b	13A	37.55	29b	14A	37.61
29b	12A	36.09	29b	13A	38.18	29b	14A	36.38
30a	12A	26.60	30a	13A	28.38	30a	14A	31.28
30a	12A	26.02	30a	13A	28.46	30a	14A	27.19
208a	12A		208a	13A		208a	14A	
208a	12A		208a	13A	39.59	208a	14A	
505	12A	33.80	505	13A	34.65	505	14A	34.36
505	12A	32.31	505	13A	37.23	505	14A	34.10
144	12A	34.82	144	13A	36.34	144	14A	35.75
144	12A	35.33	144	13A	39.91	144	14A	38.17
451	12A	22.89	451	13A	24.52	451	14A	24.50
451	12A	22.20	451	13A	24.26	451	14A	25.21
125	12A	26.68	125	13A	29.27	125	14A	30.88
125	12A	26.50	125	13A	30.36	125	14A	30.21

U6	12B	31.37	U6	13B	32.11	U6	14B	34.25
U6	12B	33.03	U6	13B	30.73	U6	14B	33.76
1	12B	30.01	1	13B	31.75	1	14B	33.80
1	12B	30.82	1	13B	31.79	1	14B	33.88
27a	12B	24.82	27a	13B	29.84	27a	14B	28.73
27a	12B	26.10	27a	13B	29.20	27a	14B	34.00
133a	12B	29.51	133a	13B	33.08	133a	14B	34.13
133a	12B	28.53	133a	13B	33.01	133a	14B	32.89
133b	12B	34.19	133b	13B	37.08	133b	14B	35.61
133b	12B	35.77	133b	13B	35.39	133b	14B	36.61
29b	12B	33.43	29b	13B	37.40	29b	14B	38.68
29b	12B	34.52	29b	13B	37.60	29b	14B	38.06
30a	12B	23.66	30a	13B	27.08	30a	14B	25.54
30a	12B	24.07	30a	13B	27.69	30a	14B	26.19
208a	12B		208a	13B		208a	14B	
208a	12B		208a	13B		208a	14B	
505	12B	32.41	505	13B	39.82	505	14B	31.88
505	12B	32.66	505	13B	34.15	505	14B	31.04
144	12B	33.57	144	13B	31.02	144	14B	32.94
144	12B	33.02	144	13B	35.38	144	14B	
451	12B	22.05	451	13B	22.26	451	14B	22.45
451	12B	22.15	451	13B	23.23	451	14B	21.69
125	12B	25.54	125	13B	28.72	125	14B	29.56
125	12B	25.30	125	13B	29.17	125	14B	29.62
U6	12C	39.57	U6	13C	34.73	U6	14C	33.27
U6	12C	38.08	U6	13C	33.22	U6	14C	31.51
1	12C	33.46	1	13C	29.28	1	14C	35.88
1	12C	31.98	1	13C	30.80	1	14C	33.33
27a	12C	28.22	27a	13C	28.02	27a	14C	27.25
27a	12C	29.41	27a	13C	28.41	27a	14C	27.70
133a	12C	32.85	133a	13C	36.00	133a	14C	30.21
133a	12C	34.91	133a	13C	30.81	133a	14C	32.63
133b	12C		133b	13C	32.55	133b	14C	
133b	12C	38.59	133b	13C	35.15	133b	14C	34.59
29b	12C	36.79	29b	13C	35.38	29b	14C	34.81
29b	12C	35.33	29b	13C	36.36	29b	14C	35.68
30a	12C	28.00	30a	13C	25.58	30a	14C	27.32
30a	12C	26.97	30a	13C	25.49	30a	14C	25.73
208a	12C		208a	13C		208a	14C	
208a	12C		208a	13C		208a	14C	
505	12C	34.37	505	13C	35.88	505	14C	31.71
505	12C	34.49	505	13C	36.15	505	14C	32.81
144	12C	34.23	144	13C	38.00	144	14C	
144	12C	33.42	144	13C	34.04	144	14C	35.23
451	12C	23.73	451	13C	22.43	451	14C	23.45
451	12C	23.78	451	13C	21.53	451	14C	22.85

125	12C	28.14	125	13C	27.71	125	14C	28.20
125	12C	28.21	125	13C	33.17	125	14C	27.22
U6	12D	32.10	U6	13D	26.95	U6	14D	32.87
U6	12D	31.53	U6	13D	26.16	U6	14D	35.12
1	12D	33.04	1	13D	31.12	1	14D	33.64
1	12D	33.06	1	13D	32.33	1	14D	31.28
27a	12D	29.10	27a	13D	29.50	27a	14D	28.56
27a	12D	29.28	27a	13D	27.68	27a	14D	27.35
133a	12D	34.19	133a	13D	30.74	133a	14D	28.87
133a	12D	33.87	133a	13D	30.41	133a	14D	28.13
133b	12D	37.29	133b	13D	39.48	133b	14D	39.80
133b	12D	38.12	133b	13D	39.24	133b	14D	36.82
29b	12D	36.80	29b	13D	35.20	29b	14D	33.15
29b	12D	36.17	29b	13D	35.16	29b	14D	34.02
30a	12D	26.38	30a	13D	25.06	30a	14D	25.08
30a	12D	26.03	30a	13D	23.07	30a	14D	25.76
208a	12D		208a	13D		208a	14D	
208a	12D		208a	13D		208a	14D	
505	12D	33.32	505	13D	32.18	505	14D	39.61
505	12D	33.74	505	13D	31.00	505	14D	33.54
144	12D	32.42	144	13D	30.69	144	14D	30.95
144	12D	32.20	144	13D	29.04	144	14D	31.52
451	12D	22.35	451	13D	19.28	451	14D	22.22
451	12D	22.29	451	13D	19.36	451	14D	23.02
125	12D	28.43	125	13D	28.64	125	14D	27.57
125	12D	28.21	125	13D	30.58	125	14D	26.66

As can be seen in table B for patient 12, 13 and 14 Cq values as obtained from RT-PCR, as can be seen from this table mIR-208a was not detected in these patients.

Table C: Sample 16, 20 and 22 Cq values as obtained by RT-PCR.

Target	Sample	Ct	Target	Sample	Ct	Target	Sample	Ct
U6	16A	32.62	U6	20A	33.26	U6	22A	33.11
U6	16A	32.80	U6	20A	31.65	U6	22A	32.92
1	16A	29.36	1	20A	31.33	1	22A	32.12
1	16A	29.62	1	20A	31.14	1	22A	31.50
27a	16A	23.64	27a	20A	26.51	27a	22A	24.20
27a	16A	24.69	27a	20A	26.08	27a	22A	25.29
133a	16A	27.22	133a	20A	30.40	133a	22A	29.32
133a	16A	27.65	133a	20A	31.06	133a	22A	29.84
133b	16A	36.80	133b	20A	35.70	133b	22A	35.98
133b	16A	33.66	133b	20A	35.79	133b	22A	33.69
29b	16A	31.45	29b	20A	35.09	29b	22A	32.90
29b	16A	32.17	29b	20A	36.08	29b	22A	36.23
30a	16A	26.38	30a	20A	24.76	30a	22A	27.52
30a	16A	25.78	30a	20A	23.94	30a	22A	24.33

208a	16A		208a	20A		208a	22A	38.44
208a	16A	39.15	208a	20A		208a	22A	
505	16A	33.14	505	20A	31.70	505	22A	32.06
505	16A	33.73	505	20A	32.69	505	22A	32.46
144	16A	33.96	144	20A	33.50	144	22A	34.47
144	16A	34.58	144	20A	36.11	144	22A	34.46
451	16A	20.25	451	20A	23.73	451	22A	21.76
451	16A	21.00	451	20A	23.11	451	22A	26.75
125	16A	24.74	125	20A	26.91	125	22A	26.73
125	16A	25.63	125	20A	27.26	125	22A	27.16
U6	16B	26.80	U6	20B	33.00	U6	22B	29.26
U6	16B	26.48	U6	20B	31.10	U6	22B	28.87
1	16B	30.81	1	20B	31.84	1	22B	32.61
1	16B	30.91	1	20B	31.15	1	22B	32.48
27a	16B	28.38	27a	20B	25.18	27a	22B	24.84
27a	16B	27.65	27a	20B	26.05	27a	22B	25.32
133a	16B	31.19	133a	20B	30.40	133a	22B	30.69
133a	16B	29.92	133a	20B	31.04	133a	22B	31.93
133b	16B		133b	20B	37.75	133b	22B	
133b	16B		133b	20B	35.89	133b	22B	
29b	16B	37.94	29b	20B	32.93	29b	22B	37.93
29b	16B	36.72	29b	20B	38.80	29b	22B	
30a	16B	25.72	30a	20B	25.71	30a	22B	23.17
30a	16B	28.73	30a	20B	26.14	30a	22B	22.31
208a	16B		208a	20B		208a	22B	
208a	16B		208a	20B		208a	22B	
505	16B	33.31	505	20B	33.98	505	22B	31.99
505	16B	36.40	505	20B	35.74	505	22B	33.43
144	16B		144	20B	31.79	144	22B	29.81
144	16B	36.06	144	20B	35.82	144	22B	28.71
451	16B	24.07	451	20B	23.71	451	22B	18.41
451	16B	24.42	451	20B	23.83	451	22B	19.26
125	16B	27.30	125	20B	27.26	125	22B	27.71
125	16B	29.90	125	20B	27.02	125	22B	28.44
U6	16C	31.13	U6	20C	25.19	U6	22C	31.53
U6	16C	31.01	U6	20C	25.32	U6	22C	30.91
1	16C	29.26	1	20C	31.90	1	22C	33.05
1	16C	29.43	1	20C	32.36	1	22C	32.75
27a	16C	27.22	27a	20C	25.31	27a	22C	25.25
27a	16C	26.40	27a	20C	24.32	27a	22C	26.38
133a	16C	31.53	133a	20C	30.31	133a	22C	31.07
133a	16C	28.68	133a	20C	30.65	133a	22C	32.67
133b	16C	39.64	133b	20C	35.63	133b	22C	39.47
133b	16C		133b	20C	35.52	133b	22C	
29b	16C		29b	20C	33.19	29b	22C	
29b	16C		29b	20C		29b	22C	33.66

30a	16C	28.49	30a	20C	24.77	30a	22C	25.26
30a	16C	27.02	30a	20C	23.79	30a	22C	25.71
208a	16C		208a	20C		208a	22C	
208a	16C		208a	20C		208a	22C	
505	16C	37.34	505	20C	33.60	505	22C	32.67
505	16C	33.77	505	20C	38.25	505	22C	34.15
144	16C	33.51	144	20C	33.02	144	22C	37.27
144	16C	38.75	144	20C	28.80	144	22C	36.32
451	16C	20.11	451	20C	19.73	451	22C	24.29
451	16C	18.67	451	20C	21.75	451	22C	24.88
125	16C	25.74	125	20C	26.91	125	22C	26.89
125	16C	24.30	125	20C	28.22	125	22C	26.90
U6	16D	33.02	U6	20D	28.69	U6	22D	32.37
U6	16D	31.74	U6	20D	29.29	U6	22D	32.49
1	16D	29.19	1	20D	33.45	1	22D	32.52
1	16D	29.42	1	20D	34.02	1	22D	32.82
27a	16D	27.09	27a	20D	27.68	27a	22D	26.47
27a	16D	26.21	27a	20D	28.06	27a	22D	28.27
133a	16D	29.24	133a	20D	32.87	133a	22D	31.43
133a	16D	28.20	133a	20D	31.72	133a	22D	30.98
133b	16D		133b	20D		133b	22D	37.86
133b	16D	36.51	133b	20D		133b	22D	39.04
29b	16D	37.49	29b	20D	35.17	29b	22D	36.22
29b	16D		29b	20D	35.86	29b	22D	37.01
30a	16D	34.07	30a	20D	30.82	30a	22D	24.77
30a	16D	28.29	30a	20D	34.35	30a	22D	26.18
208a	16D		208a	20D		208a	22D	
208a	16D		208a	20D		208a	22D	
505	16D	35.71	505	20D	34.68	505	22D	35.93
505	16D	33.98	505	20D	34.38	505	22D	31.58
144	16D	37.10	144	20D	33.83	144	22D	37.02
144	16D	38.49	144	20D	38.23	144	22D	39.86
451	16D	24.65	451	20D	24.20	451	22D	26.11
451	16D	27.81	451	20D	22.11	451	22D	25.07
125	16D	25.64	125	20D	29.12	125	22D	30.55
125	16D	26.39	125	20D	29.46	125	22D	27.64

As can be seen in table c for Sample 16, 20 and 22 Cq values as obtained by RT-PCR, as can beseen from this table mIR-208a could not be detected in any of these samples.

Table D: Patient 23, 26 and 29 Ct values as obtained by RT PCR

Target	Sample	Ct	Target	Sample	Ct	Target	Sample	Ct
U6	23A	33.29	U6	26A	31.56	U6	29A	31.04
U6	23A	33.58	U6	26A	33.52	U6	29A	29.81
1	23A	31.57	1	26A	33.33	1	29A	31.67

1	23A	32.14	1	26A	33.93	1	29A	32.53
27a	23A	25.38	27a	26A	27.19	27a	29A	28.50
27a	23A	24.89	27a	26A	27.29	27a	29A	26.44
133a	23A	31.01	133a	26A	31.55	133a	29A	31.42
133a	23A	29.57	133a	26A	31.75	133a	29A	
133b	23A	32.74	133b	26A	35.26	133b	29A	35.47
133b	23A	33.43	133b	26A	35.09	133b	29A	
29b	23A	33.57	29b	26A	33.70	29b	29A	35.94
29b	23A	34.51	29b	26A	34.73	29b	29A	35.21
30a	23A	24.12	30a	26A	25.67	30a	29A	28.33
30a	23A	24.20	30a	26A	25.45	30a	29A	27.71
208a	23A		208a	26A		208a	29A	
208a	23A		208a	26A	39.03	208a	29A	
505	23A	31.54	505	26A	34.11	505	29A	32.88
505	23A	31.73	505	26A	34.26	505	29A	33.16
144	23A	32.98	144	26A	32.37	144	29A	29.23
144	23A	32.87	144	26A	32.58	144	29A	29.45
451	23A	23.08	451	26A	24.70	451	29A	21.30
451	23A	23.02	451	26A	24.54	451	29A	20.71
125	23A	26.54	125	26A	30.29	125	29A	26.69
125	23A	26.79	125	26A	29.31	125	29A	28.25
U6	23B	34.33	U6	26B	30.49	U6	29B	
U6	23B	33.05	U6	26B	31.11	U6	29B	37.68
1	23B	32.29	1	26B	34.27	1	29B	28.97
1	23B	31.78	1	26B	33.85	1	29B	28.49
27a	23B	26.24	27a	26B	27.26	27a	29B	25.02
27a	23B	26.36	27a	26B	26.99	27a	29B	25.56
133a	23B	30.96	133a	26B	30.28	133a	29B	29.29
133a	23B	34.29	133a	26B	30.69	133a	29B	36.35
133b	23B	35.54	133b	26B	33.05	133b	29B	38.10
133b	23B		133b	26B	33.93	133b	29B	38.38
29b	23B	33.24	29b	26B	32.76	29b	29B	34.17
29b	23B	33.44	29b	26B	33.30	29b	29B	
30a	23B	33.53	30a	26B	25.53	30a	29B	26.59
30a	23B	27.62	30a	26B	25.39	30a	29B	24.11
208a	23B		208a	26B	39.15	208a	29B	
208a	23B		208a	26B		208a	29B	
505	23B	32.29	505	26B	34.10	505	29B	31.01
505	23B	31.97	505	26B	32.94	505	29B	31.63
144	23B	32.47	144	26B	30.38	144	29B	32.68
144	23B		144	26B	30.34	144	29B	32.20
451	23B	22.39	451	26B	21.98	451	29B	22.78
451	23B	22.52	451	26B	22.03	451	29B	23.09
125	23B	26.72	125	26B	28.24	125	29B	25.94
125	23B	27.29	125	26B	28.43	125	29B	26.93
U6	23C	33.49	U6	26C	34.26	U6	29C	36.96

U6	23C	32.57	U6	26C	33.72	U6	29C	32.38
1	23C	33.10	1	26C	33.93	1	29C	29.06
1	23C	33.17	1	26C	33.34	1	29C	29.73
27a	23C	26.41	27a	26C	28.27	27a	29C	28.13
133a	23C	30.90	133a	26C	30.44	133a	29C	28.67
133a	23C	31.94	133a	26C	32.53	133a	29C	27.83
133b	23C		133b	26C	36.23	133b	29C	
133b	23C	39.06	133b	26C	36.17	133b	29C	33.20
29b	23C		29b	26C	35.75	29b	29C	36.09
29b	23C	35.19	29b	26C	35.66	29b	29C	36.25
30a	23C	35.25	30a	26C	25.94	30a	29C	30.11
30a	23C		30a	26C	26.28	30a	29C	24.02
208a	23C		208a	26C		208a	29C	
208a	23C		208a	26C		208a	29C	39.71
505	23C	32.99	505	26C	32.22	505	29C	30.62
505	23C	33.59	505	26C	33.61	505	29C	30.97
144	23C	33.44	144	26C	33.70	144	29C	35.48
144	23C	37.79	144	26C	33.04	144	29C	35.11
451	23C	24.74	451	26C	23.75	451	29C	23.50
451	23C	27.00	451	26C	23.35	451	29C	25.72
125	23C	27.25	125	26C	27.52	125	29C	26.61
125	23C	27.42	125	26C	27.47	125	29C	26.44
U6	23D	32.35	U6	26D	29.12	U6	29D	31.69
U6	23D	33.27	U6	26D	29.00	U6	29D	30.23
1	23D	31.90	1	26D	32.38	1	29D	29.59
1	23D	32.09	1	26D	32.03	1	29D	30.91
27a	23D	27.01	27a	26D	26.08	27a	29D	30.16
27a	23D	26.97	27a	26D	26.22	27a	29D	
133a	23D	32.42	133a	26D	29.16	133a	29D	28.36
133a	23D	34.10	133a	26D	29.85	133a	29D	29.74
133b	23D	35.41	133b	26D	33.10	133b	29D	
133b	23D	33.53	133b	26D	32.55	133b	29D	37.50
29b	23D		29b	26D	32.42	29b	29D	37.01
29b	23D	33.85	29b	26D	32.53	29b	29D	37.62
30a	23D	25.76	30a	26D	23.00	30a	29D	29.05
30a	23D	26.77	30a	26D	22.47	30a	29D	28.77
208a	23D		208a	26D		208a	29D	
208a	23D		208a	26D		208a	29D	
505	23D	31.91	505	26D	31.17	505	29D	32.31
505	23D	32.93	505	26D	30.99	505	29D	32.99
144	23D	33.00	144	26D	25.78	144	29D	33.77
144	23D	34.67	144	26D	25.96	144	29D	35.32
451	23D	27.56	451	26D	17.99	451	29D	26.10
451	23D	25.36	451	26D	17.99	451	29D	24.15
125	23D	30.34	125	26D	27.53	125	29D	28.06
125	23D	26.54	125	26D	26.54	125	29D	26.02

As can be seen in table D for patient 23, 26 and 29 Ct values as obtained by RT PCR, as can be seen from this table mIR-208 could not be detected in these samples.

Table E: Patient 30, 31 and 32 CT values as obtained by RT-PCR.

Target	Sample	Ct	Target	Sample	Ct	Target	Sample	Ct
U6	30A	30.97	U6	31A	31.22	U6	32A	
U6	30A	33.28	U6	31A	31.19	U6	32A	33.12
1	30A	31.74	1	31A	31.81	1	32A	37.58
1	30A	35.01	1	31A	33.61	1	32A	35.33
27a	30A	28.04	27a	31A	30.30	27a	32A	30.69
27a	30A	30.48	27a	31A	31.01	27a	32A	31.30
133a	30A	33.07	133a	31A	32.49	133a	32A	35.74
133a	30A	32.88	133a	31A	32.93	133a	32A	34.05
133b	30A	37.02	133b	31A	34.19	133b	32A	39.89
133b	30A	37.41	133b	31A	33.40	133b	32A	37.87
29b	30A	37.20	29b	31A		29b	32A	
29b	30A		29b	31A		29b	32A	38.87
30a	30A	25.34	30a	31A	26.19	30a	32A	29.48
30a	30A	25.36	30a	31A	32.64	30a	32A	28.43
208a	30A		208a	31A		208a	32A	
208a	30A		208a	31A		208a	32A	
505	30A	32.18	505	31A	33.33	505	32A	35.03
505	30A	32.05	505	31A	32.37	505	32A	34.75
144	30A	35.52	144	31A	36.75	144	32A	
144	30A	34.65	144	31A	35.50	144	32A	
451	30A	24.16	451	31A	24.33	451	32A	29.12
451	30A	24.02	451	31A	23.56	451	32A	27.33
125	30A	27.12	125	31A	34.12	125	32A	29.27
125	30A	27.62	125	31A	30.16	125	32A	30.04
U6	30B		U6	31B	31.58	U6	32B	29.84
U6	30B		U6	31B		U6	32B	
1	30B		1	31B	35.81	1	32B	33.95
1	30B	39.09	1	31B	35.42	1	32B	33.86
27a	30B	30.86	27a	31B	28.36	27a	32B	29.76
27a	30B	32.23	27a	31B	28.73	27a	32B	28.68
133a	30B	34.33	133a	31B	31.49	133a	32B	33.28
133a	30B	34.72	133a	31B	32.71	133a	32B	34.95
133b	30B		133b	31B	33.81	133b	32B	37.61
133b	30B		133b	31B	34.60	133b	32B	38.06
29b	30B	38.27	29b	31B		29b	32B	37.18
29b	30B		29b	31B	37.43	29b	32B	38.31
30a	30B	28.03	30a	31B	26.74	30a	32B	26.93
30a	30B	27.17	30a	31B	27.25	30a	32B	26.49

208a	30B		208a	31B		208a	32B	
208a	30B		208a	31B		208a	32B	
505	30B	33.51	505	31B	31.49	505	32B	33.05
505	30B	33.34	505	31B	32.58	505	32B	32.74
144	30B	35.18	144	31B	36.31	144	32B	39.33
144	30B	35.76	144	31B	39.63	144	32B	36.65
451	30B	23.60	451	31B	23.33	451	32B	25.77
451	30B	24.97	451	31B	24.40	451	32B	24.70
125	30B	30.01	125	31B	28.74	125	32B	26.49
125	30B	31.10	125	31B	25.03	125	32B	27.07
U6	30C	35.97	U6	31C		U6	32C	
U6	30C	38.05	U6	31C		U6	32C	33.79
1	30C		1	31C	35.18	1	32C	36.61
1	30C	38.45	1	31C	34.27	1	32C	34.43
27a	30C	31.68	27a	31C	28.80	27a	32C	29.89
27a	30C	31.21	27a	31C	29.16	27a	32C	29.86
133a	30C	36.11	133a	31C	30.96	133a	32C	36.68
133a	30C	37.04	133a	31C	33.74	133a	32C	33.86
133b	30C		133b	31C	34.17	133b	32C	36.51
133b	30C		133b	31C	37.75	133b	32C	37.62
29b	30C	38.73	29b	31C	37.41	29b	32C	
29b	30C		29b	31C	36.51	29b	32C	
30a	30C	28.36	30a	31C		30a	32C	26.05
30a	30C	28.11	30a	31C	27.01	30a	32C	26.29
208a	30C		208a	31C		208a	32C	
208a	30C		208a	31C		208a	32C	
505	30C	33.05	505	31C	33.11	505	32C	35.77
505	30C	33.66	505	31C	31.72	505	32C	34.34
144	30C	33.87	144	31C	35.03	144	32C	37.47
144	30C	35.02	144	31C	37.49	144	32C	39.43
451	30C	25.26	451	31C	24.20	451	32C	24.21
451	30C	24.19	451	31C	25.72	451	32C	24.59
125	30C	29.97	125	31C	28.17	125	32C	26.68
125	30C	29.46	125	31C	27.89	125	32C	26.93
U6	30D	37.93	U6	31D	36.53	U6	32D	30.96
U6	30D	32.75	U6	31D		U6	32D	34.70
1	30D	37.81	1	31D	34.35	1	32D	35.02
1	30D		1	31D	31.97	1	32D	31.14
27a	30D	29.05	27a	31D	32.39	27a	32D	31.78
27a	30D	31.10	27a	31D	31.17	27a	32D	28.24
133a	30D	32.33	133a	31D	33.60	133a	32D	31.78
133a	30D	33.74	133a	31D	31.84	133a	32D	30.14
133b	30D	38.49	133b	31D		133b	32D	33.54
133b	30D		133b	31D	39.69	133b	32D	32.99
29b	30D		29b	31D		29b	32D	38.68
29b	30D	37.21	29b	31D	38.18	29b	32D	38.36

30a	30D	27.81	30a	31D	28.81	30a	32D	25.92
30a	30D	28.43	30a	31D	28.78	30a	32D	25.49
208a	30D		208a	31D		208a	32D	38.60
208a	30D		208a	31D	39.04	208a	32D	
505	30D	33.52	505	31D	31.50	505	32D	34.57
505	30D	33.92	505	31D	32.06	505	32D	33.85
144	30D	35.16	144	31D	36.49	144	32D	35.54
144	30D	35.15	144	31D	36.65	144	32D	35.26
451	30D	22.92	451	31D	32.38	451	32D	22.65
451	30D	24.71	451	31D	25.28	451	32D	23.51
125	30D	29.39	125	31D	30.45	125	32D	29.09
125	30D	31.68	125	31D	29.31	125	32D	27.57

As can be seen in table E for patient 30, 31 and 32 CT values as obtained by RT-PCR. As can be seen from this table mIR-208a could not be detected in these samples.

References

Adachi, T., Nakanishi, M., Otsuka, Y., Nishimura, K., Hirokawa, G., Goto, Y., Nonongi, H., Iwai, N. (2010) 'Plasma microRNA 499 as a biomarker of acute myocardial infarction. Clinical Chemistry [online] 56, 1183-1185 <http://clinchem.aaccjnls.org/content/56/7/1183?ijkey=9c2b37d405aecfb642b08d194fac6a84fb73f389&keytype2=tf_ipsecsha> [1st September 2017]

Bartel, D. P. (2004) 'MicroRNAs: genomics, biogenesis, mechanism, and function'. Cell [online] 116, 281–297 available at <https://www.ncbi.nlm.nih.gov/pubmed/14744438>[29 September 2015]

Beiki, O., Hall, P., Elbom, A., Moradi, T (2012) 'Breast cancer incidence and case fatality among 4.7 million women in relation to social and ethnic background: a population-based cohort study'. Breast Cancer Research [online] 14(1), 1-13 available from <https://www.ncbi.nlm.nih.gov/pmc/articles/PMC3496120/pdf/bcr3086.pdf>?> [1November 2015]

Bovelli, D., Plataniotis, G., Roila, F (2010) 'Cardiotoxicity of chemotherapeutic agents and radiotherapy-related heart disease: ESMO Clinical Practice Guidelines' Annals of Oncology [online] 21(5) 277-282 available from <https://oup.silverchair-cdn.com/oup/backfile/Content_public/Journal/annonc/21/suppl_5/10.1093/annonc/mdq200/2/mdq200.pdf?Expires=1495054225&Signature=OmZ8FVeSVNG4FcRrm9aUXuKkvfIflzzSVgg6Op2UFk2vOQanuiiiWrzFRssV9wLdqOKf6nog4McnKBd~q7ij8iIKhhZypDGYEoh6ysV2Ia0T9EMvRqdBq6GKNPBDPYgWJF-i6EhsRc1J3DwByLWRViOOkB7yTP6CyeBn--T8VVnJiJvjih6NfU9URRmsrxGeIZg2GYC9SGYwIi9ZOIozkYKyBeGY-~asJMYSRbA4-1v3nq4NAfbDKtg5xc9K8PL5a5WSqIxedKSMf15sRYMfhcUis-CSqtjVUmVCAQ6EvO148xAvapFM4DivnvF1TGLeKQvz-rteKkPmYcXTvhBpyQ__&Key-Pair-Id=APKAIUCZBIA4LVPAVW3Q?? [3 May 2017]

Brosius, F., Waller, B., Roberts, W (1981) Radiation heart disease. Analysis of 16 young (aged 15 to 33 years) necropsy patients who received over 3,500 rads to the heart. American Journal of Medicine [online] 70(3), 519-525 available from <https://www.ncbi.nlm.nih.gov/pubmed/6782873> [17th September 2017]

Chapman, J., Meng, D., Shepherd, L., Parulekar, W., Ingle, J., Muss, H., Palmer, M (2008) Journal of National Cancer Institute [online] 100(4), 252-260 available from <https://www.ncbi.nlm.nih.gov/pubmed/18270335> [27 May 2017]

Chen, J. F., Mandel, E. M., Thomson, J. M., Wu, Q., Callis, T. E.,Hammond, S. M., Conlon, F. L. and Wang, D. Z. (2006) The role of microRNA-1 and microRNA-133 in skeletal muscle proliferation and differentiation. Nat. Genet. 38, 228–233

Collinson, P. O., Boa, F. G. and Gaze, D. C. (2005) Measurement of cardiac troponins. Annals of Clinical Biochemistry [online] 38, 423–449 available from <https://ccforum.biomedcentral.com/articles/10.1186/cc3776> [2 May 2017]

Corsten, M. F., Dennert, R., Jochems, S., Kuznetsova, T.,
Devaux, Y., Hofstra, L., Wagner, D. R., Staessen, J. A.,
Heymans, S. and Schroen, B. (2010) Circulating microRNA-208b and microRNA-499 reflect myocardial damage in cardiovascular disease. Circ. Cardiovasc. Genet. 3, 499–506

Carr, Z., Land, C., Kleinerman, R., Weinstock, R., Stovall, M., Griem, M., Mabuchi, K (2005) 'Coronary heart disease after radiotherapy for breast cancer' International Journal of Radiation Oncology, Biology and Physics 61(3), 842-850 available from <https://www.ncbi.nlm.nih.gov/pubmed/15708264? [7 April 2017]

Chen, J. F., Mandel, E. M., Thomson, J. M., Wu, Q., Callis, T. E.,
Hammond, S. M., Conlon, F. L. and Wang, D. Z. (2006) The role of microRNA-1 and microRNA-133 in skeletal muscle proliferation and differentiation. Nat. Genet. 38, 228–233

Cutuli, B., Lemaniski, C., Fourquet, A., Lafontan, B., Giard, S. (2009) British Journal of Cancer [online] 100(7), 1048-1054 available at https://www.ncbi.nlm.nih.gov/pmc/articles/PMC2670007/> [3rd March 2016]
D'Alessandra YDevanna P, Limana F, Straino S, Di Carlo A, Brambilla PG, Rubino M, Carena MC, Spazzafumo L, De Simone M, Micheli B, Biglioli P, Achilli F, Martelli F, Maggiolini S, Marenzi G, Pompilio G, Capogrossi MC (2017) Circulating microRNAs are new and sensitive biomarkers of myocardial infarction. European Heart Journal [online] 31(22):2765-73 available from <https://www.ncbi.nlm.nih.gov/pubmed/20534597> [10 May 2017]

Devaux, Y., Hofstra, L., Wagner, D. R., Staessen, J. A.,

Heymans, S. and Schroen, B. (2010) Circulating microRNA-208b and microRNA-499 reflect myocardial damage in cardiovascular disease. Circ. Cardiovasc. Genet. 3, 499–506

Darby, S., Ewertz, M., McGale, P., Bennet, A., Blom-Goldman, A, Cutter, D., Gangliardi, G., Gigante, G., Hensen M. Nisbet, A, Peto, R, Rahimi, K., Taylor, C (2013) Risk of Ischemic Heart Disease in Women after Radiotherapy for Breast Cancer. The New England Journal of Medicine [online] 368, 978-998 available from <http://www.nejm.org/doi/full/10.1056/NEJMoa1209825? [3 May 2017]

Dimov, I., Jankovic, V. L. and Stefanovic, V. (2009) Urinary exosomes. Sci. World J. 9, 1107–1118

Donnellan, E., Phelan, D., McCarthy, C., Collier, P., Desai, M., Griffin, B (2016) 'Radiation-induced heart disease; A practical guide to diagnosis and management. Cleveland Clinic Journal of Medicine 83(12), 914-922 [online] available from <http://www.mdedge.com/sites/default/files/issues/articles/Donnellan_Radiation-InducedHeartDisease.pdf> [14th May 2017]

Etheridge, A., Lee, I., Hood, L., Galas, D. and Wang, K. (2011) Extracellular microRNA: a new source of biomarkers. Mutat. Res. 717, 85–90

Erven, K., Weltens, J., Giusca, S., Ector, J., Wildiers, H., Bogaert, V., Voigt, J (2011) Acute radiation effects on cardiac function detected by strain rate imaging in breast cancer patients'. International Journal of Radiation oncology, Biology and Physics [online] 79 (5), 1444-51 available at <https://www.ncbi.nlm.nih.gov/pubmed/20605341> [1 March 2017]

Ferlay, J., Stelia-Foucher, E., Lortet-Tieulent, J., Rosso, S., Coebergh, J., Comber, H., Forman, D., Bray, F (2013) 'Cancer incidence and mortality patterns in Europe: Estimates for 40 countries in 2012' European Journal of Cancer [online] 49, 1374-1403 available from <https://www.iarc.fr/en/mediacentre/iarcnews/pdf/Ferlay%20J_EJC_2013.pdf> [1 November 2015]

Friedman, R. C., Farh, K. K., Burge, C. B. and Bartel, D. P. (2009) Most mammalian mRNAs are conserved targets of microRNAs. Genome Res. 19, 92–105

Gayed, IW., Liu, H., Wei, X., Liao, Z., Yusuf, S., Chang, JY, Basset, R., Komaki, R (2009) 'Patterns of cardiac perfusion abnormalities after chemoradiotherapy in patients with lung

cancer.' Journal of Thoracic Oncology 4(2), 179-184 [online] available at <https://www.ncbi.nlm.nih.gov/pubmed/19179893>[1 May 2017]

Giordano, S., Kuo, YF., Freeman, J., Buchholz, T., Hortobagyi, G., Goodwin, J (2005) 'Risk of cardiac death after adjuvant radiotherapy for breast cancer.' Journal of the national cancer institute [online] 97(6), 419-424 available from <https://www.ncbi.nlm.nih.gov/pubmed/15770005> [12 December 2016]

Gilad, S., Meiri, E., Yogev, Y., Benjamin, S., Lebanony, D., Yerushalmi, N., Benjamin, H., Kushnir, M., Cholakh, H., Melamed, N. et al. (2008) Serum microRNAs are promising novel biomarkers. PLoS ONE 3, e3148

He, B., Xiao, J., Ren, A. J., Zhang, Y. F., Zhang, H., Chen, M., Xie, B., Gao, X. G. and Wang, Y. W. (2011) Role of miR-1 and miR-133a in myocardial ischemic postconditioning. J. Biomed. Sci. 18, 22

Horie, T., Ono, K., Nishi, H., Nagao, K., Kinoshita, M., Watanabe, S., Kuwabara, Y., Nakashima, Y., Takanabe-Mori, R., Nishi, E. et al. (2010) Acute doxorubicin cardiotoxicity is associated with miR-146a-induced inhibition of the neuregulin-ErbB pathway. Cardiovasc. Res. 87, 656–664

Jacob, S., Pathnak, A., Franzk, D., Latorzeff, I., Jiminez, G (2016] Early detection and prediction of cardiotoxicity after radiation therapy for breast cancer: the BACCARAT prospective cohort study. Radiation Oncology [online] 10 (124) 1289-1294 available from <https://ro-journal.biomedcentral.com/articles/10.1186/s13014-016-0627-5> [3rd November 2015]

Jaffe, A. S., Ravkilde, J., Roberts, R., Naslund, U., Apple, F. S., Galvani, M. and Katus, H. (2000) It's time for a change to a troponin standard. Circulation [online] 102, 1216–1220 available from <https://www.ncbi.nlm.nih.gov/pmc/articles/PMC1277047/> [3 May 2017]

Ji, X., Takahashi, R., Hiura, Y., Hirokawa, G., Fukushima, Y. and Iwai, N. (2009) Plasma miR-208 as a biomarker of myocardial injury.Clinical Chemistry, 55, 1944–1949

Jagsi, R., Pottow, J., Griffith, K., Bradley, C., Hamilton, J., Graff, S., Katz, S., Hawley, T (2014) 'Long-Term Financial Burden of Breast Cancer: Experiences of a Diverse Cohort of

Survivors Identified Through Population-Based Registries'. Journal of Clinical Oncology [online] 22 (12) 1269-1276 available from <http://ascopubs.org/doi/pdf/10.1200/JCO.2013.53.0956? [2November 2015]
Joshi, S., Khan, F., Pant, I., Shukla, A (2007) 'Role of Radiotherapy in Early Breast Cancer: An Overview' 1 (2), 259-264 available from <https://www.ncbi.nlm.nih.gov/pmc/articles/PMC3068638/> [2November 2015]

Hoekstra, M., van der Lans, C. A., Halvorsen, B., Gullestad, L., Kuiper, J., Aukrust, P., van Berkel, T. J. and Biessen, E. A. (2010) The peripheral blood mononuclear cell microRNA signature of coronary artery disease. Biochem.Biophys. Res. Commun. 394, 792–797

Kim, M., Craft, D., Orton, C (2016) Within the next five years, most radiotherapy treatment schedules will be designed using spatiotemporal optimization. The Journal of Medical Physics Research [online] 43(5), 2009-2012 available at <
Madan, R., Benson, R., Sharma, D., Julka, P., Rath, G (2015) 'Radiation induced heart disease: Pathogenesis, management and review literature' Journal of Eqyptian National Cancer Institute [online] 27 (4), 187-193, available at <http://onlinelibrary.wiley.com/doi/10.1118/1.4943383/abstract>http://www.sciencedirect.com/science/article/pii/S1110036215000631> [2 March 2016]

Lagos-Quintana, M., Rauhut, R., Yalcin, A., Meyer, J.,Lendeckel, W. and Tuschl, T. (2002) Identification of tissue-specific microRNAs from mouse. Curr. Biol. 12, 735–739

Lancelloti, P., Nkomo, V., Badano, L., Klein, J., Bogaert, J., Davin, L (2013) 'Expert consensus for multi-modality imaging evaluation of cardiovascular complications of radiotherapy in adults: a report from the European Association of Cardiovascular Imaging and the American Society of Echocardiography.' European Heart Journal Cardiovascular Medicine [online] 14(8) 721-740 available from <https://www.ncbi.nlm.nih.gov/pubmed/23847385? [2 March 17]

Marks LB, Yu, X, Prosnitz, RG., Zhou, SM., Hardenbergh, PH., Blazing, M (2005) The incidence and functional consequences of RT-associated cardiac perfusion defects. International Journal of Radiation Oncology Biology Physics (2005) [online] 63(1), 214-218 available from <https://www.ncbi.nlm.nih.gov/pmc/articles/PMC4332338/#B40> [1st October 2017]

Michael, A., Bajracharya, S. D., Yuen, P. S., Zhou, H., Star, R. A.,

Illei, G. G. and Alevizos, I. (2010) Exosomes from human saliva as a source of microRNA biomarkers. Oral Dis. 16, 34–38

Mitchell, P. S., Parkin, R. K., Kroh, E. M., Fritz, B. R., Wyman, S. K., Pogosova-Agadjanyan, E. L., Peterson, A., Noteboom, J., O'Briant, K. C., Allen, A. et al. (2008) Circulating microRNAs as stable blood-based markers for cancer detection. Proc. Natl. Acad. Sci. U.S.A. 105, 10513–10518

Maisal, A., Khrishnaswarmy, P., Richard, M., Nowak, M (2002) McNeely, M., Kristin, L., Rowe, B., Klassen, T., Mackey, J., Courneya, K (2006) 'Effects of exercise on breast cancer patients and survivors: a systematic review and meta-analysis'. Canadian Medical Association Journal [online] 175 (1), 34-41 available from <https://www.ncbi.nlm.nih.gov/pmc/articles/PMC1482759> [2nd November 2015]

Nicoli, S., Standley, C., Walker, P., Hurlstone, A., Fogarty, K. E. and Lawson, N. D. (2010) MicroRNA-mediated integration of haemodynamics and VEGF signalling during angiogenesis. Nature 464, 1196–1200

Nilsson, G., Holmberg, L., Garmo, H., Duvernoy, O., Sjogren, I., Lagergvist, B., Holmberg, L., Garmo, H., Duvernoy, O., Sjogren, J., Lagergvist, B., Biomgvist, C (2012). Distribution of coronary artery stenosis after radiation for breast cancer. Journal of Clinical Oncology [online] 30(4), 380-386 available from <https://www.ncbi.nlm.nih.gov/pubmed/22203772> - 3rd October 2017]

National Institute of Clinical Excellence (2009) 'Early and locally advanced breast cancer: diagnosis and treatment [online] available from < https://www.nice.org.uk/guidance/cg80> [11th May 2016]

O'Toole, A. S., Miller, S., Haines, N., Zink, M. C. and Serra, M. J. (2006) Comprehensive thermodynamic analysis of 3_ double-nucleotide overhangs neighboring Watson-Crick terminal base pairs. Nucleic Acids Res. 34, 3338–3344

Sandri, M. T., Salvatici, M., Cardinale, D., Zorzino, L., Passerini, R., Lentati, P., Leon, M., Civelli, M., Martinelli, G. and Cipolla, C.M. (2005) N-terminal pro-B-type natriuretic peptide after high-dose chemotherapy: a marker predictive of cardiac dysfunction? Clin. Chem. 51, 1405–1410

Sharma, S., Jackson, P., Makan, J (2004) 'Cardiac Troponins'. Journal of Clinical Pathology [online] available at <https://www.ncbi.nlm.nih.gov/pmc/articles/PMC1770452/> [5 May 2016]

Schmidt, M., Paes, K., De Mazi`ere, A., Smyczek, T., Yang, S., Gray, A., French, D., Kasman, I., Klumperman, J., Rice, D. S.and Ye, W. (2007) EGFL7 regulates the collective migration of endothelial cells by restricting their spatial distribution. Development 134, 2913–2923

Shimuzu, Y., Kodama, K., Nishi, N., Ksagi, F., Syama, A (2010) 'Radiation exposure and circulatory disease risk: Hiroshima and Nagasaki atomic bomb survivor data, 1950-2003' British Medical Journal [online] 320, 1-8 available at <http://www.bmj.com/content/bmj/340/bmj.b5349.full.pdf> [12 May 2017]

Siegel, R., Miller, K., Jemal, A (2017) 'Cancer Statistics, 2017' CA: A Cancer Journal for Clinicians' [online] 67 (1), 7-30 available from <http://onlinelibrary.wiley.com/doi/10.3322/caac.21387/full?> [2 November 2015]
Taunk, N., Haffty, B., Kostis, J., Goyal, S (2015) 'Radiation-Induced Heart Disease: Pathologic Abnormalities and Putative Mechanisms'. Frontiers in Oncology [online] 5(39) 1-27 available at <https://www.ncbi.nlm.nih.gov/pmc/articles/PMC4332338/pdf/fonc-05-00039.pdf> [19 February 2017]

Stewart, J., Fajardo, L (1984) Radiation induced heart disease; an update. Progressive Cardiovascular Disease [online] 27(3), 173-194 available from <https://www.ncbi.nlm.nih.gov/pubmed/6387801> [3rd September 2017]

Strender, L., Lindahl, J., Larsson, L (1986) Incidence of heart disease and functional significance of changes in the electrocardiogram 10 years after radiotherapy for breast cancer. Cancer [online] 57(5), 929-937 available from <https://www.ncbi.nlm.nih.gov/pubmed/3943028?> [11th March 2017]

Tijsen, A. J., Creemers, E. E., Moerland, P. D., de Windt, L. J., van der Wal, A. C., Kok, W. E. and Pinto, Y. M. (2010) MiR423-5p as a circulating biomarker for heart failure. Circ. Res. 106, 1035–1039

Taghian, A., Jeong, J., Eleftherious, M., David, S., Deutsch, M., Costantino, J., Wolmark, N (2006) 'Low Locoregional Recurrence Rate Among Node-Negative Breast Cancer Patients With Tumors 5 cm or Larger Treated by Mastectomy, With or Without Adjuvant Systemic

Therapy and Without Radiotherapy: Results From Five National Surgical Adjuvant Breast and Bowel Project Randomized Clinical Trials' Journal of Clinical Oncology [online] 24(24), 3927-3932 available from <http://ascopubs.org/doi/full/10.1200/jco.2006.06.9054> [3rd November 2015]

Taylor, C., Nisbet, A., McGale, P., Darby, S (2007) 'Cardiac exposures in breast cancer radiotherapy: 1950s-1990s' International Journal of Radiation Oncology, Biology and Physics [online] 1(69) 1484-1495 available at <https://www.ncbi.nlm.nih.gov/pubmed/18035211> [4 May 2017]

Thum, T., Gross, C., Fiedler, J., Fischer, T., Kissler, S., Bussen,M., Galuppo, P., Just, S., Rottbauer, W., Frantz, S. et al. (2008)MicroRNA-21 contributes to myocardial disease by stimulating MAP kinase signalling in fibroblasts. Nature 456, 980–984

Valadi, H., Ekstrom, K., Bossios, A., Sjostrand, M., Lee, J. J.
and Lotvall, J. O. (2007) Exosome-mediated transfer of mRNAs and microRNAs is a novel mechanism of genetic exchange between cells. Nat. Cell Biol. 9, 654–659

Vasu, S., Hundley, G (2013) 'Understanding cardiovascular injury after treatment for cancer: an overview of current uses and future directions of cardiovascular magnetic resonance'. Journal of Cardiovascular Magnetic Resonance [online] 15(66), 57-69 available at <https://jcmr-online.biomedcentral.com/articles/10.1186/1532-429X-15-66> [1 March 2016]

Veinot, J., Edwards, W (1996) Pathology of radiation-induced heart disease: a surgical and autopsy study of 27 cases. Human Pathology [online] 27(8), 776-773 [online] available from <https://www.ncbi.nlm.nih.gov/pubmed/8760008> [30th March 2017]

Vogel, B., Keller, A., Frese, K., Leidinger, P., Sedaghat-Hamedani., F., Kayvanpour, E. (2013) Multivariate miRNA signatures as biomarkers for non-ischaemic systolic heart failure. European Heart Journal [online] 34, 2812–2823 available at <10.1093/eurheartj/eht256> [30thSeptember 2017].
Wang, J., Song, Y., Zhang, Y., Xiao, H., Sun, Q., Hou, N., Guo,
S., Wang, Y., Fan, K., Zhan, D. et al. (2012) Cardiomyocyte overexpression of miR-27b induces cardiac hypertrophy and dysfunction in mice. Cell Res. 22, 516–527

Whelan, T., Levine, M (2003) 'Randomized Trial of Breast Irradiation Schedules after Lumpectomy for Women With Lymph Node-Negative Breast Cancer'. Journal of the National Cancer Institute [online] 95 (10) 759-764 available from

<https://academic.oup.com/jnci/article/95/10/759/2520231/RESPONSE-Re-Randomized-Trial-of-Breast-Irradiation> [2nd November 2015]

Vasan, R. S. (2006) Biomarkers of cardiovascular disease:
molecular basis and practical considerations. Circulation 113, 2335–2362

Veinot JP, Edwards WD. Pathology of radiation-induced heart disease: a surgical and autopsy study of 27 cases. Hum Pathol (1996) 27(8):766–73.10.1016/S0046-8177(96)90447

Xu, S., Witmer, P., Lumayg, S., Kovacs, B., Valle, D (2007) 'MicroRNA (miRNA) transcriptome of mouse retina and identification of a sensory organ-specific miRNA cluster' The journal of Biological Chemistry [online] 282(34), 25053-25066 available at <https://www.ncbi.nlm.nih.gov/pubmed/17597072> [14 August 17]

Yang, B., Lu, Y., Wang, Z (2008) Control of Cardiac Excitability by microRNAs. Cardiovascular Research [online] 4(1), 571-580 available from <https://academic.oup.com/cardiovascres/article/79/4/571/347433/Control-of-cardiac-excitability-by-microRNAs> [1st October 2017]

Zampetaki,A., Willeit, P., Tilling, L (2012) Prospective study on circulating MicroRNAs and risk of myocardial infarction. Journal of American College of Cardiology 60(4), 290-299 available from <https://www.ncbi.nlm.nih.gov/pubmed/22813605> [14 May 2017]

Zhao, T., Li, G., Mi, S., Li, S., Hannon, G. J., Wang, X. J. and Qi,
Y. (2007) A complex system of small RNAs in the unicellulargreen alga Chlamydomonas reinhardtii. Genes Dev. 21, 1190–1203